

Aus der Klinik für Anästhesiologie des Universitätsklinikums Heidelberg  
der Universität Heidelberg

Ärztlicher Direktor: Univ.-Prof. Dr. med. Markus A. Weigand

# **Pathophysiology of methylglyoxal-associated endothelial damage in experimental sepsis**

Inauguraldissertation

zur Erlangung des *Doctor scientarum humanarum* (Dr. sc. hum.) an der Medizinischen Fakultät  
Heidelberg der Ruprechts-Karls-Universität

vorgelegt von Nadia Gallenstein

aus Mannheim

2023

Dekan: Herr Univ.-Prof. Dr. med. Dr. h.c. Hans-Georg Kräusslich

Doktorvater: Herr Univ.-Prof. Dr. med. Markus A. Weigand

# Content

Table of figures.....	5
Abbreviations .....	6
1. Introduction.....	10
1.1 Inflammation and Sepsis .....	10
1.2 Endothelium and pathogen – initial action.....	12
1.3 Neuroendocrine aspects of sepsis.....	13
1.4 Metabolic aspects of sepsis .....	14
1.5 Endothelium in sepsis.....	15
1.6 ROS and RNS in sepsis.....	17
1.7 Endothelium and ROS/RNS in sepsis .....	18
1.8 Reactive Carbonyl Species (RCS)—Underdogs of reactive metabolites .....	19
1.9 MG-derived carbonyl stress in sepsis .....	19
1.10 Pathophysiology of MG-derived carbonyl stress in sepsis.....	21
1.11 Regulation of MG-derived carbonyl stress in sepsis.....	22
1.12 What we know from Diabetes mellitus and other AGE-related diseases.....	22
1.12.1 Diabetes mellitus.....	23
1.12.2 Atherosclerosis.....	24
1.12.3 Hypertension.....	24
1.12.4 Cancer.....	25
1.13 Therapeutic options to limit MG .....	25
1.13.1 Aminoguanidine.....	25
1.13.2 N-Acetylcysteine.....	26
1.13.3 L-carnosine.....	26
1.13.4 L-Anserine .....	26
1.14 Aim of the study.....	27
2. Material and Methods.....	29
2.1 Materials.....	29
2.1.1 Devices.....	29
2.1.2 Consumables.....	30
2.1.3 ELISA, Activity Assays and Kits.....	30
2.1.4 Antibodies and dyes.....	31
2.1.5 Reagents for Immunofluorescence and Immunohistochemistry.....	31
2.1.6 Reagents for cell culture.....	32

2.1.7 Reagents and chemicals for HPLC.....	33
2.1.8 Reagents and chemicals for FACS.....	34
2.1.9 Reagents and chemicals for Zymography.....	34
2.1.10 Animals, drugs, and reagents for animal experiment.....	35
2.1.11 Software.....	35
2.2 Methods.....	36
2.2.1 Mouse model.....	36
The cecal ligation and puncture (CLP).....	36
Intraperitoneal (i.p.) administration of drugs.....	36
Intravenous (i.v.) Evans Blue Injection.....	36
Further processing of organs.....	37
Preparation of organ samples for staining.....	37
Evans Blue Extraction and Quantification.....	37
Immunofluorescence (IF) staining for localization microscopy.....	37
Immunohistochemistry.....	38
Determination of Anserine.....	38
2.2.2 Cell culture.....	39
Conditions.....	39
Passaging cells.....	39
Determination of the cell number.....	39
Cryoconservation of cells.....	40
Reactivation of cryo conserved cells.....	40
Cell stimulation.....	40
2.2.3 Experiments.....	41
The transendothelial electrical resistance (TER, Ohm's Law Method).....	41
Immunofluorescence staining for localization microscopy.....	41
In Situ Trypan blue staining.....	42
Paracellular permeability assay.....	42
Bicinchoninic acid assay.....	43
Zymography.....	43
FACS.....	44
2.2.4 Commercial Assays.....	45
Enzyme-linked Immunosorbent Assay (ELISA).....	45
Human Active MMP-1 Fluorescent Assay.....	46
Lactate Dehydrogenase (LDH) Assay.....	46

Caspase Assay.....	47
Cytokine Array.....	47
2.2.5 Statistics.....	48
3 Results.....	49
3.1 Endothelial barrier integrity and paracellular transport <i>in vitro</i> .....	49
3.1.1 MG impairs the endothelial barrier by disturbing the monolayer integrity and increasing paracellular leakage.....	49
3.1.2 Anserine prevents effects of patho- and supraphysiological MG doses.....	51
3.1.3 The effects of Anserine exceed those of previously described scavengers.....	55
3.1.4 MG disrupts endothelial barrier proteins.....	55
3.2 Anserine effects in a murine model of sepsis ( <i>in vivo</i> ) .....	58
3.3 Mechanisms of action of MG and Ans <i>in vitro</i> .....	62
3.3.1 MG, Ans and the extracellular matrix .....	62
3.3.2 Immunological effects of MG.....	65
4. Discussion.....	75
4.1 Ans shows protective and restoring effects against MG induced endothelial damage <i>in vitro</i> .....	75
4.2 Ans reduces MG-induced endothelial leak, tissue AGE formation and improves survival in septic mice ( <i>in vivo</i> ) .....	76
4.3 MG does not increase MMP shedding or activity in HUVEC <i>in vitro</i> .....	79
4.4 MG induces inflammation by activating the NLRP3 inflammasome <i>in vitro</i> .....	80
4.5 MG activates MAPKs via RAGE-dependent and -independent pathways <i>in vitro</i> .....	83
4.6 Limitations of the study .....	86
4.7 Outlook.....	86
5. Summary .....	87
6. Zusammenfassung.....	89
7. References.....	91
8. Personal contribution to data collection .....	114
Curriculum Vitae .....	115
Acknowledgements.....	116
Eidesstattliche Versicherung (Affidavit) .....	118

## Table of figures

Figure 1: Inflammatory cascade in sepsis .....	13
Figure 2: Endothelial permeability in sepsis .....	16
Figure 3: FACS Gating Strategy for HUVEC.....	45
Figure 4: MG impairs the endothelial barrier comparable to LPS and TNF.....	50
Figure 5: MG leads to increased paracellular leakage .....	51
Figure 6: Ans prevents MG-induced TER loss and improves paracellular leakage of small molecules..	52
Figure 7: Ans prevents TER loss and paracellular leakage of supraphysiological MG dosages.....	53
Figure 8: Ans shows TER restoring effects .....	54
Figure 9: MG-scavengers and antioxidants show moderate effects in MG-induced TER loss.....	56
Figure 10: MG leads to disruption of endothelial barrier forming proteins.....	57
Figure 11: Ans improves survival of septic mice by stably increasing Ans tissue concentrations.....	59
Figure 12: Ans improves capillary leak of septic mice.....	60
Figure 13: Ans effect of barrier forming proteins in vivo .....	61
Figure 14: Ans functions as an effective MG-scavenger in vivo.....	62
Figure 15: MG in pathophysiological dosages activates MMP1.....	64
Figure 16: Inflammatory cytokine profile from MG- and Ans stimulated HUVEC.....	70
Figure 17: MG leads to caspase-1 activation in HUVEC independent of cell death. ....	71
Figure 18: MG dose-dependently increases human pro IL-1beta secretion from HUVEC.....	72
Figure 19: The MG effect on TER is RAGE-dependent .....	72
Figure 20: MG activates MAPK but not the NF- $\kappa$ B subunit or Akt kinase .....	73
Figure 21: Ans does not exert effects on MG-induced p38- or c-Jun phosphorylation .....	74
Figure 22: c-Jun but not p38 phosphorylation by MG is RAGE dependent .....	75

## Abbreviations

4',6-diamidino-2-phenylindol	DAPI
activator protein-1	AP-1
adenosine triphosphate	ATP
advanced glycation end-products	AGEs
alternating current	AC
aminoguanidine	AG
bicinchoninic acid	BCA
blood brain barrier	BBB
body weight	bw
bovine serum albumin	BSA
cardiovascular diseases	CVD
carnosinase 1	CN1
carnosinase 2	CN2
C-C motif chemokine ligand 24	CCL24
cecal ligation and puncture	CLP
cluster of differentiation	CD
compensatory anti-inflammatory response syndrome	CARS
C-reactive protein	CRP
C-X-C motif chemokine ligand 1	CXCL1
damage associated molecular patterns	DAMPs
deoxyribonucleic acid	DNA
dihydroxyacetone phosphate	DHAP
dimethyl sulfoxide	DMSO
distilled water	ddH <sub>2</sub> O
Dulbecco's phosphate buffered saline	DPBS
endothelial cells	EC
endothelial nitric oxide synthase	eNOS
enzyme-linked immunosorbent assay	ELISA
Escherichia coli	E. coli
estimated glomerular filtration rate	eGFR

ethanol	EtOH
ethylenediaminetetraacetic acid	EDTA
Evans blue	EB
extracellular signal-regulated kinases	ERK
fetal calve serum	FCS
fluorescein isothiocyanate	FITC
fluorescence activated cell sorting	FACS
forward scatter	FSC
forward scatter area	FSC-A
forward scatter height	FSC-H
glutathione	GSH
glyceraldehyde-3-phosphate	GAP
glyoxalase-1	GLO-1
glyoxalase-2	GLO-2
granulocyte colony-stimulating factor	G-CSF
granulocyte colony-stimulating factor	GM-CSF
heat shock protein	Hsp
heme oxygenase-1	HO-1
high performance liquid chromatography	HPLC
high-density-lipoprotein	HDL
human umbilical vein endothelial cells	HUVEC
hydrogen oxidases	NOXs
I $\kappa$ B signalosome dependent phosphorylation of NF- $\kappa$ B inhibitors	I $\kappa$ B inhibitors
immunofluorescence	IF
inducible NO-synthase	iNOS
inhibitor of NF-KB	IKB
intercellular adhesion molecule 1	ICAM-1
interferon regulatory factor 3	IRF3
interleukin-1 receptor-associated kinases	IRAK
interleukins	IL
intra peritoneal	i.p.



intravenous	i.v.
lactate dehydrogenase	LDH
L-anserine	Ans
L-carnosine	Cns
lipopolysaccharides	LPS
low-density-lipoprotein	LDL
LPS-binding protein	LBP
MAPK kinases	MKKs
mean fluorescence intensity	MFI
metalloproteinases	MMPs
methylglyoxal-derived hydroimidazolones	MG-H1
mitogen-activated protein kinases	MAPKs
mixed-lineage kinases	MLKs
MKK kinases	MKKKs
mouse cardiac endothelial cells	MCEC
multiple organ dysfunction syndrome	MODS
myeloid Differentiation factor 2	MD-2
myeloid differentiation primary response 88	MyD88
N-acetylcysteine	NAC
nicotinamide adenine dinucleotide phosphate	NADPH
nitric oxide	NO
NOD-like receptor containing pyrin domain 3	NLRP3
N-terminal c- Jun kinases	JNKs
nuclear factor 2	Nrf2
nuclear factor- $\kappa$ B	NF- $\kappa$ B
nucleotide-binding oligomerization domain	NOD
p-amino phenylmercuric acetate	APMA
paraformaldehyde	PFA
pathogen associated molecular patterns	PAMPs
pattern recognition receptors	PRRs
peptidoglycans	PGN

peripheral blood mononuclear cells	PBMCs
phosphatidylinositol 3-kinase	PI3K
platelet and endothelial cell adhesion molecule 1	PECAM-1
procalcitonin	PCT
protein kinase B	Akt
radio-immunoprecipitation assay	RIPA
reactive carbonyl species	RCS
reactive oxygen species	ROS
reactive nitrogen species	RNS
receptor of advanced glycation end-product	RAGE
regulatory T cell	Treg
relative fluorescence units	RFU
side scatter	SSC
sodium chloride	NaCl
soluble RAGE	sRAGE
soluble TNF receptor	sTNFR
standard deviations	SD
standard error mean	SEM
systemic inflammatory response syndrome	SIRS
T helper 17 cells	TH17
tight junctions	TJs
TNF receptor-associated factor 6	TRAF6
toll-interleukin-1 receptor (TIR)-domain-containing adapter-inducing interferon- $\beta$	TRIF
toll-like receptor 4	TLR 4
transendothelial electrical resistance	TER
tumor necrosis factor	TNF
type 1 and type 2 Diabetes mellitus	T1D, T2D
vascular cell adhesion molecule 1	VCAM-1
vascular endothelial cadherin	VE-cadherin
water-soluble tetrazolium salts	WSTs
zonula-occludens-1	ZO-1

# 1. Introduction

## 1.1 Inflammation and Sepsis

Sepsis is defined as a life-threatening organ dysfunction caused by a dysregulated host response to infection (Singer et al., 2016) and is associated with a high morbidity and mortality. The occurrence is not limited to low- and middle-income countries. Millions of people are also affected in high-income countries – and in some of them, the rate of sepsis continues to rise. In 2017, more than 49 million sepsis cases occurred worldwide, causing about 11 million deaths (Rudd et al., 2020). In recent years, the definition of sepsis has undergone few modifications, owed to the lack of specific and quick diagnostic tools and a quite non-specific clinical presentation. Although sepsis is caused by an infection, the dysregulated generalized host response ultimately results in severe multi-organ dysfunction and death (Singer et al., 2016). The underlying pathophysiological mechanisms have not been fully clarified yet; however, the innate immune system seems to control the initial phase of the disease.

Systemic inflammatory response syndrome (SIRS) is an overstated defense response of the organism to a harmful stressor (e.g., infection, trauma, surgery, acute inflammation, ischemia/reperfusion, or malignancy) to localize and then to abolish the endogenous or exogenous source of the insult. It involves the release of acute-phase proteins, which directly mediate far-reaching autonomic, endocrine, hematological, and immunological changes in the patient (Chakraborty and Burns, 2023). Even though the purpose is defensive, the dysregulated immune response can cause a massive inflammatory cascade leading to reversible or irreversible end-organ dysfunction and even death (Bone et al., 1992). SIRS with a suspected source of infection is called sepsis, and hemodynamic instability despite intravascular volume administration is referred to as septic shock. Together they represent a physiological process with an increasingly deteriorating balance between the body's pro-inflammatory and anti-inflammatory responses (Chakraborty and Burns, 2023).

At a molecular level, the etiopathogenesis broadly divides into unspecific and highly conserved antigens, so-called pathogen associated molecular pattern (PAMPs), (Ritthaler et al., 1995, Weigand et al., 2004, Carré and Singer, 2008, Hotchkiss and Karl, 2003, Jalbout et al., 2007) and damage associated molecular patterns (DAMPs), which are associated with components of host cells that are released during cell damage or death (Kumar et al., 2011). Both are recognized by pattern recognition receptors (PRR) on immune and endothelial cells and thereby trigger a diversified stress response. PAMPs comprise bacterial cell wall components such as lipopolysaccharides (LPS) or peptidoglycans (PGN) and lead to degranulation, phagocytosis, upregulation of adhesion molecules, release of pro-inflammatory cytokines, and activation of complement pathways, ultimately causing a procoagulant state (Ritthaler

et al., 1995, Weigand et al., 2004, Carré and Singer, 2008, Hotchkiss and Karl, 2003, Jalbout et al., 2007).

In addition, many metabolic changes occur as a result of inflammation, which lead to the release of reactive oxygen (ROS, e.g. superoxide) and nitrogen (RNS; e.g. nitric oxide) species. Reactive carbonyl species (RCS) are another crucial group of highly reactive metabolites (Lide, 2005) that have not yet been adequately studied in the context of sepsis. However, RCS could contribute massively to the changes triggered by the infection. Usually, the inflammatory response is limited to the infection and responds with a balanced production and elimination of cytokines and free radicals (Gutteridge and Mitchell, 1999). In the case of sepsis, the physiological conditions become enormously imbalanced. This often leads to a hyperdynamic cardiovascular situation, fever, and a changed number of white blood cells (Hotchkiss and Karl, 2003, Levy et al., 2003).

Roger Bone outlined a sepsis cascade beginning with SIRS and progressing to multiple organ dysfunction syndrome (MODS) unless counteracted by a compensatory anti-inflammatory response or alleviation of the primary causative etiology (Bone et al., 1997). This compensatory anti-inflammatory response syndrome (CARS) is triggered shortly after the onset of sepsis (Preiser et al., 2014). The goal of these reactions is to restore homeostasis after systemic inflammation by downregulation of the immune system. Otherwise, early deaths from the acute hyperinflammatory phase of sepsis often occur (Singer et al., 2016). Sepsis is a systemic condition, virtually affecting all organs and tissues, with the endothelium being one of the first to be attacked and to respond to the insult. In sepsis, the endothelial cells (EC) have two evident roles: one is to amplify the immune response and the other is the activation of the coagulation system. The activation, but also a dysfunction of the endothelium fundamentally contributes to an end organ damage in sepsis. Moreover, the endothelium provides not only a connection between the local and systemic immune responses but is also a target as well as a source of inflammation at the same time (Hack and Zeerleder, 2001). When being stimulated, EC produce vasoactive composites, inflammatory cytokines as well as chemoattractants and express adhesion molecules, consequently switching from an anticoagulant to a procoagulant state. Local endothelial activation is needed to fight the source of infection, however systemic activation results in microvascular thrombosis, capillary leak, hypotension, hypoxia and finally in tissue damage (Reinhart et al., 2002).

## 1.2 Endothelium and pathogen – initial action

When there is an injury that allows a pathogen to enter the bloodstream, there is generalized inflammation from exposure to bacterial components and tissue breakdown products. Not only the immune cells provide a sufficient response to the insult, but also the endothelium is activated and directs as well as modulates the inflammatory response (Hack and Zeerleder, 2001). During the course of severe inflammation, as seen in sepsis, the pathogen leads to activation of the inflammatory cascade, resulting in a cytokine storm. Cytokines include interleukins (IL), chemokines, interferons, tumor necrosis factor (TNF), as well as growth factors (Stober et al., 2019), which are produced and released mainly by immune cells (Dinarello, 2007). Infection will ultimately activate the cytokine system, which consists of pro-inflammatory and anti-inflammatory cytokines. The equilibrium between these counter-regulatory pathways ultimately determines the inflammatory activity of the cytokine system (Fig.1). In both, inflammatory cells and ECs respond to cytokines or bacterial cell wall components (LPS). Nuclear factor- $\kappa$ B (NF- $\kappa$ B) plays a crucial role in the cell (both inflammatory cells and ECs) (Li et al., 1997). A complex is formed by LPS with LPS-binding protein (LBP), Myeloid Differentiation factor 2 (MD-2), toll-like receptor 4 (TLR4), and cluster of differentiation (CD) 14, which further initiates an intracellular signaling cascade (Kuzmich et al., 2017). The pathways can be roughly divided into two competitive cascades: TLR4/ toll-interleukin-1 receptor (TIR)-domain-containing adapter-inducing interferon- $\beta$  (TRIF)/ interferon regulatory factor 3 (IRF3) and TLR4/ myeloid differentiation primary response 88 (MyD88)/NF- $\kappa$ B. The TLR4/TRIF/IRF3 cascade involves activation of TRIF, internalization of the TLR4/TRIF complex within endosomes and subsequent activation of interferon regulatory transcription factor-3 (IRF3) and interferon production. Simultaneously, the activation of the TLR4/MyD88/NF- $\kappa$ B cascade leads to phosphorylation of MyD88 and interleukin-1 receptor-associated kinases 1 and 4 (IRAK1 and IRAK4). IRAKs in turn phosphorylate TNF receptor-associated factor 6 (TRAF6), that forwards the degradation of inhibitor of NF- $\kappa$ B (IKB) and nuclear translocation of NF- $\kappa$ B. TRAF6 also activates mitogen-activated protein kinases (MAPKs), finally resulting in the activation of activator protein-1 (AP-1) (Kuzmich et al., 2017). Inflammatory cytokines, like TNF, can activate similar pathways resulting in nuclear translocation of NF- $\kappa$ B, further increasing cytokine production (Wu et al., 2016). Activation of NF- $\kappa$ B can result in nucleotide-binding oligomerization domain (NOD)-like receptor containing pyrin domain 3 (NLRP3), proIL-1 $\beta$  and proIL-18 expression. NLRP3 senses different PAMPs and DAMPs, which induce the assembly of the NLRP3 inflammasome, activating Caspase-1 followed by the cleavage of the pro-inflammatory cytokines proIL-1 $\beta$  and -18. Subsequent secretion of the mature and active cytokines induces inflammation (Hennig et al., 2018). As noted above, LPS exerts its effects on endothelial cells via binding to TLR4; thus, intervening in LPS binding to TLR4 as well as targeting the downstream signaling pathways are potential treatment strategies for Gram-negative sepsis (Ding and Liu, 2019). While designed to be

protective by its nature, in cases when the stimulus becomes overwhelming, the TLR4 pathway can contribute to the pathologic downward spiral of sepsis. However, the immunoinflammatory and the neuroendocrine stress responses lead coordinately to profound metabolic changes during sepsis (Preiser et al., 2014), affecting the vascular system.

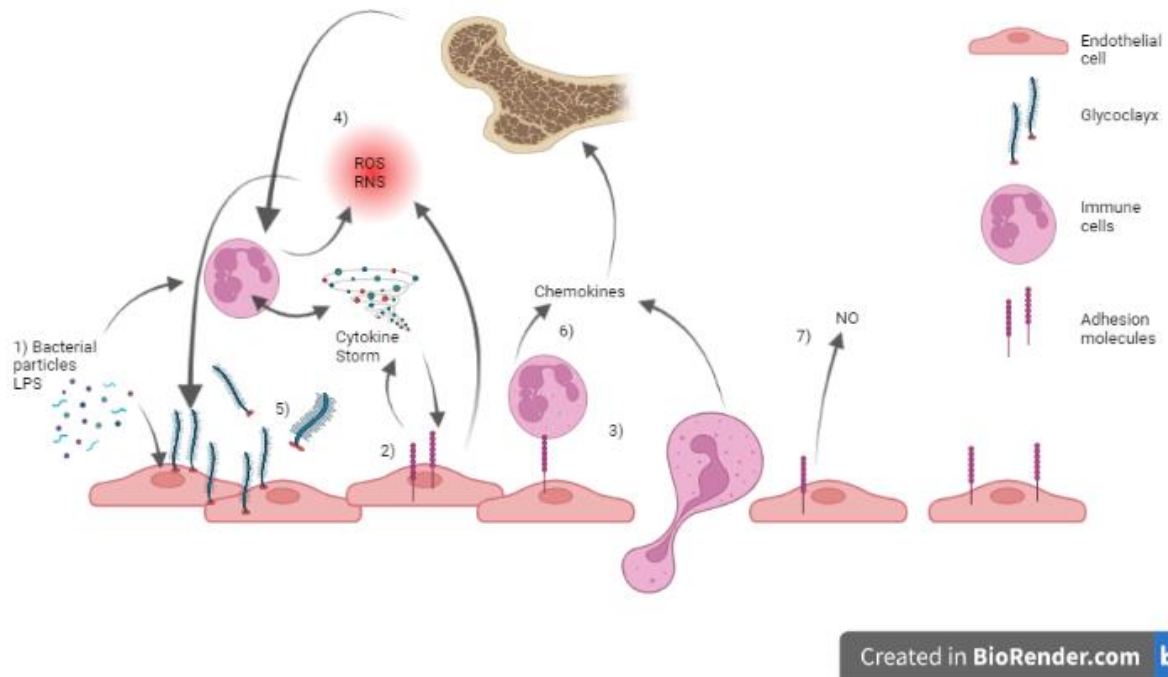


**Figure 1: Inflammatory cascade in sepsis**

1) Bacterial components activate both immune and endothelial cells inducing cytokine production, which is self-perpetuating. 2) Endothelial cells become activated and express adhesion molecules, to which immune cells bind. 3) This initiates the process of transmigration of immune cells to the site of injury. 4) ROS secreted by immune and endothelial cells further augment the inflammatory response. 5) The combination of these insults leads to a shedding of the glycocalyx, induction of adhesion molecules, increased endothelial permeability, and endothelial apoptosis. 6) Chemokines secreted by immune and endothelial cells recruit immune cells from the bone marrow. 7) The shift in the eNOS/iNOS balance results in excess NO synthesis and vasodilation. **Abbreviations:** ROS: reactive oxygen species; RNS: reactive nitrogen species; NO: nitric oxide; LPS: lipopolysaccharide. Adapted from: Dolmatova, E. V., Wang, K., Mandavilli, R., & Griendling, K. K. (2021). The effects of sepsis on endothelium and clinical implications. *Cardiovascular research*, 117(1), 60–73. <https://doi.org/10.1093/cvr/cvaa070>. Created with biorender.com

### 1.3 Neuroendocrine aspects of sepsis

During sepsis a variety of stress associated hormones like cortisol, epinephrine, norepinephrine, and vasopressin are inevitably released in addition to both insulin and glucagon (Carré and Singer, 2008, Hotchkiss and Karl, 2003, Jalbout et al., 2007). This response is controlled by the hypothalamic-pituitary axis and the sympathetic nervous system (Preiser et al., 2014). The first phase of sepsis is often characterized by a hyper-hemodynamic state. Furthermore, the excessive release of stress hormones also leads to substantial changes in the metabolic state. Epinephrine and norepinephrine induce

hepatic gluconeogenesis, glycogenolysis and glycolysis (Dungan et al., 2009). This hyperglycemic state is even worsened by an additional cortisol release (e.g. due to inflammatory mediators like TNF, IL-1, IL-6 and C-reactive protein (CRP)), which stimulates hepatic gluconeogenesis and induces insulin resistance (Dungan et al., 2009, Marik and Bellomo, 2013).

#### 1.4 Metabolic aspects of sepsis

As aforementioned, sepsis as well as septic shock result from infection, neuroendocrine as well as metabolic changes, or abnormalities. The combined immunoinflammatory and neuroendocrine responses to an infection lead to an apparent catabolic state, which is accompanied by insulin resistance. Consequently, hyperglycemia is a frequent observation in sepsis (Dungan et al., 2009, Marik and Raghavan, 2004, Marik and Bellomo, 2013) and associated with a higher mortality and morbidity in critically ill patients (Krinsley, 2003, Capes et al., 2000, Gale et al., 2007, Langley and Adams, 2007, Wiener et al., 2008). A possible explanation for that could be the impaired glucose usage of mitochondria during systemic inflammation (Fink, 2001, Fink, 2015). This might be due to the fact that the electron transport chain is uncoupled or altered during systemic inflammation (Fink, 2015), resulting in a greater dependence on glycolysis for the energy supply. In comparison to oxidative phosphorylation, glycolysis is much less effective in producing adenosine triphosphate (ATP), accounting for the temporarily large demands for glucose consumed to cover the energy amounts. Alongside, the glucose supply in sepsis is further impeded by a deranged microcirculation (Dungan et al., 2009, Marik and Bellomo, 2013, Losser et al., 2010). This metabolic switch seems to have high importance within the immune responses (O'Neill et al., 2016) of all activated immune cells. First described in tumor cells (Warburg, 1924), the concept of the so called „Warburg effect“ was expanded to include immune cells as well (Rodríguez-Prados et al., 2010, Krawczyk et al., 2010, Doughty et al., 2006, Michalek et al., 2011, Donnelly et al., 2014, Palsson-McDermott and O'Neill, 2013). With regard to ATP production, glycolysis provides important coenzymes and intermediate products essential for cell growth, proliferation and cytokine assembly. Further, enhanced glycolysis is closely linked to an upregulation of the pentose phosphate pathway, which supplies not only nucleotide intermediates but also nicotinamide adenine dinucleotide phosphate (NADPH), which is required for the so-called respiratory burst. Besides its role in activated immune cells to adapt to particular energy demands of the target tissues, glycolysis appears to be involved in additional cell lineage-specific signaling pathways that promote inflammation and immune cell differentiation (O'Neill et al., 2016). For example, hexokinase, the rate limiting enzyme of glycolysis has been demonstrated to be an activator of the NLRP3 inflammasome in macrophages, which in turn regulates caspase-1 (Moon et al., 2015). Caspase-1 then produces IL-1 $\beta$ , IL-18 and can induce pyroptosis. Also, in T cells, another crosslink

between glucose metabolism, inflammatory condition and phenotype was demonstrated (Jha et al., 2015, Gerriets et al., 2015, Beier et al., 2015). Inhibition of glycolysis has been shown to induce the conversion of T helper 17 (TH17) cells to regulatory T (Treg) cells (Shi et al., 2011). From one perspective, hyperglycemia seems to provide the energy supply in systemic inflammation and enables the immune system to access a proinflammatory state respectively to exert its delegated functions. From the other perspective, when systemic inflammation becomes dysregulated, it can eventually become a vicious cycle that leads to damage to endothelial cells, dysfunction of multiple organs, and eventual death (Marik and Bellomo, 2013).

## 1.5 Endothelium in sepsis

Immune cells and the endothelium are influential interactors during sepsis and endothelial cell damage accounts for much of the pathology in septic shock. The endothelial barrier is highly selective and fundamental to preserve the fluid balance in the tissue and to sustain normal organ function (Kása et al., 2015). During sepsis the endothelium is characterized by increased permeability or a loss of barrier function, which possibly lead to a shift in the circulating elements and tissue edema (Ferro et al., 2000). Vascular endothelial (VE)-cadherin is the main component of the endothelial adherens junctions. These are tightly regulated protein complexes that connect neighbouring ECs and prevent leukocyte migration and vascular leakage. Inflammatory mediators lead to distinct suppressive and activating cascades (Allingham et al., 2007), resulting in phosphorylation of VE-cadherin, dissociation from catenin and induction of its own endocytosis (Radeva and Waschke, 2018). This self-propelled endocytosis of VE-cadherin alone is capable of triggering gap formation between ECs, ultimately leading to a higher permeability (Lee and Slutsky, 2010). Likewise, to adherent junctions, the disruption of endothelial tight junctions (TJ) has been reported as well in sepsis, along with a decrease of occludin and zonula-occludens-1 (TJ protein 1; ZO-1) protein levels (He et al., 2018, Ni et al., 2019). As described before, TNF is one of the central cytokines in sepsis and leads to disturbance of claudin 5 at cell-cell junctions of ECs through the NF- $\kappa$ B cascade (Clark et al., 2015).

The endothelial glycocalyx is a critical regulator of the endothelial barrier integrity during sepsis. Positioned between the vessel wall and the blood, the endothelial glycocalyx is built up from a membrane-bound negatively charged network of proteoglycans, glycoproteins, glycolipids, glycosaminoglycans (i.e. heparan sulphate), and adherent plasma proteins (Weinbaum et al., 2007). Inflammation, and in particular sepsis, lead to changes in the glycocalyx, resulting in endothelial damage and microvascular dysfunction (Chelazzi et al., 2015). Enzymes such as metalloproteinases (MMP), heparanase, and hyaluronidase also participate in glycocalyx degradation. LPS, ROS and pro-inflammatory cytokines are described to be involved in activation of such shedding enzymes. These



enzymes cleave the extracellular parts of the transmembrane proteins (e.g. syndecan), which in turn uncover ECs for leukocyte and platelet adhesion, increase inflammation, lead to increased vascular permeability, dysregulation of vascular homeostasis and activate the coagulation cascade (Chappell et al., 2009, Goligorsky and Sun, 2020, Uchimido et al., 2019, Cao et al., 2019a). Along with increased vascular permeability, one of the most severe complications in sepsis and septic shock is disseminated intravascular coagulation (Iba et al., 2019). Even though ECs coordinate the clotting cascade and activation as well as aggregation of platelets, activated platelets are also capable of the secretion of numerous cytokines which stimulate immune cells and promote their adhesion to the endothelium (Thomas and Storey, 2015). The combined extreme inflammatory stimuli cause the endothelium to separate, to produce gaps between the ECs and to finally end up in a significantly increased permeability. Reactive metabolites such as ROS, RNS and RCS may also play a greater role here than previously assumed.

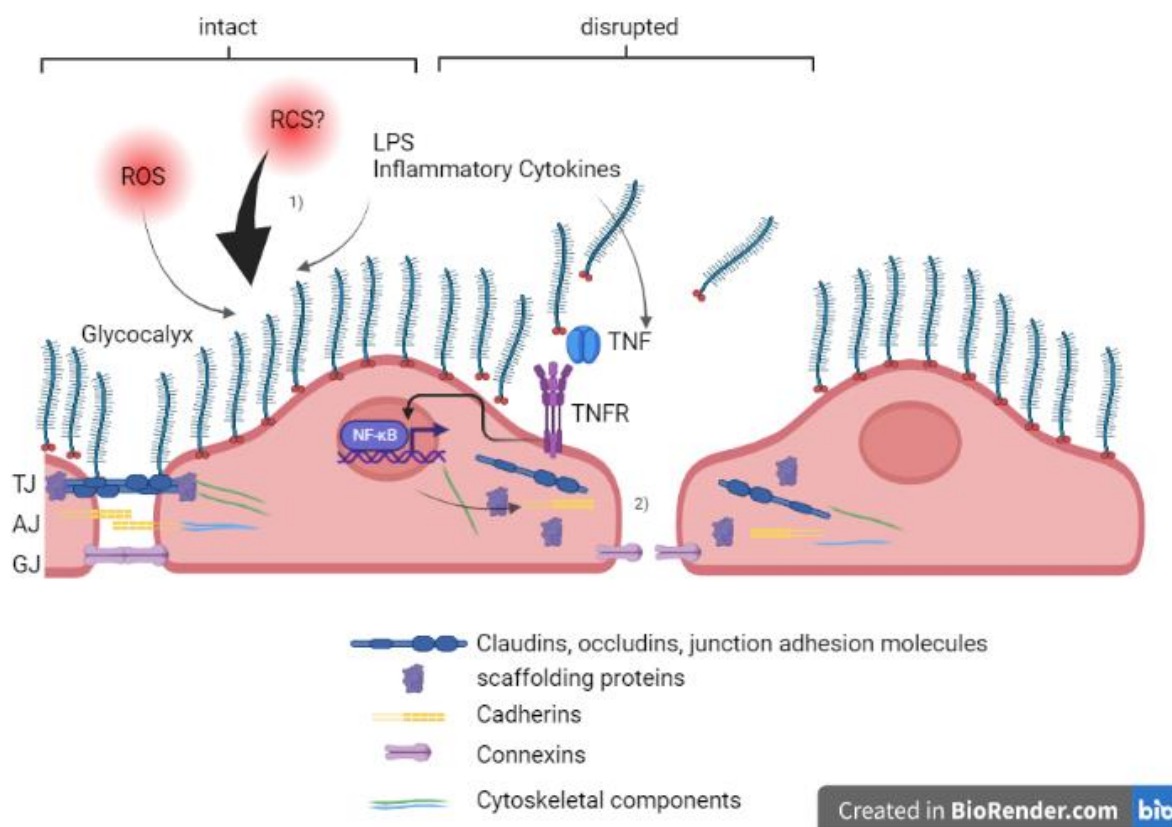


**Figure 2: Endothelial permeability in sepsis**

1) ROS and bacterial components (i.e., LPS) damage the glycocalyx. 2) LPS and inflammatory cytokines result in disruption of tight junctions (TJ), adherens junctions (AJ), and gap junctions (GJ) via activation of TNF- $\alpha$  and Ang2 pathways. The above-mentioned effects increase endothelial permeability. **Abbreviations:** ROS: reactive oxygen species; RCS: reactive carbonyl species; LPS: lipopolysaccharide; TJ: tight junctions; AJ: adherens junctions; GJ: gap junctions; TNF: tumor necrosis factor; TNFR: TNF receptor; NF- $\kappa$ B: nuclear factor  $\kappa$ B. Adapted from: Dolmatova, E. V., Wang, K., Mandavilli, R., & Griendling, K. K. (2021). The effects of sepsis on endothelium and clinical implications. *Cardiovascular research*, 117(1), 60–73. <https://doi.org/10.1093/cvr/cvaa070>. Created with biorender.com

## 1.6 ROS and RNS in sepsis

In order to eliminate invaders and in the course of the innate immune response, phagocytes such as macrophages and neutrophils release extensive quantities of ROS ( $O_2^-$  and  $H_2O_2$ ). As part of this process, the so called “respiratory burst”, NADPH-oxidases are the main source of ROS (Dahlgren and Karlsson, 1999). This process uses large amounts of oxygen (Baldridge and Gerard, 1932). Furthermore, ROS produced by the respiratory burst appear to exert also paracrine effects, by activating adjacent EC but also altering their function. In proper sequence, EC rise the intracellular ROS and RNS production. Beside the ROS production by NADPH-oxidases, ROS can be also produced by uncoupling of respiratory chain complexes of the mitochondria (Cepinskas and Wilson, 2008, Ince et al., 2016). Besides the increased nitric oxide (NO) production by the inducible NO-synthase (iNOS), various pathways contribute to ROS production and inflammation. NO stimulates not only the mitochondrial  $H_2O_2$  and  $O_2^-$  formation by inhibiting cytochrome-c oxidases (Poderoso et al., 1996),  $H_2O_2$  also induces the upregulation of iNOS in a NF- $\kappa$ B dependent manner (Han et al., 2001). Moreover, NO and  $H_2O_2$  react to form peroxynitrite and other RNS (Cuzzocrea et al., 2006, West et al., 2011). In addition, it is indicated that the mitochondrial complexes I and IV are vulnerable to RNS (Beltrán et al., 2000, Arulkumaran et al., 2016), which further impairs mitochondrial respiration (Boulos et al., 2003). Several animal models support the idea of an altered mitochondrial function in sepsis and septic shock. An impaired mitochondrial function was observed in the heart (Vanasco et al., 2014, Levy et al., 2004), liver (Lowe et al., 2013, Brealey et al., 2004) and intestine (Crouser et al., 1999, King et al., 1999). Moreover, in skeletal muscle biopsies of non-surviving septic patients compared to survivors and post-operative controls, a reduced mitochondrial complex I activity has been detected (Brealey et al., 2002). In platelets of septic patients an increased mitochondrial respiration has been observed (Sjövall et al., 2010, Sjövall et al., 2014). Due to uncoupling, the oxidative phosphorylation became less effective after all (Sjövall et al., 2014). As a result, increased mitochondrial respiration during the early phase of systemic inflammation has been correlated inversely with survival of these patients (Sjövall et al., 2010).

It is noteworthy, that ROS are not only antimicrobials (Babior, 2000), but also serve as powerful activators of the innate immune system (Arulkumaran et al., 2016, Zhou et al., 2011, Mao et al., 2013, Emre et al., 2007, Rousset et al., 2006, West et al., 2011b), considering that mitochondrial dysregulation in sepsis and septic shock might be part of the directed stress response in systemic inflammation. From this perspective, the metabolic switch from mitochondrial citrate cycle to cytosolic glycolysis may not only be the result of defective mitochondrial function but also a required action to allow mitochondrial uncoupling in order to strengthen the pathogen defense. Along these lines, besides to ROS and RNS production, hyperglycemic alterations in mitochondrial function are features of the legitimate stress response, eventually being dysregulated in sepsis and septic shock. Accordingly,

moderate levels of ROS have been shown to act as second messengers in signaling pathways and gene regulation, including nuclear factor 2 (Nrf2) and NF- $\kappa$ B, however elevated levels of ROS encourage apoptosis or even necrosis (Hensley et al., 2000, Lander, 1997, Genestra, 2007, Tonks, 2005, Aslan and Ozben, 2003, Schreck et al., 1991).

## 1.7 Endothelium and ROS/RNS in sepsis

As described before, activated immune cells deliver reactive molecules that are originally intended to fight germs but can also damage the affected tissue (Prauchner, 2017). Direct interaction of ROS and the endothelium leads to increased vascular permeability, worsening hypotension, and decreased colloid osmotic pressure of the plasma. Likewise, they affect tissue oxygen consumption and accelerate organ failure (Parihar et al., 2008). Current data clearly indicates that ROS damage the endothelial glycocalyx (Ince et al., 2016) and dramatically affect the endothelial barrier function, ultimately resulting in increased neutrophil recruitment and trafficking (Usatyuk et al., 2003). Whether *in vitro* or *in vivo*, the interaction of EC and ROS results in a remodeling of the cytoskeleton and upregulation of the adhesion molecules intercellular adhesion molecule 1 (ICAM-1), platelet and endothelial cell adhesion molecule 1 (PECAM-1), vascular cell adhesion molecule 1 (VCAM-1), and P-selectin, followed by increased neutrophil adhesion to the endothelium (Gaboury et al., 1994). There are several proposed mediators of the ROS induced increase in endothelial permeability, among other things, the activation of MAPK p38 (Usatyuk et al., 2003). ROS are also associated with the disruption of endothelial TJ proteins. H<sub>2</sub>O<sub>2</sub> e.g., reorganizes occludin on the cell surface, reducing its association with ZO-1 and thereby increasing endothelial permeability (Kevile et al., 2000). ROS can also be formed by EC themselves through the mitochondrial electron transport chain, nicotinamide adenine dinucleotide phosphate hydrogen oxidases (NOXs), uncoupled endothelial nitric oxide synthase (eNOS), and xanthine oxidase (Cai and Harrison, 2000). ROS induced signaling at physiological levels is fundamental for the maintenance of the vascular tone and also enables angiogenesis as well as acute inflammatory responses in defense of the invading pathogens (Craigie et al., 2015). Under pathological conditions such as sepsis, when the ROS response is overwhelming, it has been shown that reducing ROS production protects against sepsis-induced organ damage (Joseph et al., 2017, Fisher et al., 2020, Hernandez et al., 2014). As described before, NO is an endogenous vasodilator and antiproliferative agent and is produced in EC by eNOS (Vanhoutte, 1998). During sepsis some of the necessary cofactors for active eNOS are completely consumed by oxidation, uncoupling eNOS, generating superoxide anions and therefore reducing NO production (Ince et al., 2016). Contemporaneously, iNOS in immune cells and endothelium becomes activated, delivering large amounts of NO. NO and superoxide anions then react to form RNS, which in turn also contribute to endothelial dysfunction (McQuaid and Keenan,

1997). Both ROS and RNS appear to have cellular adverse effects through their role in protein and lipid oxidation and DNA damage. Regardless of the excessive ROS production during sepsis, the usefulness of ROS measurement in diagnosing sepsis and predicting mortality remains limited. In part, this can be attributed to the instability of ROS, which makes it difficult to measure them accurately in a clinical setting, as well as the relative non-specificity of the ROS response (Lopes-Pires et al., 2022).

## 1.8 Reactive Carbonyl Species (RCS)—Underdogs of reactive metabolites

ROS and RNS are extremely unstable compounds, and their harmful effects are narrowed to their place of origin and its immediate surroundings. Another group of highly reactive metabolites, RCS have been overlooked for years, although they interact with a large number of biomolecules (Lide, 2005). RCS are more stable but still highly reactive and represent a large heterogeneous group of low molecular carbonyls. They show the ability to react with proteins, deoxyribonucleic acid (DNA) or phospholipids, forming advanced glycation end-products (AGEs). These modifications include structural and functional changes resulting in dysfunction or complete inoperability of the initial protein (Ahmed and Thornalley, 2005, Dobler et al., 2006). These harmful effects are reminiscent of those of ROS, whereas RCS, in contrast, are far more stable and also have a systemic effect (Kalapos, 2008). One of the most important representatives of RCS with a clear pathophysiological relevance is methylglyoxal (MG). In multicellular organisms, MG mainly arises as a by-product during glycolysis and is formed by non-enzymatic degradation of triose phosphates, glyceraldehyde-3-phosphate (GAP) and dihydroxyacetone phosphate (DHAP) (Kalapos, 2008, Thornalley et al., 1999). Commonly only small amounts between 0.05 % to 0.1 % of the glycolytic flux are converted into MG (Veech et al., 1969), resulting in physiological concentrations of 50-150 nM in human plasma (Rabbani and Thornalley, 2014, Rabbani et al., 2016). Because there is a proportionality between MG production and glycolytic flux, it stands to reason that in diseases associated with increased glycolytic flux (such as diabetes mellitus or sepsis), elevated MG levels predominate. In addition, MG appears to be more than just a substitute for imbalanced glucose metabolism, since it is clearly associated with the occurrence of diabetic complications such as nephropathy and retinopathy (Beisswenger et al., 2003, Vander Jagt, 2008).

## 1.9 MG-derived carbonyl stress in sepsis

Until to date, the amount of data showing a direct association between human sepsis and MG is limited. Many studies at best create a bridge of ideas or are performed *in vitro* respectively *ex vivo*. For example, during sepsis eryptotic activity is elevated within the plasma and often results in eryptosis

hemolytic syndrome (Kempe et al., 2007). A study that was carried out at the same time found that MG impaired energy production and anti-oxidative defense of isolated circulating erythrocytes. Those effects contributed to an enhanced phosphatidyl serine exposure of those circulating erythrocytes and were found to result in anemia and deranged microcirculation (Nicolay et al., 2006). Like ROS, MG production appears to be a necessary defense mechanism against pathogens. Various *in vitro* studies report e.g. that macrophages infected with *Mycobacterium tuberculosis* (Zhang et al., 2016) had increased MG levels, as well as neutrophils infected with Group A *Streptococcus* (Rachman et al., 2006). Other studies demonstrated that bacteria also have the ability to produce MG and could also contribute to the carbonyl stress during bacterial sepsis and septic shock (Baskaran et al., 1989, Booth et al., 2003, Cooper, 1984, Ferguson et al., 1998). In some *Escherichia coli* (*E. coli*) strains, MG production allows them to adapt to carbon rich environments giving them time to adapt to adverse environmental conditions and to survive (Ferguson et al., 1998). In 2014, Brenner et al. made the first direct link between MG-induced carbonyl stress in critically ill patients. Septic patients showed significantly higher MG plasma levels in comparison to postoperative as well as healthy controls. In addition, MG outperformed the incumbent inflammation and infection markers such as procalcitonin (PCT), CRP, soluble CD14 subtype and IL-6, with a view to early and effective detection of sepsis in this study. Moreover, they identified MG as an independent predictor of mortality in sepsis (Brenner et al., 2014). It is still unexplored whether the elevated MG levels in sepsis come from endogenous or exogenous sources. However, the data situation now speaks more for the direction of endogenous carbonyl stress production in systemic inflammation. In addition to the increased MG levels in postoperative controls (Brenner et al., 2014), significantly increased MG levels could also be detected in patients following liver transplantation (Brenner et al., 2013) as well as in severely traumatized patients (Uhle et al., 2015). Both of these patient groups were clearly suffering from germ-free/sterile inflammation. In this context, a direct influence of MG on the dysregulated systemic inflammation seems no longer deniable. The phenomenon of metabolic tolerance has also been observed in a monocytic cell line as well as primary human monocytes, meaning that high levels of AGEs were capable to activate immune cells at first, but induced a secondary state of hypo-responsiveness in these cells (Uhle et al., 2017). Recent data described LPS administration *in vitro* as well as *in vivo* (murine model) to lead robustly to increased levels of MG-adducts and to polarize macrophages into a proinflammatory M1 phenotype. Furthermore, exogenous MG was able to block redox activities in mitochondria which was associated with membrane permeability and induced an increased C-X-C Motif Chemokine Ligand 1 (CXCL1) gene expression (Prantner et al., 2021). Driessen et al. investigated the effect of inflammation and hypoxia on the MG pathway in humans *in vivo* and found that glyoxalase-1 (GLO-1, the MG converting enzyme) expression was significantly downregulated in healthy males receiving LPS but was not influenced by hypoxia. Downregulation of GLO-1 could be a

possible mechanism leading to cell damage and multi-organ failure in sepsis (Driessen et al., 2021). As of today, it appears that MG does not have "just a singular" effect, but influences sepsis and septic shock in many ways. However, with regard to RCS and the endothelium in sepsis there is no data available despite from the following work.

### 1.10 Pathophysiology of MG-derived carbonyl stress in sepsis

Under physiological conditions, MG reacts with modified arginine, lysine and cysteine residues in proteins (Lo et al., 1994a), with arginine appearing to be most susceptible. Furthermore, MG can modify human albumin *in vivo*. In the majority of albumin modifications, arginine residues are most frequently modified, resulting in the formation of hydroimidazolone N-ornithine (Ahmed and Thornalley, 2005). This modified albumin can, inter alia, induce the synthesis and secretion of IL-1 (Westwood and Thornalley, 1996, Abordo et al., 1996). Simultaneously MG-modified arginine residues gain chemoattractant capabilities, provoking receptor-mediated endocytosis and degradation (Westwood et al., 1997). Over and beyond, MG-mediated oxidation leads to misfolding of enzymes, leading to proteolysis (Du et al., 2006). The interaction between RCS and DNA can result in further cell damage. This creates nucleotide-AGEs, which can lead to strand breaks and point mutations (Hoon et al., 2011).

The influence of carbonyl stress on mitochondria and its importance for ROS formation could be of great interest in the context of critical diseases. It is very likely that ROS, RNS and RCS constitute a self-sustaining system in which the factors stimulate each other (Kalapos, 2008, Wu, 2005). The fact that MG concentrations are significantly increased during hydrogen peroxide-induced necrotic cell death supports this theory (Abordo et al., 1999). Inhibition of the downstream glycolytic enzymes leads to an accumulation of GA3P and DHAP (Hyslop et al., 1988). Vice versa, decreased MG levels are observed to be associated with decreased ROS levels (Abordo et al., 1999, Yao and Brownlee, 2010). At the same time, RCS can severely impair mitochondrial function. Several studies described MG-derived carbonyl stress to be harmful to mitochondrial proteins (Morcos et al., 2008), to increase ROS levels and to induce apoptosis via the mitochondrial pathway (Chan et al., 2007) as well as to significantly increase the permeability of the mitochondrial membrane (Seo et al., 2014). Summarized, MG-derived carbonyl stress can not only affect the effector functions of immune cells under infection but also affect basic metabolic pathways such as glycolysis and mitochondrial respiration. Consequently, it could have an impact on the development of sepsis-induced MODS.

### 1.11 Regulation of MG-derived carbonyl stress in sepsis

In healthy individuals, MG is normally detoxified via the glyoxalase system. This includes the enzymes GLO-1 and glyoxalase-2 (GLO-2) (Brownlee, 2001, Thornalley et al., 2003), metabolizing MG into D-lactate by using NADPH and glutathione (GSH) (Thornalley et al., 2003, Lohmann, 1932). As described by Driessen et al. 2021, this way of MG detoxification seems to be severely disrupted during critical illness (Driessen et al., 2021). As already known, systematic inflammation produces large amounts of ROS, which must be rendered harmless, but these detoxification mechanisms also require larger amounts of GSH (Rabbani and Thornalley, 2008). This high consumption of GSH thus also influences the glyoxalase pathway. Furthermore, it is known that "hyperoxide" (a ROS) can directly inhibit GLO-1 (Kanwar and Kowluru, 2009). This is in line with the findings that critically ill patients show increased levels of both ROS and RCS, which is paralleled by an impaired GLO-1 expression in patients with septic shock (Brenner et al., 2014). It was suggested that the downregulation of GLO-1 is receptor AGE (RAGE)-dependent (Bierhaus et al., 1997, Bierhaus et al., 2006, Lander et al., 1997, Thornalley, 1998). In both patients with septic shock (Hofer et al., 2016) and patients following severe trauma (Uhle et al., 2015) monocytes exhibited an elevated RAGE expression and increased plasma levels of soluble RAGE (sRAGE). Consistent with these results and increased AGE formation by MG, a regulatory cycle can be mapped. This includes the MG-AGE-RAGE-GLO-1-MG axis leading to the formation of ROS, RNS and RCS during systemic inflammation.

### 1.12 What we know from Diabetes mellitus and other AGE-related diseases

Results from experimental and preclinical research show with unequivocal certainty that increased MG formation in hyperglycemia contributes to the development of vascular complications. MG is associated not only with diabetic hyperglycemia but also with other risk factors for diabetic vascular difficulties such as dyslipidemia, hypertension, and obesity. Furthermore, there is increasing evidence that MG also alters insulin resistance (Mey and Haus, 2018). Incidentally, MG is directly associated with insulin resistance due to MG interference with the complex molecular signaling pathways of insulin in muscle cells (Riboulet-Chavey et al., 2006), EC (Nigro et al., 2014), and beta cells (Fiory et al., 2011). Therefore, MG reflects the hyperglycemic flux, and can also encourage insulin resistance and beta cell dysfunction by itself, thus predisposing to type 2 Diabetes mellitus (T2D) (Moraru et al., 2018). Since glycolysis is also increased during inflammation and hypoxia, these conditions may also contribute to MG formation. In addition, the expression as well as the activity of GLO-1 are impaired under these conditions, which can also contribute to the increased MG levels (Haik et al., 1994). This fact clarifies why MG is related with many other age-related chronic inflammatory diseases, such as atherosclerosis,

hypertension, cancer, and disorders of the central nervous system (Maessen et al., 2015, Schalkwijk, 2015).

### 1.12.1 Diabetes mellitus

After discovering that high glucose concentrations result in MG formation (Schalkwijk et al., 2004, Schalkwijk et al., 2006, Shinohara et al., 1998, Thornalley, 1988) and that both type 1 and type 2 Diabetes mellitus (T1D, T2D) patients suffer from higher plasma levels of MG and AGEs (Beisswenger et al., 1999, van Eupen et al., 2013) subsequent studies have highlighted the relevance of MG in diabetes-associated complications, especially in the vessels. E.g. Diabetes-related endothelial dysfunction represents an initial factor in the pathogenesis of diabetic micro- and macroangiopathy (Rohlenova et al., 2018, Schalkwijk and Stehouwer, 2005) and is outlined by increased levels of oxidative stress and inflammation as well as alterations in vasoregulation and barrier function of the endothelium (Eringa et al., 2013, Schalkwijk and Stehouwer, 2005). It is hypothesized that four independent biochemical pathways in endothelial cells are overactivated in hyperglycemia by an intracellular excess of glucose flux. These pathways are thought to be linked by a single upstream event, namely the mitochondrial overproduction of ROS (Giacco et al., 2013). Several experimental models demonstrate the importance of MG for endothelial dysfunction in diabetes. Administration of MG in animal models results in diabetes-like microvascular changes, including impaired vasodilation (Berlanga et al., 2005, Sena et al., 2012), degenerative changes in microvasculature with loss of endothelial cells, thickening of the basement membrane (Berlanga et al., 2005), and increased oxidative stress (Sena et al., 2012). Higher MG plasma levels in the kidney contribute to the development of diabetic nephropathy (Hanssen et al., 2019, Rabbani and Thornalley, 2018) and are associated with an increased incidence of chronic kidney disease (Beisswenger et al., 2005, Lu et al., 2011, Nakayama et al., 2008) and an increased risk of lower estimated glomerular filtration rate (eGFR) and albuminuria in T1D and T2D (Hanssen et al., 2017, Hanssen et al., 2018, Jensen et al., 2016). However, the most common microvascular complication in diabetes is retinopathy (Yau et al., 2012) with the greatest risk factor for its development being chronic hyperglycemia (Stitt et al., 2016). It is postulated that increased MG levels in the eyes impair the regulation of retinal blood flow and thus contribute to diabetic retinopathy or alter the blood-retinal barrier (Díaz-Coránguez et al., 2017). In the rat model, the injection of MG into the eye leads to a hyperpermeability of the blood-retinal barrier via the loss of TJ proteins and the activation of matrix metalloproteinases (Hanssen et al., 2014a). Studies using RAGE<sup>-/-</sup> mice showed that they accumulated less MG in their retinas and that activation of GLO-1 protected them against microglial activation and vasoregression (McVicar et al., 2015), underlining the role of MG in the pathogenesis of diabetic retinopathy. Despite the large number of



studies in diabetic animal models and humans that show that glycation plays a key role in the formation of diabetic neuropathy (Cullum et al., 1991, Ryle and Donaghy, 1995, Sugimoto et al., 2008, Vlassara et al., 1983) only a handful specifically focus on the importance of MG and GLO-1. Due to its high energy requirements, neuronal tissue absorbs large amounts of glucose independently of insulin. Therefore, neuronal tissue and cells are at high risk for MG accumulation (Thornalley et al., 2003). This has already been identified as a risk factor for the development of polyneuropathy in T2D patients (Anderson et al., 2018). Furthermore, MG activates p38 MAPK in Schwann cells, which ultimately leads to apoptosis (Fukunaga et al., 2004). Pathophysiological MG plasma concentrations lead to depolarization of sensory neurons and cause post-translational modifications that increase blood flow in brain regions involved in pain processing (Bierhaus et al., 2012).

### 1.12.2 Atherosclerosis

MG seems to play a major role in the development of atherosclerosis (Hanssen et al., 2014b). Elevated plasma MG levels are associated with cardiovascular diseases (CVD), myocardial infarction and lower extremity amputation (Hanssen et al., 2020), all-cause (CVD) mortality in diabetic patients, as well as thickening of the intima media (Ogawa et al., 2010). These studies confirm previous assumptions that plasma concentrations of certain MG-adducts are associated with the occurrence of CVD in diabetes (Hanssen et al., 2015, Nin et al., 2011). Activation of the endothelium and the expression of adhesion molecules are the essential reason for atherosclerosis and MG is directly linked to diabetes-induced activation of endothelial cells (Brouwers et al., 2010, Brouwers et al., 2011, Brouwers et al., 2013, Brouwers et al., 2014, Mäkinen et al., 2014, Stratmann et al., 2016). The protein content of low-density-lipoprotein (LDL) is a target for MG modification in atherosclerosis and changes both the physiochemical and biological properties of LDL (Brown et al., 2005, Rabbani et al., 2011, Turk et al., 2011) as well as the formation of methylglyoxal-derived hydroimidazolones (MG-H1) and atherogenic LDL particles (Rabbani et al., 2010, Rabbani et al., 2011). MG modification of high-density-lipoprotein (HDL) forwards its degradation, impairs functionality and could be in part responsible for diabetic CVD. It is important to note that MG is also involved in non-diabetic atherosclerosis (Brownlee, 2001). MG-AGEs can be found in atherosclerotic plaques and are associated with rupture-prone phenotypes of diabetic as well as non-diabetic plaques (Ghirlanda et al., 1997, Schalkwijk and Miyata, 2012).

### 1.12.3 Hypertension

Some studies report that AGE-RAGE interaction is involved in the pathophysiology of hypertension by stiffness by cross-linking of collagen in the arterial media leading to an increased arterial stiffness and by functional changes of the vascular cells (Prasad and Mishra, 2017). MG might be involved in the

pathophysiology of hypertension by structural and functional alterations of the arteries. *In vitro* experiments revealed that MG was able to induce the described cross-linking of type 1 collagen. This led to changes in physical properties, including a physiologically relevant reduced viscoelasticity (Fessel et al., 2014, Gautieri et al., 2017, Lederer and Klaiber, 1999, Li et al., 2013, Stehouwer et al., 1992).

#### 1.12.4 Cancer

Cancer is portrayed by proliferation and uncontrolled growth of abnormal cells. Because of oxygen deficiency, tumor cells depend on the “Warburg effect”. In compensation for the insufficient energy supply, tumor cells exert a higher glycolysis rate and take up higher amounts of glucose, consequently forming intracellular MG (Bellahcène et al., 2018). Cancer cells with high glycolytic rates therefore require a high detoxification capacity for MG, and high expression of GLO-1. This is a reasonable survival and growth mechanism for tumors with high glycolytic fluxes and an increased formation of MG. Truly, an association between high GLO-1 expression and tumor progression in numerous cancer types including colorectal cancer (Sakellariou et al., 2016) and gastric cancer (Hosoda et al., 2015) has been reported and the reduction of intracellular MG by increased GLO-1 expression is probably an explanation for the survival promoting effects. Through ROS generation and GSH depletion (Amicarelli et al., 2003), inhibition of cellular respiration (Ghosh et al., 2011), DNA modification and DNA-protein cross-link resulting in DNA instability (Jandial et al., 2018, Tamae et al., 2011, Wuenschell et al., 2010), MG can induce apoptosis in cancerous cells.

#### 1.13 Therapeutic options to limit MG

Several strategic therapeutic approaches to lower MG have been developed over the years, however none of these applications could be transferred into clinical routine.

##### 1.13.1 Aminoguanidine

Aminoguanidine (AG) is a derivative of the organic base guanidine and a strong scavenging agent of MG because of its dicarbonyl-directing guanidine group (Brings et al., 2017, Brownlee et al., 1986, Lo et al., 1994b). In animal models of diabetes, AG has been effective in lowering AGE formation and prevented nephropathy (Soulis-Liparota et al., 1991, Soulis et al., 1996), retinopathy (Hammes et al., 1991), and neuropathy (Kihara et al., 1991). In two large clinical trials with T1D (Bolton et al., 2004) and T2D (Freedman et al., 1999) patients, however, AG did not show convincing results. In T1D, the goal to decrease the doubling time of serum creatinine was unfortunately missed and the study in T2D patients was prematurely stopped because of ineffectiveness and safety concerns about gastrointestinal disturbance, lupus-like illness, abnormal liver function, flu-like symptoms, and

vasculitis. The further assessment of aminoguanidine in humans was discontinued due to an unfavorable perceived benefit-risk ratio (Löbner et al., 2015).

### 1.13.2 N-Acetylcysteine

N-Acetylcysteine (NAC, obsolete mercapturic acid) is a derivative of the naturally occurring amino acid cysteine and a potent antioxidant, found in several dietary supplements. It can induce protein phosphatase and reduce GSH, neutralizing MG to nonreactive and non-toxic forms such as hemithioacetal, s-lactoyl-GSH, and D-lactate (Dhar et al., 2010, Allaman et al., 2015, Mokhtari et al., 2017, Echeverri-Ruiz et al., 2018, Jo, 2011). In *in vitro* experiments NAC inhibited the MG-induced AGE/RAGE expression in keratinocytes (Yang et al., 2017) and improved the MG-induced neurotoxicity in hippocampal neurons (Zhou et al., 2009). Although NAC is a familiar substance, its long-term use is limited through negative side effects like vomiting, rash, and high fever (Schmidt and Dalhoff, 2001).

### 1.13.3 L-carnosine

L-carnosine (Cns, beta-alanyl-L-histidine) is a naturally occurring dipeptide with MG-scavenging activities (Colzani et al., 2016, Vistoli et al., 2017). In rodent models of metabolic syndrome and cardiovascular disease the benefit of Cns as a potential pharmacological agent could be highlighted (Aldini et al., 2011, Barski et al., 2008). In an interventional study of overweight and obese individuals, subjects received a daily dose of L-carnosine. This dose could prevent insulin sensitivity and secretion and normalized glucose tolerance compared to the placebo group (de Courten et al., 2016). Due to rapid hydrolysis of the peptide by carnosinases, the therapeutic potential of Cns in humans is limited (Anderson et al., 2018).

### 1.13.4 L-Anserine

Anserine (Ans,  $\beta$ -alanyl-3-methylhistidine) is a dipeptide (Garrett RH, 2012) and a methylated derivative of Cns. It is found in the skeletal muscle and brain of mammals and birds (Blancquaert et al., 2016) and can also be found in high levels within human kidneys (Peters et al., 2018). Both Ans and Cns show copper chelating capacities (Kohen et al., 1988). Cns as well as Ans can be digested by carnosinase 1 (CN1, EC 3.4.13.20) and at a high pH by carnosinase 2 (CN2, EC 3.4.13.18) (Teufel et al., 2003). Serum CN1 has a higher activity for Cns compared to Ans (Peters et al., 2011). Ans is more stable in serum and resistant to degradation than Cns due to its methylation (Everaert et al., 2019). When contained in Ans, the acid constant of the imidazole ring of histidine is 7.04, which makes it an effective buffer at physiological pH (Wu, 2020, Kaneko et al., 2017). The positive effects of Ans on cell and organ function

have been described in several publications (Vistoli et al., 2016, Hobart et al., 2004). The fact that Ans delays and (in one case) reverses non-enzymatic glycation is here of special interest. Cns and Ans can serve as alternative and competing glycation targets, thereby protecting proteins from modulation. Another mechanism by which these two peptides can retard, or reverse glycation involves the decomposition of the very first intermediates of the non-enzymatic glycation by nucleophilic attack of Cns and/or Ans on the preformed aldosamine such as glucosyl-lysine (Szwergold, 2005). *In vitro*, as little as 5 mM Ans is sufficient to significantly reduce the glycation of human serum albumin by 25 mM glucose, measured as free lysine residues (Lee, 1999). In neuronal cells the anti-radical capacity for Ans was shown to be higher than Cns (Boldyrev et al., 2004). By activating the intracellular defense system under oxidative stress Ans, but not Cns has been observed to play an important role, by activating heat shock protein (Hsp) expression. Hsps have multiple cell protective effects like cellular repair, interaction with cytoskeletal structures, protein transport and cleavage (Beck et al., 2000, Chebotareva et al., 2017) and post-inflammatory processes (Bellia et al., 2011). In line with that, Ans upregulated Hsp70 expression under conditions of oxidative and glycating stress in tubular cells in a T2D mouse model, and reduced blood glucose levels, vascular permeability, and proteinuria (Peters et al., 2018). Under glucose stress, Ans also increased the concentration of heme oxygenase-1 (HO-1), an enzyme mediating cyto- and tissue protective processes against a broad spectrum of injurious insults (Ryter et al., 2006). Due to the 200-fold lower degradation rate of CN1 for Ans, Ans appears to be a promising therapeutic tool for humans (Peters et al., 2011). To date, there is no data available elucidating the potential protective effects of Ans in sepsis and septic shock in relation to carbonyl stress.

### 1.14 Aim of the study

The aim of the here presented project was to investigate to what extent and via which mechanism the MG-related carbonyl stress contributes to the occurrence and progression of septic multi-organ failure, which is closely associated with a disturbed endothelial barrier function. In this context, it seems quite plausible to first investigate the influence of MG-induced carbonyl stress on the endothelium, since this must be considered to be directly exposed to MG through its direct contact with the bloodstream. In addition to increased radical formation as part of the MG metabolism, MG also promotes oxidative stress directly by increasing the activity of prooxidative enzymes such as p38 MAPK (Akhand et al., 2001, Ward and McLeish, 2004) and N-terminal c-Jun kinases (JNKs) (Amicarelli et al., 2003). These in turn play a central role in regulating TJ permeability and regulating the barrier function (Xiong et al., 2020), which has been shown both *in vitro* (Wang et al., 2019) and *in vivo* (Meir et al., 2019). In the context of sepsis, classic inflammatory mediators such as TNF or LPS were able to induce TJ dysregulation by upregulating MAPK expression (Borgonetti et al., 2022, Petecchia et al., 2012). It has

also been described for the proinflammatory RAGE pathway that receptor binding by AGEs on the endothelial cell surface also leads to an induction of MAPK kinases (Goldin et al., 2006). This is of interest since MG leads to relevant AGE formation via glycation of proteins (Waqas et al., 2022). However, it is not yet known to what extent MG, via a RAGE-dependent mechanism, is able to impair the endothelial barrier function in sepsis in the sense of a capillary leak and thus induces or maintains the full picture of septic shock. To test this hypothesis on the morphological and functional cell level (*in vitro*), primary endothelial cells were analyzed under sepsis-like conditions and the modulation of systemic disease severity was examined in the murine sepsis model of cecal ligation and puncture. For the development of a possible therapeutic approach, a close cooperation with MG-associated diabetes researchers was established (SFB 1118, Reactive metabolites as a cause of diabetic consequential damage, sub-project C05, Prof. (apl.) Dr. rer. nat. Verena Peters and Prof. (apl.) Dr. med. Claus Peter Schmitt). To answer the question to what extent a limitation of MG-related carbonyl stress is able to reverse endothelial MG damage and thus have a positive impact on the course of sepsis, the dipeptide Ans was examined as a therapeutic agent.

## 2. Material and Methods

### 2.1 Materials

#### 2.1.1 Devices

Centrifuge <i>Multifuge 3 S-R</i>	Heraeus Hanau, DE
Centrifuge <i>Micro 200R</i>	Hettich Tuttlingen, DE
Coverslips	VWR International GmbH Darmstadt, DE
Freezing container <i>Mr. Frosty™</i>	ThermoFisher Scientific Inc. Waltham, USA
Heat block <i>Thermomixer compact</i>	Heraeus Hanau, DE
Incubator <i>HeraCell</i>	Heraeus Hanau, DE
Light microscope <i>Axiovert25</i>	Zeiss Oberkochen, DE
<i>Milli-Q® Reference Water Purification System</i>	Merck Darmstadt, DE
Microplate Spectrophotometer <i>Epoch 2</i>	BioTek Bad Friedrichshall, DE
<i>Invitrogen™ XCell SureLock™ Mini-Cell</i>	ThermoFisher Scientific Inc. Waltham, USA
Neubauer improved cell counting chamber	neoLab Migge GmbH Heidelberg, DE
Peleus ball	VWR International GmbH Darmstadt, DE
pH meter <i>ph 211</i>	HANNA instruments Voehringen, DE
Pipets 10 µl, 100 µl, 1000 µl	Eppendorf Hamburg, DE
Pipetting aid	Eppendorf Hamburg, DE
High performance liquid chromatography (HPLC)-Column	Jupiter® 5 µm C18 300Å, LC Column 250 × 4.6 mm, Phenomenex (Aschaffenburg, DE)
Scale <i>Kern EG4200-2NM</i>	Kern & Sohn GmbH Balingen, DE
Shaker <i>Rotamax120</i>	Heidolph Schwabach, DE
<i>Chemiluminescence imaging systems, Fusion FX7</i>	Vilber Collégien, FR
Multi-function printer and scanner <i>CX923dte</i>	Lexmark Lexington, USA
Sterile bench <i>HeraSafe</i>	Heraeus Hanau, DE
Vortex Mixer <i>72020</i>	neoLab Migge GmbH Heidelberg, DE

Water bath 3048	Koettermann GmbH Uetze, DE
Tecan Infinite F200 Fluorescence Microplate Reader	Tecan Group AG Männedorf, CH
Acquifer Imaging Machine	ACQUIFER Imaging Heidelberg, DE
Tecan Spark® Multimode Microplate Reader	Tecan Group AG Männedorf, CH
Fluorescence activated cell sorting (FACS) lyric	BD Franklin Lakes, USA

### 2.1.2 Consumables

Pipet tips 10 µl, 100 µl, 1000 µl <i>Axygen Scientific Maximum Recovery</i>	Corning Corning, USA
Gloves <i>TouchNTuff</i>	Ansell Richmond, AUS
Reaction tubes 0.5 ml, 1.5 ml, 2 ml	Sarstedt Nuernbrecht, DE
Reaction tubes 15 ml, 50 ml <i>CELLSTAR®</i>	Greiner Bio One International GmbH Frickenhausen, DE
Laboratory towels <i>TORK Wash Cloth</i>	SCA Goeteborg, SWE
Cryo tubes 2 ml <i>Cryo.s™</i>	Greiner Bio One International GmbH Frickenhausen, DE
Serological pipets 5 ml, 10 ml, 25 ml <i>CELLSTAR®</i>	Greiner Bio One International GmbH Frickenhausen, DE
Filter top T75 cell culture flask <i>CELLSTAR®</i>	Greiner Bio One International GmbH Frickenhausen, DE
24-well plate, adherent <i>CELLSTAR®</i>	Greiner Bio One International GmbH Frickenhausen, DE
24-well plate, adherent <i>CELLSTAR®</i>	Greiner Bio One International GmbH Frickenhausen, DE
96-well plate, adherent <i>CELLSTAR®</i>	Greiner Bio One International GmbH Frickenhausen, DE
Cell scraper, rotatable, 13 mm	TPP Techno Plastic Products AG Trasadingen, CH
Round-Bottom Polystyrene Tubes, Disposable, Falcon® 5ml	Corning Corning, USA
Transwell plates Costar 0.4 µm pore size, polyester, 24 well and 6 well	Corning Corning, USA

### 2.1.3 ELISA, Activity Assays and Kits

Target	Catalogue number	Company
Caspase-Glo® 1 Inflammasome Assay	G9951	Promega Madison, USA
Human pro IL-1beta ELISA Kit	HUF102788	Assay Genie Dublin, Ireland
Human MMP-1 ELISA Kit	RAB0361-1KT	Sigma- Aldrich St. Louis, USA

Human MMP-2 ELISA Kit	RAB0365-1KT	Sigma- Aldrich St. Louis, USA
Human MMP-9 ELISA Kit	RAB0372-1KT	Sigma- Aldrich St. Louis, USA
Micro BCA™ Protein-Assay-Kit	23235	Thermo Fisher Scientific Waltham, USA
Human Active MMP-1 Fluorokine E Kit	F1M00	R & D Systems Minneapolis, USA
Pierce lactatedehydrogenase (LDH) Cytotoxicity Assay Kit	88953	Thermo Fisher Scientific Waltham, USA
Human Cytokine Array C3 and C7	AAH-CYT-3-2 AAH-CYT-7-2	RayBiotech Life Peachtree Corners, USA

#### 2.1.4 Antibodies and dyes

Target	Catalogue number	Company
Anti-ZO-1 ZO-1 Monoclonal Antibody (ZO1-1A12), Alexa Fluor™ 647	MA3-39100-A647	Thermo Fisher Scientific Waltham, USA
PE Mouse anti-NF-κB p65 (pS529)	558423	BD Franklin Lakes, USA
Claudin 5 Monoclonal Antibody (4C3C2), Alexa Fluor™ 488, Invitrogen™	ab131259	Thermo Fisher Scientific Waltham, USA
Phospho-c-Jun (Ser73) (D47G9) XP® Rabbit mAb (PE Conjugate)	#8752	Cell Signaling Technology Danvers, USA
Phospho-Akt (Ser473) (D9E) XP® Rabbit mAb (Alexa Fluor® 647 Conjugate)	#4075	Cell Signaling Technology Danvers, USA
Phospho-p38 MAPK (Thr180/Tyr182) (28B10) Mouse mAb (Alexa Fluor® 488 Conjugate)	#4551	Cell Signaling Technology Danvers, USA
Phospho-IRF-3 (Ser386) (E7J8G) XP® Rabbit mAb (Alexa Fluor® 647 Conjugate)	#96421	Cell Signaling Technology Danvers, USA
Anti-AGE Rabbit pAb	ab23722	abcam Cambridge, UK
4',6-diamidino-2-phenylindol (DAPI)	D9542	Sigma- Aldrich St. Louis, USA

#### 2.1.5 Reagents for Immunofluorescence and Immunohistochemistry

100 % Ethanol (EtOH)	Thermo Fisher Scientific Waltham, USA
Gibco™ Dulbecco's phosphate-buffered saline (DPBS) w/o Ca2+ and Mg2+	Thermo Fisher Scientific Waltham, USA
Triton X-100	Sigma- Aldrich St. Louis, USA
Albumin Fraction V, protease-free, (bovine serum albumin, BSA) Europe	Carl Roth Karlsruhe, DE



Paraformaldehyde (PFA), 4% w/v aq. soln., methanol free	Thermo Fisher Scientific Waltham, USA
Dako Antibody Diluent with Background Reducing Components	Agilent Santa Clara, USA
Dako Liquid 3,3'-diaminobenzidine (DAB) + Chromogen	Agilent Santa Clara, USA
Dako Liquid DAB+ Substrate Buffer	Agilent Santa Clara, USA
Dako REAL™ Peroxidase-Blocking Solution	Agilent Santa Clara, USA
Dako Target Retrieval solution	Agilent Santa Clara, USA
Gibco™ DPBS w/o Ca <sup>2+</sup> and Mg <sup>2+</sup>	Thermo Fisher Scientific Waltham, USA
96 % Ethanol	Thermo Fisher Scientific Waltham, USA
70 % Ethanol	Thermo Fisher Scientific Waltham, USA
xylene	Sigma- Aldrich St. Louis, USA
ProLong™ Gold Antifade Mountant	Thermo Fisher Scientific Waltham, USA
Ammonium chloride	Thermo Fisher Scientific Waltham, USA

#### 2.1.6 Reagents for cell culture

Reagent	Company
Dimethyl sulfoxide (DMSO)	Sigma-Aldrich, St. Louis, USA
40 % Methylglyoxal	Sigma-Aldrich, St. Louis, USA
LPS ultrapure	InvivoGen San Diego, USA
L-Anserine	AKScientific, Inc Union City, USA
L-Carnosine	Sigma-Aldrich, St. Louis, USA
rhTNFa	PeproTech, Inc. Rocky Hill, USA
N-Acetylcysteine	Sigma-Aldrich, St. Louis, USA
Aminoguanidine	Sigma-Aldrich, St. Louis, USA
Fluorescein isothiocyanate (FITC)-Dextran (4, 10, 70 kDa)	Sigma-Aldrich St. Louis, USA
Dextran (4, 10, 70 kDa)	Sigma-Aldrich, St. Louis, USA

Fetal calve serum (FCS)	Cell concepts Umkirch, DE
Ethylenediaminetetraacetic acid (EDTA)-Trypsin	Cell concepts Umkirch, DE
Gibco™ Penicillin-Streptomycin	Thermo Fisher Scientific Waltham, USA
RAGE-Antagonist FPS-ZM1	Sigma- Aldrich St. Louis, USA
MMP Inhibitor I, CAS 124168-73-6	Sigma- Aldrich St. Louis, USA
MMP-2/MMP-9-Inhibitor I - CAS 193807-58-8	Sigma- Aldrich St. Louis, USA
Trypan blue 0.4 %	Sigma- Aldrich St. Louis, USA
Gibco™ DPBS w/o Ca <sup>2+</sup> and Mg <sup>2+</sup>	Thermo Fisher Scientific Waltham, USA

Media		Company
<i>Endothelial Cell Growth Medium Kit</i> FCS (0.02 ml/ml) Endothelial Cell Growth Supplement (0.004 ml/ml) Epidermal Growth Factor (recombinant human) (0.1 ng/ml) Basic Fibroblast Growth Factor (recombinant human) (1 ng/ml) Heparin (90 µg/ml) Hydrocortisone (1 µg/ml) 1 % Penicillin-Streptomycin	C-22010	PromoCell - Heidelberg, DE
<i>Stop Medium</i> Gibco™ DPBS w/o Ca <sup>2+</sup> and Mg <sup>2+</sup> 10 % FCS		
<i>Cryo Medium</i> 50 % Endothelial Cell Growth Medium 40 % FCS 10 % DMSO		

### 2.1.7 Reagents and chemicals for HPLC

Radio-Immunoprecipitation Assay (RIPA) buffer	Thermo Fisher Scientific Waltham, USA
sulfosalicylic acid 99 %	Sigma- Aldrich St. Louis, USA
borate buffer 0.4 M	Agilent
carbazole-9-carbonyl chloride	Sigma- Aldrich St. Louis, USA
hydroxylamine	Sigma- Aldrich St. Louis, USA
hydroxylamine hydrochloride	Sigma- Aldrich St. Louis, USA
sodium hydroxide	Carl Roth Karlsruhe, DE

methanol	Carl Roth Karlsruhe, DE
acetonitrile	Sigma- Aldrich St. Louis, USA
acetic acid	Sigma- Aldrich St. Louis, USA
Acetate buffer <i>Solution 1: Acetic acid 50 mM</i> <i>Solution 2: Sodium acetate 80 mM</i> Mix 2:1, pH 4.37	
<i>buffer A</i> 820 ml 50 mM Na-Acetate buffer 180 ml <i>buffer B</i>	
<i>buffer B</i> 70 % (v/v) Acetonitrile 25 % (v/v) Methanol 5 % (v/v) Tetrahydrofuran	
Tetrahydrofuran	Sigma- Aldrich St. Louis, USA
Sodium acetate	Sigma- Aldrich St. Louis, USA

#### 2.1.8 Reagents and chemicals for FACS

PFA, 4 % w/v aq. soln., methanol free	Thermo Fisher Scientific Waltham, USA
Gibco™ DPBS w/o Ca <sup>2+</sup> and Mg <sup>2+</sup>	Thermo Fisher Scientific Waltham, USA
Albumin Fraction V, bovine serum albumin (BSA), protease-free, Europe	Carl Roth Karlsruhe, DE
methanol	Carl Roth Karlsruhe, DE
Iso buffer 2 mM EDTA 0.5 % BSA In DPBS 1x	

#### 2.1.9 Reagents and chemicals for Zymography

Novex Tris-Glycine SDS-sample buffer	LC2676	Thermo Fisher Scientific Waltham, USA
Novex Tris-Glycine SDS-running buffer	LC2675	Thermo Fisher Scientific Waltham, USA
Novex Zymogram Renaturing buffer	LC2670	Thermo Fisher Scientific Waltham, USA
Novex Zymogram development buffer	LC2671	Thermo Fisher Scientific Waltham, USA
Invitrogen™ Colloidal Blue Staining Kit	LC6025	Thermo Fisher Scientific Waltham, USA
Novex™ 10% Zymogram Plus (Gelatin) Protein Gels, 1.0 mm, 12-well	ZY00102BOX	Thermo Fisher Scientific Waltham, USA

### 2.1.10 Animals, drugs, and reagents for animal experiment

<b>Product</b>		<b>Company</b>
C57/BL6	9-12 weeks	Charles River
Xylazine	20 mg/ml	Euridco BV Heesch, NL
Ketamine	Ketanest S 25 mg/ml	Pfizer NY, USA
Buprenorphine	Buprenovet sine 0.3 mg/ml	Bayer Vital GmbH Leverkusen, DE
Bepanthen	Eye and nose ointment	Hoffmann-La Roche Basel, CH
Skin antiseptic	Octeniderm	Schülke & Mayr Norderstedt, DE
Sodium chloride (NaCl)	0.9 %	B. Braun Melsungen Melsungen, DE
Surgical cutlery		
Rhodent electric razor <i>Isis</i>		Aesculap Melsungen, DE
Seam material <i>Prolene monofil blue 6-0, with needle, P 3 Prime</i> <i>Ethicon Vicryl Plus violet, with needle, absorbable 6-0</i>		Ethicon, Inc. Somerville, USA
Evans blue	A16774-18	Thermo Fisher Scientific Waltham, USA
PFA, 4 % w/v aq. soln., methanol free		Thermo Fisher Scientific Waltham, USA
Formamide		Thermo Fisher Scientific Waltham, USA
L-Anserin		AK Scientific, Inc Union City, USA
Sterile syringes 1-20 ml		BD Franklin Lakes, USA
Gauge needles 27G, 23G, 20G <i>Sterican®</i>		B. Braun Melsungen, DE

### 2.1.11 Software

Aperio ImageScope v.12.4	Leica Wetzlar, DE
Fiji (ImageJ)	National Institutes of Health (Schindelin et al., 2012)
GraphPad Prism 9	GraphPad Software San Diego, USA
Microsoft Office Home and Student 2021	Microsoft Redmond, USA
BD FACS suite	BD Franklin Lakes, USA

## 2.2 Methods

### 2.2.1 Mouse model

All animal experiments were carried out in accordance with the guidelines and with the approval of the Animal Care and Use Committee at the Regierungspräsidium Karlsruhe (AZ 35-9185.81/G-72/18). All mice were maintained in a pathogen-free environment and housed in clear shoebox cages in groups of three animals per cage with constant temperature (20-22 °C) and humidity and 12 h:12 h light-dark cycle, within a specialized facility for interfaculty biomedical research at Heidelberg University. All animals always had access to water and were fed *ad libitum*. All experiments were performed in adult female mice (9-12 weeks of age).

### The cecal ligation and puncture (CLP)

The CLP septic mouse model was performed as described previously (Toscano et al., 2011). Anesthesia for CLP was performed by intra peritoneal (i.p.) injection of ketamine (100 mg/kg body weight (bw))/xylazine (3 mg/kg bw) in 0.9 % saline. During anesthesia eye ointment was used to prevent drying of and damage to the cornea. In brief, the cecum of female mice (C57BL/6) was exposed through a 1.0– 1.5 cm abdominal midline incision and subjected to a ligation 7 mm apart from the cecal tip followed by a single puncture with a 23-gauge needle. A small amount of feces was expelled from the puncture to ensure patency. The cecum was replaced into the peritoneal cavity, into which a 0.9 % NaCl bolus is given, and the abdominal incision was closed layer by layer (Toscano et al. 2011). Mice were either observed over a time course of seven days or sacrificed after 6 h, 24 h and 36 h. All surgical interventions were performed on 37.5 °C heat plates. The first 36 h after surgery the cages were kept on the heat plates.

### Intraperitoneal (i.p.) administration of drugs

Ans (300 mg/ml in 0.9 % NaCl) was used as pretreatment (before CLP) in a dose of 1.500 mg/kg bw every 12 h for 3 days (72 h). Starting from wound closure, Ans was used as posttreatment (after CLP) in a dose of 1.500 mg/kg bw every 8 h for a maximum 2 days (48 h). The control animals received the same volume of 0.9 % NaCl as vehicle.

### Intravenous (i.v.) Evans Blue Injection

200 µl of 1 % sterile Evans blue (EB) solution in 0.9 % NaCl was slowly injected into the tail vein of the mouse. The mouse was put back into its cage and was observed for 15 min. Mice were anesthetized

and sacrificed through final blood collection. The organs (lung, heart, kidney, small intestine, colon) were harvested and further analyzed (Radu and Chernoff, 2013) .

Further processing of organs

One part of the organs was used for the EB extraction and quantification, one part was fixed in 4 % PFA and the remaining part was snap frozen in liquid nitrogen and kept in -80 °C. Parts of those cryo samples were used for the detection of Ans.

Preparation of organ samples for staining

The organs were kept for 40 h in 4 % PFA, were watered for a minimum of 2 h and dried with a tissue. In an embedding mold, a small amount of O.C.T-Compound (Tissue-Tek) was prepared, and the respective tissue was added. The tissue was covered with O.C.T-Compound (Tissue-Tek) and snap frozen in liquid nitrogen. 2 µm cryo slices were produced with Leitz 1720 digital Kryostat.

Evans Blue Extraction and Quantification

Organs of interest were weighted and 500 µl formamide was added to each tissue sample tube. The tubes were transferred to a 55 °C water bath and incubated for 48 h to extract EB from tissue. The formamide/EB mixture was centrifuged to pellet any remaining tissue fragments. Measure absorbance was at 610 nm, 500 µl formamide was used as blank. Extravasated ng EB per mg tissue were calculated (Radu and Chernoff, 2013).

Immunofluorescence (IF) staining for localization microscopy

The slides were fixed for 5 min with absolute EtOH in -20 °C. The fixative was removed and washed five times with DPBS. For permeabilization of the cells, 0.5 % Triton X in DPBS were added and incubated for 8 min in room temperature. After washing five times with DPBS, the antigens were demasked by boiling the slides in Citrate buffer pH 6.0 in a pressure cooker. The slides were then rinsed for 30 min with distilled water. Tissue autofluorescence was blocked with 50 mM NH<sub>4</sub>Cl in DPBS for 10 min. The slides were washed three times with DPBS and then blocked with 5 % BSA in DPBS for 1 h in room temperature. The anti-Cld5 488 was added 1:200 and incubated over night at 4 °C. The next day, the solution was removed and washed five times with DPBS. The first antibody was fixed with 4 % PFA for 20 min at room temperature. The fixative was removed and washed five times with DPBS. To start with the second immunostaining, again 5 % BSA in DPBS was added and incubated for 1 h in room temperature to block unspecific binding sites. Anti-ZO-1 647 was added 1:200 and incubated for 1 h in

room temperature. The solution was removed and washed five times with DPBS. For nuclear staining, 30 nM DAPI in distilled water (ddH<sub>2</sub>O) were incubated for 15 min in room temperature. The solution was removed and the filters with the fixed and stained cells were cut out using 23-Gauge needles and placed on a glass slide. 10 µl of antifading mount medium was added and the cover slip was put on top. Before imaging, the slides were hardened for 24 h in the dark at room temperature. The experiment was repeated for 3 times. From every image, six randomly selected excerpts were further densitometrically analyzed for IF intensity on selected membrane areas in gray scales as described previously (Bartosova et al., 2020).

#### Immunohistochemistry

Tissue sections were hydrated for 5 min each in Xylol (2x), 100 % absolute ethanol (2x), 96 % ethanol, 70 % ethanol and were 2x washed with distilled water. To unmask the antigens, the slides were cooked in citrate buffer pH 6.0 and cooled down for 30 min in distilled water. In a humidified chamber, slides were washed 3x with DPBS. Endogenous peroxidase activity was quenched with DAKO buffer for 8 min. Slides were washed 3x with DPBS and blocked for 30 min with DAKO universal blocking buffer (1:10 in distilled water). The target antibody (αAGE; 1:10000) was incubated over night at 4 °C. The incubation with the corresponding secondary antibody (diluted 1:3000) took place after washing three times with DPBS for 30 min. The secondary antibody incubation was terminated by washing three times and the slides were incubated with R.T.U. vectastain ABC reagent for 15 min. The primary antibody binding was counterstained with DAB and the cell nuclei were stained with hematoxylin. Finally, the sections were dehydrated by incubation in 70 % ethanol, 96 % ethanol, twice in 100 % ethanol and twice in xylol (5 min each).

#### Determination of Anserine

Ans concentrations were determined fluorometrically using HPLC according to Schönherr et al. (Schönherr, 2002). For this purpose, 30 mg of cryopreserved mouse kidney tissue samples was lysed in 500 µl of RIPA buffer and centrifuged off at 10000 x g for 10 min. 200 µl of the supernatant were deproteinized using 37.5 µl of sulfosalicylic acid, incubated on ice for 30 min and centrifuged off at 10000 x g for 5 min. For derivatization, the supernatant was diluted 1:3 with borate buffer, 180 µl mixed with an equivalent volume of carbazole-9-carbonyl chloride solution, incubated for 90 s and then with 108 µl of a hydrosylamine solution (150 mmol/l hydroxylamine hydrochloride, 68 mmol/l sodium hydroxide, 2 % methanol v/v) for 3 min and the derivatization was stopped using 252 µl acetonitrile in acetic acid (8:2 v/v). Ans was separated using a Jupiter C18 column, the mobile phase consisting of a gradient of buffer A (82 %) and buffer B (18 %). The fluorometric detection took place

at  $\lambda_{\text{ex}}=283$  nm and  $\lambda_{\text{em}}=340$  nm. For validation, each sample was measured in duplicate, each duplicate having 0.6  $\mu\text{g}/\text{ml}$  Ans added to it.

### 2.2.2 Cell culture

Primary human umbilical vein endothelial cells (HUVEC) were purchased cryopreserved from pooled donors from Promocell (Heidelberg). For transendothelial electrical resistance (TER) and paracellular transport experiments cells were grown on special membrane filters, so called transwell permeable supports. These inserts provide access to both sides of the monolayer, giving the opportunity to study transport and other metabolic activities. For all other experiments classical cell culture plates for adherent cells were used.

#### Conditions

HUVEC were cultured in Endothelial Cell Growth Medium, supplemented with Growth Kit in T75 cell culture flasks and kept under physiological conditions (37.5 °C, 95 % humidity, 5 % CO<sub>2</sub> fumigation) in the incubator. Sterile activities were performed under a laminar flow sterile bench. All culture media were stored at 4 °C until use and only preheated in a water bath at 37 °C in case of direct application. All experiments were performed in Endothelial cell basal medium supplemented with 2 % FCS.

#### Passaging cells

After reaching approximately 75 % confluence, the cells were split. Here fore, the old media was aspired, and the cells were washed with DPBS. The DPBS was aspired again, and EDTA-Trypsin was added to the cells. The closed culture flask was incubated for 5 min under physiological conditions. The detachment of the cells was supported with a light tap from the outside of the culture flask and checked with a microscope. The cell suspension was transferred into a reaction tube and centrifuged for 3 min at 750 x g. The supernatant was discarded, and the pellet solved in 1 mL media for subsequent counting.

#### Determination of the cell number

To perform all experiments under the same conditions, it is crucial to work with the same cell numbers for every experiment. Dilutions of the cell suspension were prepared in a 96-well plate (1:4- 1:32) with Trypan blue. The Trypan blue staining is based on the principle, that vital cells with intact cell membranes are not colored. Since alive cells have a semi permeable membrane, they will not take up the dye, whereas the dye passes the membrane in dead cells. Hence, alive cells will reveal a clear



cytoplasm under the microscope, whereas dead cells appear as blue colored. Because viable cells are excluded from the staining, this technique is also described as a dye exclusion method (Strober, 2015). In this case, the cell number in a suspension was determined with the help of a Neubauer improved cell counting chamber using the following formula:

Cells/mL = counted cells per square x dilution factor x chamber factor  $10^4$

10  $\mu$ l of the cell suspension was diluted as stated before and 10  $\mu$ l of the cell - Trypan blue - compound was added into the Neubauer chamber. The cells were counted under the microscope and the final cell number was determined with the aforementioned formula.

#### Cryoconservation of cells

To conserve cells over a longer duration of time, the cells were stored at  $-196\text{ }^\circ\text{C}$  in liquid nitrogen. Therefore, a special cryo medium containing DMSO and high amounts of FCS was used. The lipophilic DMSO reduces the water content of the cell and thus prevents the formation of ice crystals, which could rupture the cell membrane. FCS contains a natural mix of growth factors, hormones, and nutrients that support cell survival and proliferation. Alike to passaging, the cells were first trypsinized and spun down. The pellet was solved in cryo medium ( $1 \times 10^6$  cells/mL), transferred into a cryo tube and frozen in a freezing container filled with isopropanol for one day at  $-80\text{ }^\circ\text{C}$ . Isopropanol provides a cooling rate of  $-1\text{ }^\circ\text{C}/\text{min}$  which is required for a successful cell cryopreservation and recovery. Later on, the cells were stored in a liquid nitrogen tank at  $-196\text{ }^\circ\text{C}$ .

#### Reactivation of cryo conserved cells

First the medium was prewarmed in a water bath at  $37\text{ }^\circ\text{C}$ . The cryo tubes containing the desired cells were removed from the nitrogen tank and thawed in the water bath for 2 min. The tube was disinfected through dipping several times into 70 % Ethanol. The thawed content was transferred into a T75 cell culture flask prepared with 10 ml preheated Endothelial cell growth medium.

#### Cell stimulation

For cell stimulation, the cells were passaged and counted. The concentration of the cell suspension was set to  $0.1 \times 10^6/\text{mL}$ , so  $0.05 \times 10^6$  cells were seeded in 0.5 mL per well on a 24-well plate. The media was changed every two days until the cells were confluent (usually between day two and three). For the stimulation, the respective substance was added to the cells in the indicated concentration for the indicated amount of time and incubated under physiological conditions.

### 2.2.3 Experiments

The transendothelial electrical resistance (TER, Ohm's Law Method)

TER of a cellular monolayer is a quantitative measurement for the integrity of the barrier. A classical setup for TER measurement is built from a cellular monolayer, that grows on semipermeable filter membranes, that help developing the apical and basal compartments of the cells. To measure the electrical resistance, two electrodes are used, commonly called chopstick electrodes: one electrode is placed in the lower and one in the upper compartment. The electrodes contain a silver or silver chloride pellet for measuring voltage and a silver electrode for the passing current. The electrodes are separated by the cells. In the classical TER systems (Voltohmmeter) an alternating current (AC) square wave is used to avoid any effects on the cells.

The measurement procedure includes measuring the blank resistance ( $R_{\text{BLANK}}$ ) of the filter insert only and the resistance across the cell layer on the semipermeable membrane ( $R_{\text{TOTAL}}$ ). The cell specific resistance ( $R_{\text{TISSUE}}$ ) in units of Ohm ( $\Omega$ ), can be obtained as:

$$R_{\text{TISSUE}}(\Omega) = R_{\text{TOTAL}} - R_{\text{BLANK}}$$

where resistance is inversely proportional (Srinivasan et al., 2015) to the effective area of the semipermeable membrane ( $M_{\text{AREA}}$ ) which is reported in units of  $\text{cm}^2$ .

$$R_{\text{TISSUE}} \propto 1 / M_{\text{AREA}}$$

TER values are reported ( $\text{TER}_{\text{REPORTED}}$ ) in units of  $\Omega \cdot \text{cm}^2$  and calculated as:

$$\text{TER}_{\text{REPORTED}} = R_{\text{TISSUE}}(\Omega) \times M_{\text{AREA}} (\text{cm}^2) \text{ (Watson et al., 2013, Haorah et al., 2008)}$$

Depending on the well or filter size, the appropriate volume was chosen. First, media was added in the lower, than into the upper compartment to moist the filters (2 h or overnight in the incubator). Cells were seeded in the respective density according to manufacturer's instructions onto the filter. To determine the differentiated monolayer, the TER was measured, reaching the plateau after 3 days. For all experiments at least one blank control (without cells) and one media control (cells in untreated culture media) were included. For all stimulations, the 0h value was measured before the application of the treatment solutions as a reference.

Immunofluorescence staining for localization microscopy

The treatment solution was removed from the trans wells and the cells were fixed for 5 min with absolute EtOH in  $-20^\circ\text{C}$ . The fixative was removed and washed five times with DPBS. For permeabilization of the cells, 0.5 % Triton X in DPBS were added and incubated for 8 min at room temperature. After washing five times with DPBS, 5 % BSA in DPBS were added and incubated for 1 h

at room temperature to block unspecific binding sites. The anti-Cld5 488 was added 1:200 and incubated overnight at 4 °C. The next day, the solution was removed and washed five times with DPBS. The first antibody was fixed with 4 % PFA for 20 min at room temperature. The fixative was removed and washed five times with DPBS. To start with the second immunostaining, again 5 % BSA in DPBS were added and incubated for 1 h at room temperature to block unspecific binding sites. Anti-ZO-1 647 was added 1:200 and incubated for 1 h at room temperature. The solution was removed and washed five times with DPBS. For nuclear staining, 30 nM DAPI in ddH<sub>2</sub>O were incubated for 15 min at room temperature. The solution was removed and the filters with the fixed and stained cells were cut out using 23-Gauge needles and placed on a glass slide. 10 µl of antifading mount medium was added and the cover slip was put on top. Before imaging, the slides were hardened for 24 h protected from light at room temperature (Bartosova et al., 2020).

#### In Situ Trypan blue staining

The cells were cultured on glass coverslips in 24-well plates and treated as indicated. Using a centrifuge plate attachment, the plates were spun at 200 × g. The media was removed, and the cells were washed for 3 min with DPBS and recentrifuged as described above. The wash was removed, and a 0.2 % Trypan Blue solution was added for 1 min. The Trypan Blue solution was removed, and cells were immediately fixed with 4 % PFA, pH 7.5, for 10 min at 20–22 °C. After fixation, cells were rinsed 3–4 times with DPBS with gentle shaking until the fluid was clear of any residual blue color. The coverslips were gently lifted to free Trypan Blue from underneath. The coverslips were dehydrated through sequential ethanol washes (1 min each in 70% and 95 %, 3× for 1 min in 100 %), followed by immersion in ROTICLEAR® clearant (a xylene substitute). Finally, the coverslips were mounted onto glass slides with a ROTI® Mount (Perry et al., 1997).

#### Paracellular permeability assay

The paracellular permeability assay gives insight into TJ integrity, as well as the rates of size-selective paracellular permeability *in vitro*. A known concentration of a labeled (apical) and unlabeled (basal) agent is added into the treatment solutions. After the indicated time, a small amount from the basal compartment is analyzed for fluorescence, using a prepared standard curve and a fluorescence plate reader (Ruiz-Remolina et al., 2017).

For the standard curve an eight-point dilution series of the labeled molecule (in this case different molecular weight Dextrans) was prepared starting at 50 µg/ml. The stock solutions were added in duplets (100 µl/well) on a black 96 well plate. Finally, the basolateral solutions were transferred in

duplets in a dilution of 1:100 in DPBS onto the plate. The plate was analyzed with a fluorescence reader in excitation 520 nm and emission 590 nm. The amount of diffused dextran is calculated by the calibration curves.

#### Bicinchoninic acid assay

This method uses bicinchoninic acid (BCA) as the detection reagent for Cu<sup>+1</sup>, which is formed when Cu<sup>+2</sup> is reduced by proteins in an alkaline environment (Smith et al., 1985). A purple reaction product is formed by the chelation of two molecules of BCA with one cuprous ion (Cu<sup>+1</sup>). This water-soluble complex exhibits a strong absorbance at 562 nm that is linear with increasing protein concentrations. The macromolecular structure of proteins, the number of peptide bonds and the presence of four amino acids (cysteine, cystine, tryptophan and tyrosine) are reported to be responsible for color formation with BCA (Wiechelman et al., 1988).

Nine BSA standards were prepared in a range from 0-200 µg/ml. 150 µL of each standard or unknown sample replicate was pipetted into a 96 well plate. 150 µL of the work reagent was added to each well and mixed thoroughly on a plate shaker for 30 sec. The plate was covered and incubated at 37 °C for 2 h. The plate was cooled to room temperature and the absorbance was measured at 562 nm on a plate reader. The average 562 nm absorbance of the blank standards was subtracted from the 562 nm reading of all standard and unknown samples. The standard curve was prepared by plotting the average Blank-corrected 562 nm reading for each BSA standard vs. its concentration in µg/ml. The standard curve was used to calculate the protein concentration of the samples (Abcam 2023).

#### Zymography

Zymography is an electrophoretic technique for the detection of hydrolytic enzymes, based on the substrate repertoire of the enzyme (Vandooren et al., 2013). In detail, gelatin in a polyacrylamide gel will be digested by active gelatinases running through the gel. After Coomassie staining, the degraded areas are visible as pale bands against a darkly stained background (Abcam 2017).

For the zymography, apical supernatants of 5 transwell experiments were concentrated with 30 K centrifugal filter units (4000 x g, 10 min). The protein concentration was determined with Micro BCA Assay. 10 µg protein in 4x sample buffer were loaded in duplets onto the gel, which was run for 110 min, 200 V. After electrophoresis the gel was removed and incubated in 1x Zymogram Renaturing Buffer for 30 min at room temperature with gentle agitation. The buffer was decanted and 1x Zymogram Developing Buffer was added to the gel. The gel was equilibrated for 30 min at room temperature with gentle agitation. The gel was incubated overnight at 37 °C. The staining solution was

prepared as instructed with the Colloidal Blue Staining Kit. The gel was shaken in staining solution for 3 h. The staining solution was removed, and the gel was washed with deionized water (Abcam 2017). After “sandwiching” into a plastic wrap, the picture was taken with a light scanner.

#### FACS

Cells were treated as indicated and washed with DPBS before detaching with EDTA-Trypsin for 5 min. The reaction was stopped with Stop medium and the solution was transferred into a round bottom polystyrene tube and spinned down for 3 min at 750 x g. The supernatant was discarded, and the pellet was washed twice with 500 µl Iso buffer for 3 min at 750 x g. After discarding the supernatant, cells were fixed with 250 µl of 4 % formaldehyde and incubated for 15 min at 37 °C in the water bath. The cells were spinned down for 3 min at 750 x g and were washed twice with 500 µl Iso buffer for 3 min at 750 x g and the supernatant was discarded. Cells were resuspended in 100 µl Iso buffer and permeabilized by adding ice-cold 100% methanol to the prechilled cells, to a final concentration of 90 % methanol. The tubes were incubated for 25 min on ice. To remove the methanol, cells were washed twice excessively in Iso buffer by centrifugation for 3 min at 750 x g. After discarding the supernatant, the cells were resuspended in 100 µl of diluted antibody (1:100) and incubated at room temperature for 1 h, protected from light. The incubation was stopped by adding excessive Iso buffer and washing by centrifugation at 750x g for 3 min. The supernatant was discarded. After a final wash with Iso buffer the cells were spinned down again for 3 min at 750 x g, the supernatant was discarded, and the cells were resuspended in 500 µl iso buffer and were analyzed in the flow cytometer (Cell Signaling Technologies, 2020). The gating strategy is described in Fig. 3.

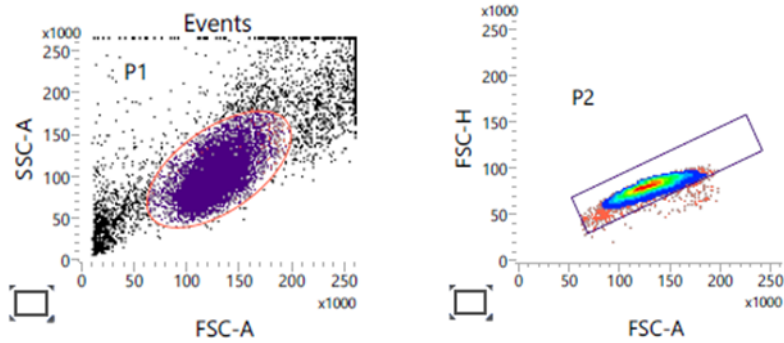


**Figure 3: FACS Gating Strategy for HUVEC**

Forward versus side scatter (FSC vs. SSC) gating was used to identify HUVEC based on size and granularity (left panel). To exclude doublets, side scatter height (SSC-H) vs. side scatter area (SSC-A) plot were used (right panel).

## 2.2.4 Commercial Assays

### Enzyme-linked Immunosorbent Assay (ELISA)

An ELISA is an antibody-based assay used for quantitative protein measurements but is also able to detect lower molecular compounds like pesticides, hormones, and toxins. The whole assay is based on the property of specific antibodies that bind to the antigen to be detected. Another antibody is linked to a reporter enzyme (e.g., horseradish peroxidase or alkaline phosphatase), which catalyzes a substrate into a colorimetric, fluorescent, or chemiluminescent product. The catalyzed reaction of the reporter enzyme serves as verification for the presence of the antigen.

The signal strength of the antigen concentration can be precisely determined with a photometer. Multiple measurements carried out can also be used for quantitative detection. The sample concentration is calculated by comparison to a dilution series with known concentrations of the antigen of interest by a standard curve (Engvall and Perlmann, 1971).

The different ELISAs were performed according strictly to the manufacturer's instructions. In general, a surface is prepared to which a known quantity of capture antibody is coupled. The target standard in known concentration and the antigen-containing sample is applied to the plate and captured by the bound antibody. The plate is washed to remove all unbound antigen. An antigen specific detection antibody is added to the plate. Here, it is possible to either use an already enzyme linked detection antibody, or another unlabeled detection antibody is added binding the detection antibody. Finally, the substrate is added, and is converted into a detectable form. For detection a microplate reader with the according wavelengths was used (R&D Systems, 2017).

### Human Active MMP-1 Fluorescent Assay

The assay is a fluorometric assay to quantitatively measure enzyme activity. A monoclonal antibody specific for human MMP-1 is precoated onto a black microplate. Added Standards and samples containing MMP-1 are bound by the immobilized antibody. After washing a fluorogenic substrate linked to quencher molecules is added and any active enzyme present will cleave the connection between the fluorophore and the quencher molecule. The cleavage extinguishes the distance depending on resonance energy transfer between the fluorophore and the quencher molecule, emitting the fluorescent signal that is proportional to the active enzyme in the sample.

The procedure was performed according to the manufacturer's recommendations. Each well was added 100  $\mu$ l of Assay Diluent and 150  $\mu$ l of sample or standard. The plate was incubated at room temperature on a horizontal plate shaker. The wells were washed four times with Wash Buffer. 200  $\mu$ l of p-amino phenylmercuric acetate (APMA) were added only to the standards. To measure only endogenous levels of active MMP-1 in samples, instead of APMA, 200  $\mu$ l of Reagent Diluent 2 was added. The plate was incubated in a humidified chamber at 37 °C and protected from light. After washing, 200  $\mu$ l of substrate was added and the plate was incubated for 20 h in a humidified chamber at 37 °C and protected from light. The relative fluorescence units (RFU) were determined using a fluorescence plate reader with excitation wavelength 320 nm and emission wavelength set to 405 nm; endpoint mode; 1x 20 mS integration time; plate speed 6 (R&D Systems, 2017).

### Lactate Dehydrogenase (LDH) Assay

The LDH assay is a cell death / cytotoxicity assay used to determine the level of plasma membrane damage in a cell population. LDH is present in all cell types and rapidly released into the cell culture supernatants when the plasma membrane is damaged. The LDH assay protocol is based on an enzymatic coupling reaction: LDH released from the cell oxidizes lactate to generate NADH, which then reacts with water-soluble tetrazolium salts (WSTs) to produce a yellow color. The intensity of the produced color correlates directly with the number of lysed cells.

First,  $3 \times 10^4$  cells / well were seeded on a 96 well plate in triplicates. The next day, the treatment was applied. LDH Positive Control was reconstituted with 100  $\mu$ l of LDH Assay Buffer. For a background control, only culture medium was used, and the values were subtracted from all other values. For the low control, triplicates of cells in culture medium were used, for the high control triplicates of cells with cell lysis solution were used. The test samples in triplicates were treated as indicated. The medium solutions (10  $\mu$ l / well) were transferred into an optically clear 96-well plate. WST Substrate Mix was reconstituted in 1.1 ml ddH<sub>2</sub>O for 10 min and mixed thoroughly. 200  $\mu$ l of WST Substrate Mix was mixed with 10.0 ml of LDH Assay Buffer. 100  $\mu$ l LDH Reaction Mix was added to each well, mixed and

incubated for 30 min at room temperature. The absorbance of all controls and samples were measured with a plate reader equipped with a 450 nm (440 nm - 490 nm) filter. The reference wavelength was 650 nm.

Data analysis is calculated as:

Cytotoxicity (%) = ((Test Sample – Low Control) / (High Control – Low Control)) X 100 (Abcam 2017).

#### Caspase Assay

The Caspase-Glo® 1 Inflammasome Assay is a bioluminescent method to measure the caspase-1 activity, an essential component of the inflammasome. After caspase cleavage of the Z-WEHD substrate (Z-WEHD-aminoluciferin), a substrate for luciferase (aminoluciferin) is released, resulting in luciferase activity and the production of light by a proprietary, thermostable, recombinant luciferase. The selective caspase-1 substrate (Z-WEHD) enables the detection of catalytically active caspase-1 in cells or culture media and the quantitative measurement of inflammasome activity. The inclusion of the proteasome inhibitor MG-132 in the reagent eliminates non-specific cleavage of the proteasome substrate, allowing sensitive detection of caspase-1. The assay includes a caspase-1 specific inhibitor (Ac-YVAD-CHO) to confirm specific activity in parallel samples and to discriminate caspase-1 activity from other caspases. Cells were grown in white opaque-walled multiwell tissue culture plates. Plates were allowed to equilibrate at room temperature for 5 minutes. 100 µL of Caspase-Glo® 1 Reagent was added to half of the wells of the 96-well plate containing 100 µL of blank, negative control cells, or treated cells in culture medium. 100 µL of Caspase-Glo® 1 YVAD-CHO reagent was added to the other half of the plate. The plate was covered and mixed gently with a plate shaker at 300-500 rpm for 30 seconds. In order to stabilize the luminescence signal, the plate was incubated at least 1 hour at room temperature. Luminescence was measured using a plate meter luminometer according to the luminometer manufacturer's instructions. All experiments were performed as three independent experiments (Promega 2019).

#### Cytokine Array

Antibody arrays immobilize a capture antibody onto a solid substrate, such as a membrane. For planar surface arrays, different capture antibodies with known binding specificities are spotted onto a nitrocellulose membrane in an addressable format. After adding the sample, a biotinylated antibody is incubated. Finally, labeled streptavidin is added, and the data can be analyzed and graphed.

The components were allowed to equilibrate to room temperature. One membrane per well was prepared. 2 ml of Blocking Buffer was pipetted into each well and incubated for 30 minutes at room



temperature. After aspirating, 1 ml of diluted or undiluted sample was added into each well and incubated for 2 h at room temperature. After aspirating samples from each well with a pipette, 2 ml of 1X Wash Buffer I was added into each well and incubated for 5 minutes at room temperature. This was repeated for a total of 3 washes using fresh buffer and aspirating out the buffer completely each time. 2 ml of 1X Wash Buffer II was added into each well and incubated for 5 minutes at room temperature. This was repeated for a total of 2 washes using fresh buffer and aspirating out the buffer completely each time. 1 ml of the prepared Biotinylated Antibody Cocktail was added into each well and incubated for 2 h at room temperature. The Biotinylated Antibody Cocktail was removed from each well and the membranes were washed 3x with Wash Buffer I and 2x with Wash Buffer II. 2 ml of 1X HRP-Streptavidin was added into each well and incubated for 2 h at room temperature. The HRP-Streptavidin was removed from each well and the membranes were washed 3x with Wash Buffer I and 2x with Wash Buffer II. The membranes were transferred, printed side up, onto a sheet of blotting paper lying on a flat surface (such as a benchtop). Any excess wash buffer was removed by blotting the membrane edges with another piece of paper. The membranes were transferred and placed, printed side up, onto a plastic sheet lying on a flat surface. Per membrane, 250  $\mu$ l of Detection Buffer C + 250  $\mu$ l of Detection Buffer D were gently added onto each membrane and incubated for 2 minutes at room temperature. Immediately afterwards, another plastic sheet was placed on top of the membranes. The membranes were "sandwiched" between two plastic sheets. The sandwiched membranes were transferred to the CCD camera and exposed (Raybiotech, 2019).

### 2.2.5 Statistics

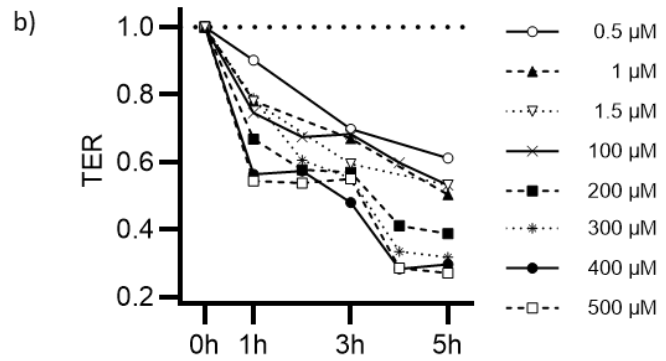
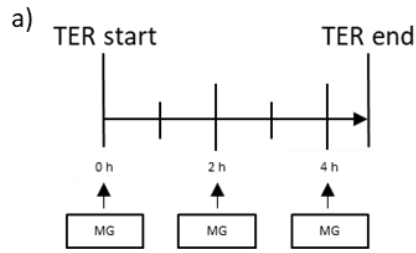
Resulting study data were entered into an electronic database (Microsoft® Excel 2016, Microsoft Corporation, Redmond, USA) and evaluated using Graphpad Prism for Windows (Version 9.0.2, GraphPad Software, San Diego California USA). Data were visualized using mean values with connecting line charts, bar charts, or for survival Kaplan-Meier plots. Correlation was visualized in scatter (xy) plots. The Kolmogorov-Smirnov test was applied to check for normal distribution. Due to non-normally distributed data, non-parametric methods for evaluation were used. The Gehan-Breslow-Wilcoxon test was used to compare two or more survival distributions. TERs, paracellular leakage, EB concentrations, Ans concentrations, relative AGE-DAB positivity and IF intensity of two groups at individual time points were compared using Mann-Whitney-U-Test. A p-value < 0.05 was considered statistically significant. Concerning symbolism: not significant: ns,  $p \leq 0.05$ : \*,  $p \leq 0.01$ : \*\*,  $p \leq 0.001$ : \*\*\*,  $p \leq 0.0001$ : \*\*\*\*.

## 3 Results

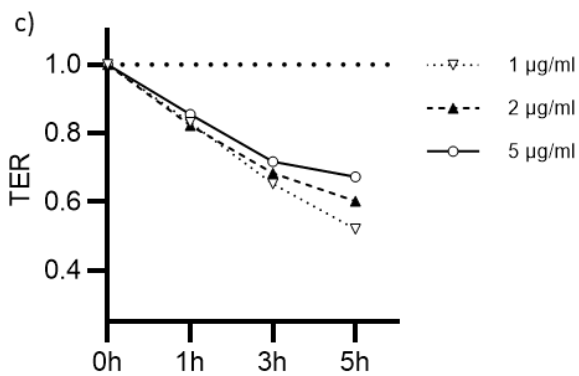
### 3.1 Endothelial barrier integrity and paracellular transport *in vitro*

#### 3.1.1 MG impairs the endothelial barrier by disturbing the monolayer integrity and increasing paracellular leakage

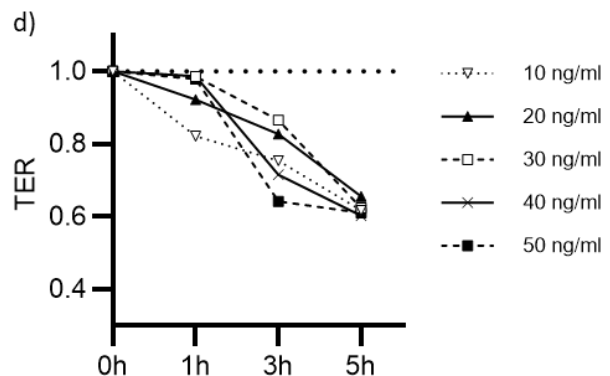
We hypothesized that MG might contribute to the disturbance of the endothelial barrier during development of septic shock. To assess the impact of MG on endothelial integrity, primary HUVEC were used, and the barrier function was evaluated by measuring the TER of HUVEC monolayers exposed to MG over a 5-hour time course. Because of the relative instability, MG was adjusted in 2-hour intervals (Fig. 4a). MG dose- and time-dependently reduced the TER of HUVEC monolayers (Fig. 4b). Comparable courses could be observed after single exposition to LPS (Fig. 4c) and TNF (Fig. 4d). To further assess if the drop in TER was related to increased paracellular leakage, the measured relative concentrations of 70 kDa dextran were compared in Fig. 4 with increasing MG doses after 2 hours (Fig. 5a) and after 5 hours (Fig. 5b). Matching the observed TER reductions in Fig. 4, a dose and time-dependent increase in the paracellular leakage could be observed at both time points (Fig. 5a, b) with increasing MG dosages. A direct comparison of the paracellular leakage of each concentration in the described time course is given in Fig. 5.



SD	0.5 $\mu$ M	1 $\mu$ M	1.5 $\mu$ M	100 $\mu$ M	200 $\mu$ M	300 $\mu$ M	400 $\mu$ M	500 $\mu$ M
1h	0.204	0.258	0.149	0.296	0.247	0.152	0.254	0.076
3h	0.204	0.226	0.088	0.254	0.091	0.181	0.171	0.106
5h	0.174	0.227	0.193	0.213	0.095	0.171	0.213	0.100



SD	1 $\mu$ g/ml	2 $\mu$ g/ml	5 $\mu$ g/ml
1h	0.157	0.277	0.263
3h	0.157	0.168	0.134
5h	0.127	0.128	0.092



SD	10 ng/ml	20 ng/ml	30 ng/ml	40 ng/ml	50 ng/ml
1h	0.217	0.206	0.175	0.312	0.259
3h	0.130	0.141	0.200	0.253	0.249
5h	0.105	0.221	0.116	0.189	0.135

**Figure 4: MG impairs the endothelial barrier comparable to LPS and TNF**

a) Dose titration scheme of MG administration for TER measurements. The given MG concentration was generated in cell media. Every 2 h the desired concentration was restored in the apical compartment. b) Time course of TER of HUVEC monolayers under MG-treatment relative to MG-free media control. Treatment was repeated every 2 h. c) Time course of TER of HUVEC monolayers under single LPS or d) single TNF administration relative to LPS- respectively TNF-free media control. Concentrations as indicated. Each point represents mean values of TER from n=6, standard deviations (SD) are presented below.

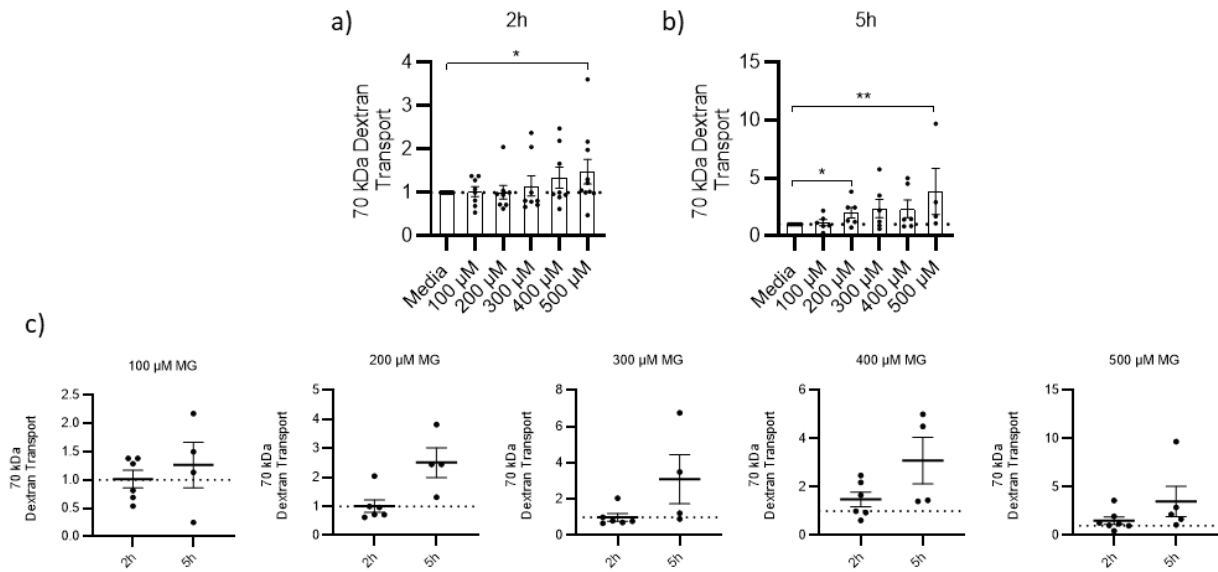


**Figure 5: MG leads to increased paracellular leakage**

a) 2 h paracellular leakage of a HUVEC monolayer for 70 kDa dextran under repeated increasing MG treatment relative to MG-free control.  
 b) 5 h paracellular leakage of a HUVEC monolayer for 70 kDa dextran under repeated increasing MG treatment relative to MG-free control.  
 c) Comparing bar graphs of the paracellular leakage under repeated increasing MG treatments relative to MG-free control. Concentrations as indicated. Data represent mean values of transport from n=6 and SEM. Mann-Whitney U-test, concerning symbols: \* p≤0.05, \*\* p≤0.01.

### 3.1.2 Anserine prevents effects of patho- and supraphysiological MG doses

Given that MG impairs the endothelial barrier *in vitro*, next it was examined whether Ans is able to shield the harmful effects of pathophysiological MG doses. For the Ans cotreatment, MG and Ans were given at the same time and MG administration was repeated in 2-hour intervals, LPS was only added at the start (Fig. 6a). TER was observed over a time course of 5 hours. A single Ans cotreatment prevented the MG induced TER drop significantly at 1 hour and stably over 5 hours (Fig. 6b). Furthermore, a single Ans cotreatment was able to prevent not only LPS induced TER drop at the time point of 5 hours (Fig. 6c), but also when MG and LPS were combined (Fig. 6d). In the measurement of 4 kDa dextran paracellular leakage, the single Ans treatment significantly decreased the molecule transport at the time point of 5 hours, regardless of whether MG was used alone or in combination with LPS (Fig. 6e). The same trend emerged for the transport of 10kDa molecules, with the effect being statistically significant only for the combination of MG and LPS (Fig. 6f). When incubated with supraphysiological dosages of 500 μM MG, Ans treatment was repeated with every MG administration (Fig. 7a) in intervals of 2 hours and TER was observed over a time course of 5 hours. Ans was titrated to a maximum of the same proportionate dose as the pathophysiological MG concentration. In fact, the same dose-response relationship could also prevent the complete loss of resistance of the supraphysiological MG dosage, whereas the next smaller Ans dosage only seemed to have an

improving effect after the second administration (Fig. 7b). The individual time courses of the increasing concentrations of Ans are shown in Fig. 7c.

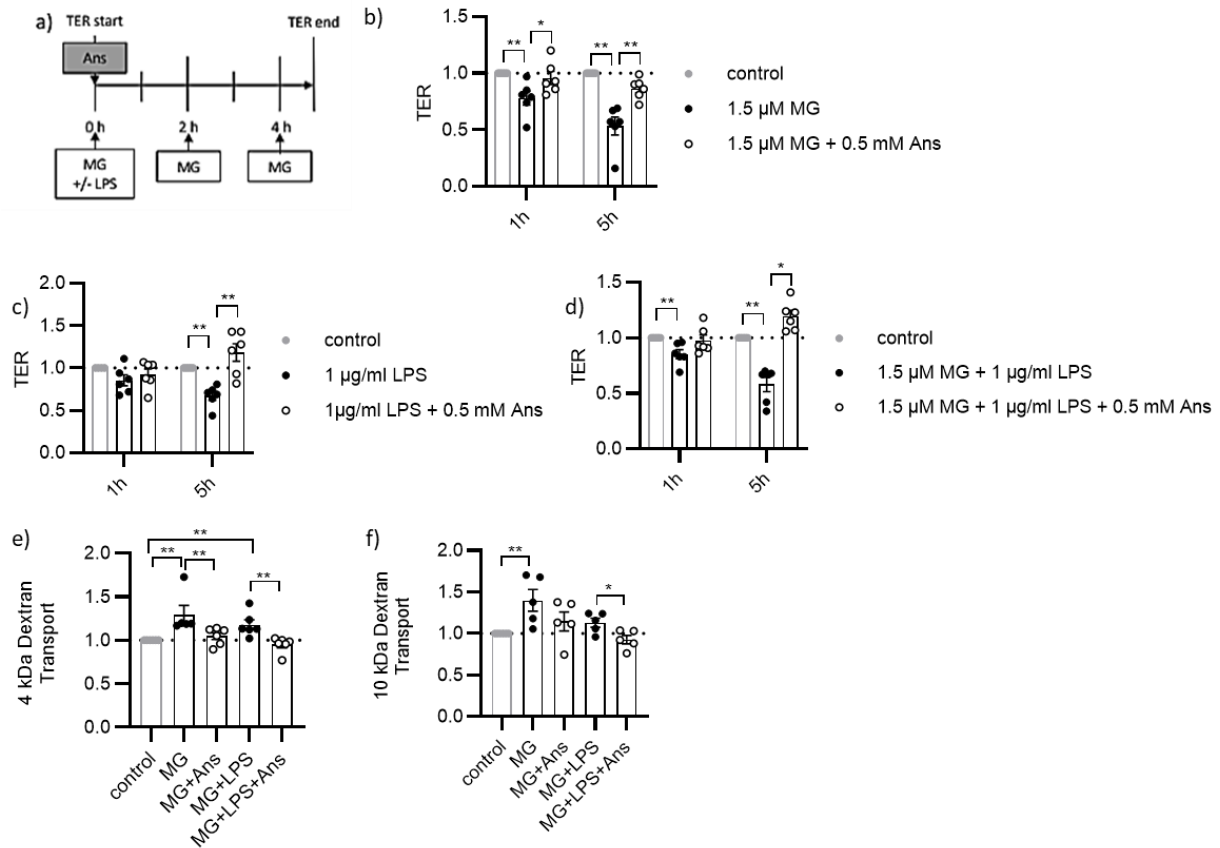


**Figure 6: Ans prevents MG-induced TER loss and improves paracellular leakage of small molecules**

a) Scheme of Ans administration for TER cotreatment measurements. The given MG concentration was generated in cell media. Every 2 h the desired concentration was restored in the apical compartment. b) Effect of repeated MG and single Ans cotreatment on the TER of a HUVEC polarized monolayer relative to MG-free control. c) Effect of single LPS and single Ans cotreatment on the TER of a HUVEC polarized monolayer relative to MG-free control. d) Effect of repeated MG, single LPS and single Ans cotreatment on the TER of a HUVEC polarized monolayer relative to MG-free control. e) 5 h paracellular leakage of a HUVEC monolayer for 4 kDa dextran under repeated MG treatment (1.5 μM), single LPS treatment (1 μg/ml) or combined repeated MG (1.5 μM) and single LPS (1 μg/ml) treatment with and without Ans (0.5 mM), relative to MG-free control. f) 5 h paracellular leakage of a HUVEC monolayer for 10 kDa dextran under repeated MG treatment (1.5 μM), single LPS treatment (1 μg/ml) or combined repeated MG (1.5 μM) and single LPS (1 μg/ml) treatment with and without Ans (0.5 mM), relative to MG-free control. Concentrations as indicated. Mann-Whitney U test; concerning symbols: \*  $p \leq 0.05$ , \*\*  $p \leq 0.01$ . Data represent mean values of TER or transport from  $n=6$  and SEM.

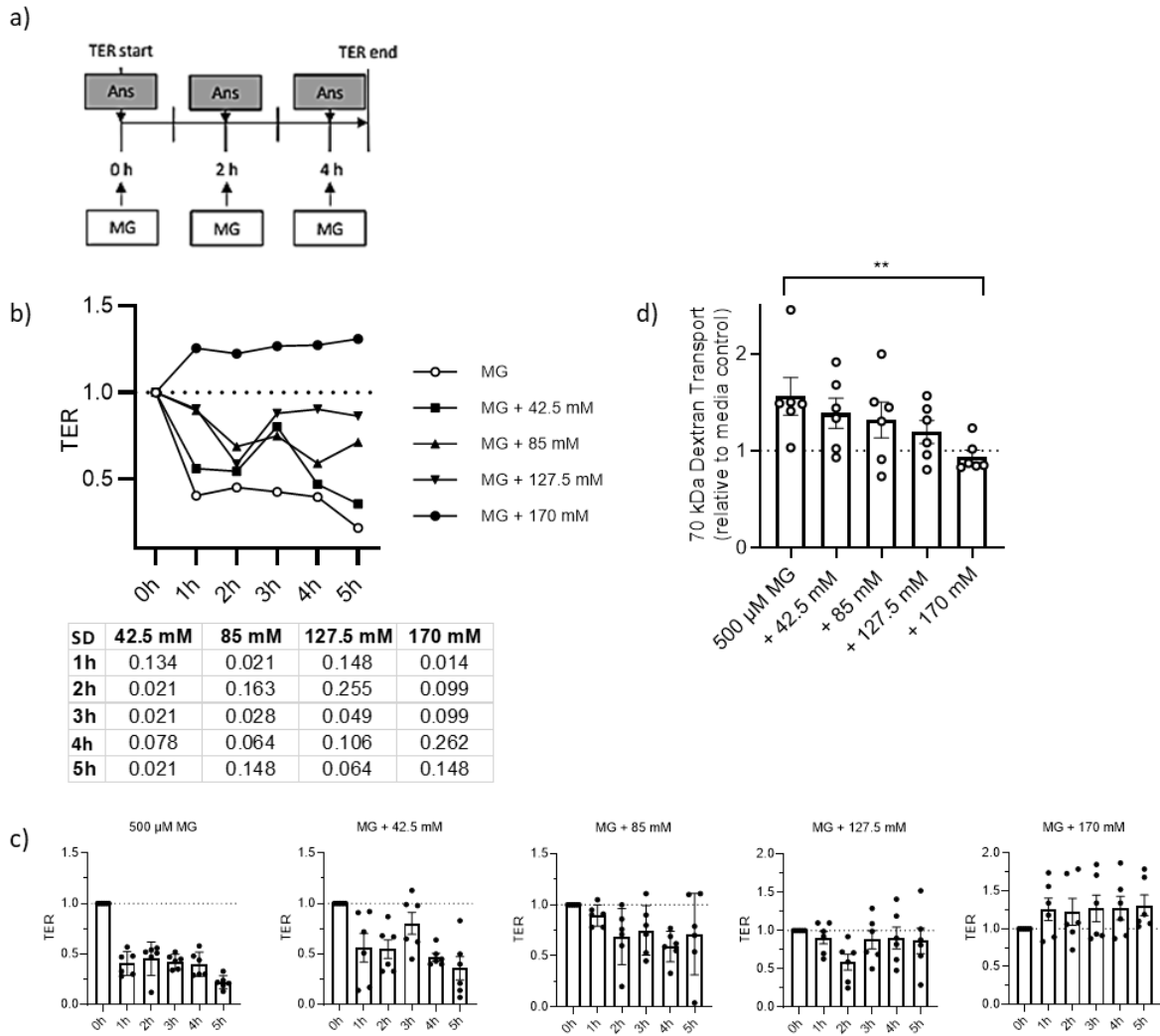


**Figure 7: Ans prevents TER loss and paracellular leakage of supraphysiological MG dosages**

a) Scheme of Ans administration for supraphysiological TER cotreatment measurements. The supraphysiological MG concentration of 500  $\mu\text{M}$  was generated in cell media. Every 2 h MG and Ans were restored in the apical compartment. b) Time course of TER of HUVEC monolayers under supraphysiological MG-treatment (500  $\mu\text{M}$ ) and increasing Ans doses relative to MG-free media control. MG and Ans treatment were repeated every 2 h. Each point represents mean values of TER from  $n=6$ , standard deviations (SD) below. c) Comparing bar graphs of a supraphysiological MG dosage and increasing Ans dosages relative to MG-free control. d) 5 h Paracellular leakage of a HUVEC monolayer for 70 kDa dextran under repeated supraphysiological MG treatment and increasing Ans concentrations relative to MG-free control. Concentrations as indicated. Mann-Whitney U test; concerning symbols: \*\*  $p \leq 0.01$ . Data represent mean values of TER or transport from  $n=6$  and SEM.

Next, it was tested, whether the protective effect of Ans could be further enhanced by a prophylactic treatment (=pretreatment). For this purpose, the cells were pretreated 2 hours beforehand with a single dosage of Ans and then again, every 2 hours with the pathophysiological dosage of MG and if indicated, a single dosage of LPS (Fig. 8a). Ans pre-treatment achieved comparable effects to co-treatment (Fig. 6b, d), regardless of whether MG was used alone (Fig. 8b) or in combination with LPS (Fig. 8c). To test whether Ans was able to restore the endothelial integrity after an MG-induced injury (=posttreatment), a single dosage of Ans was added 3 hours after the start of MG and MG+LPS exposure (Fig. 8d). TER was all together observed in total over 5 hours. The Ans posttreatment

significantly re-established the TER previously decreased by MG and restored a comparable level of resistance to that of the MG-free medium control (Fig. 8e). A comparable effect was observed when inducing the TER loss with a combination of MG and LPS (Fig. 8f).

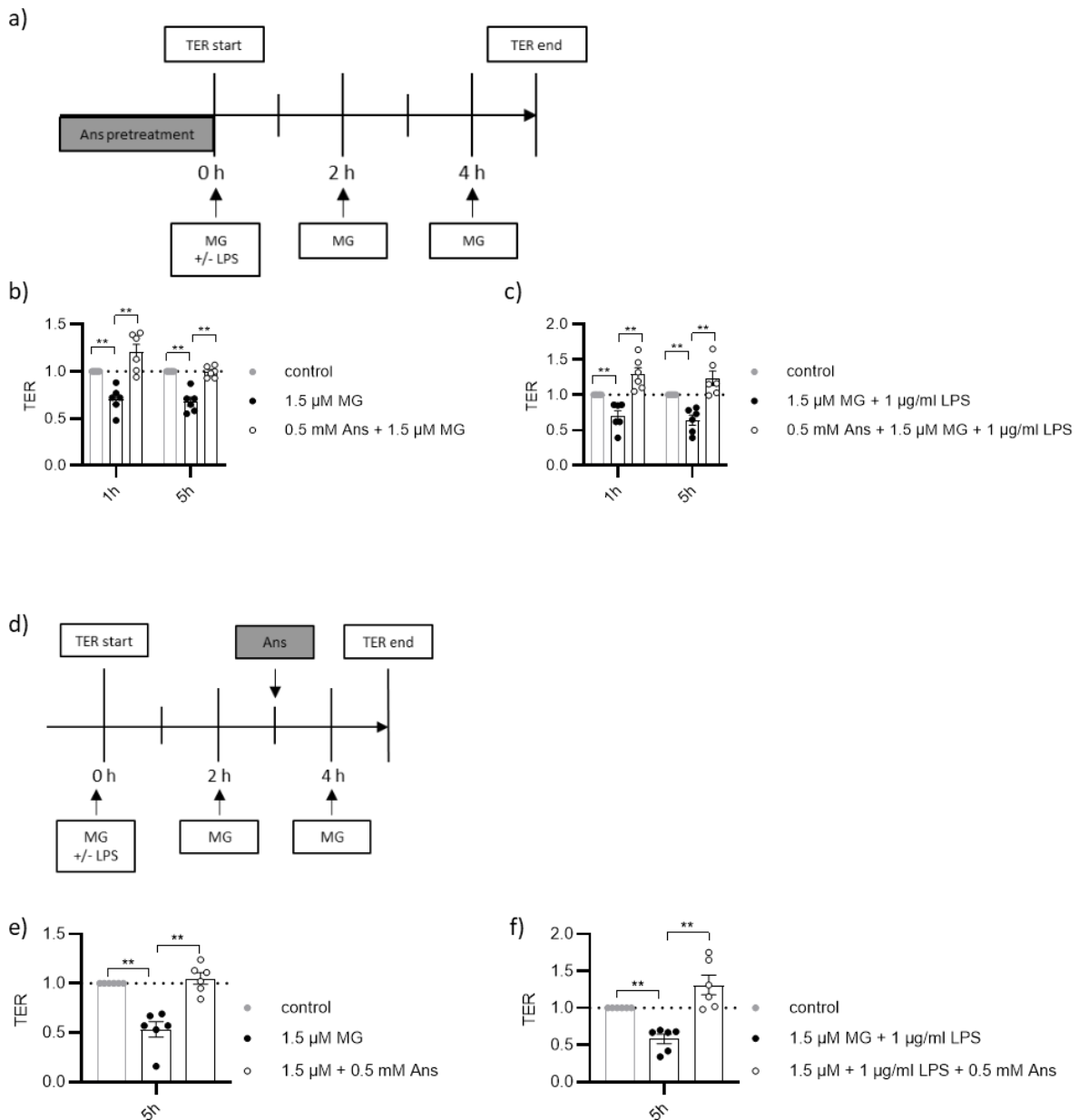


**Figure 8: Ans shows TER restoring effects**

a) Scheme of Ans administration for TER pretreatment measurements. Cells were pretreated 2 h before MG administration. The given MG concentration was generated in cell media. Every 2 h the desired concentration was restored in the apical compartment. b) Effect of repeated MG and single Ans pretreatment on the TER of a HUVEC polarized monolayer relative to MG-free control. c) Effect of repeated MG, single LPS and single Ans pretreatment on the TER of a HUVEC polarized monolayer relative to MG-free control. d) Scheme of Ans administration for TER posttreatment measurements. After 3 h of repeated MG treatment or repeated MG- and single LPS treatment, a single dose Ans was added. e) Effect of repeated MG and single Ans posttreatment on the TER of a HUVEC polarized monolayer relative to MG-free control. f) Effect of repeated MG, single LPS and single Ans posttreatment on the TER of a HUVEC polarized monolayer relative to MG-free control. Concentrations as indicated. Mann-Whitney U test; concerning symbols: \*\*  $p \leq 0.01$ . Data represent mean values of TER from  $n=6$  and SEM.

### 3.1.3 The effects of Anserine exceed those of previously described scavengers

To prove the scavenger activities of Ans, different medications respectively described MG-scavengers were tested in the TER system as cotreatments. All the medications were given at the same time as the first MG dosage and MG treatment was repeated in 2-hour intervals (Fig. 9a). Cns significantly prevented the TER loss induced by MG alone (Fig. 9b) and MG and LPS (Fig. 9d) at 1 hour, however it could not be obtained over 5 hours (Fig. 9b, d). For LPS treatment alone, Cns cotreatment showed no differences at any time point (Fig. 9c). The effect of the AG co-treatment was exactly the opposite: at the time point of 1 hour, no effect was seen with either MG alone (Fig. 9e) or in combination with LPS (Fig. 9g), but there was a significant difference in both cases after 5 hours (Fig. 9e, g). AG cotreatment significantly prevented the TER loss induced by LPS alone at 1 hour, however it could not be obtained over 5 hours (Fig. 9f). Cotreatment with the antioxidant NAC did not show any effect at any time point with MG alone (Fig. 9h), however for LPS, NAC cotreatment significantly improved TER after 5 hours (Fig. 9i). A similar effect was observed for the combination of MG and LPS after 5 hours (Fig. 9j), whereby the effect appeared probably due to the LPS.

### 3.1.4 MG disrupts endothelial barrier proteins

It was then investigated whether the loss of TER induced by MG and improved with the Ans treatment was dependent from a loss or restructuring of TJs or TJ associated proteins. Therefore, the TJ claudin 5 and the TJ associated protein ZO-1 were chosen. Pathophysiological doses of MG were sufficient to induce a loss of claudin 5 as well as ZO-1 at 5 hours. Anserin cotreatment visually improved the distribution of those endothelial barrier forming proteins. When combined with LPS, MG rather led to a redistribution or clustering of claudin 5 and ZO-1 which also could be improved by Ans cotreatment (Fig. 10a). The densitometric analysis revealed and confirmed a highly significant rarefication of claudin 5 (Fig. 10b) and ZO-1 for both MG alone and combined MG and LPS (Fig. 10c), which could be improved with a single Ans cotreatment in both cases (Fig. 10b, c).



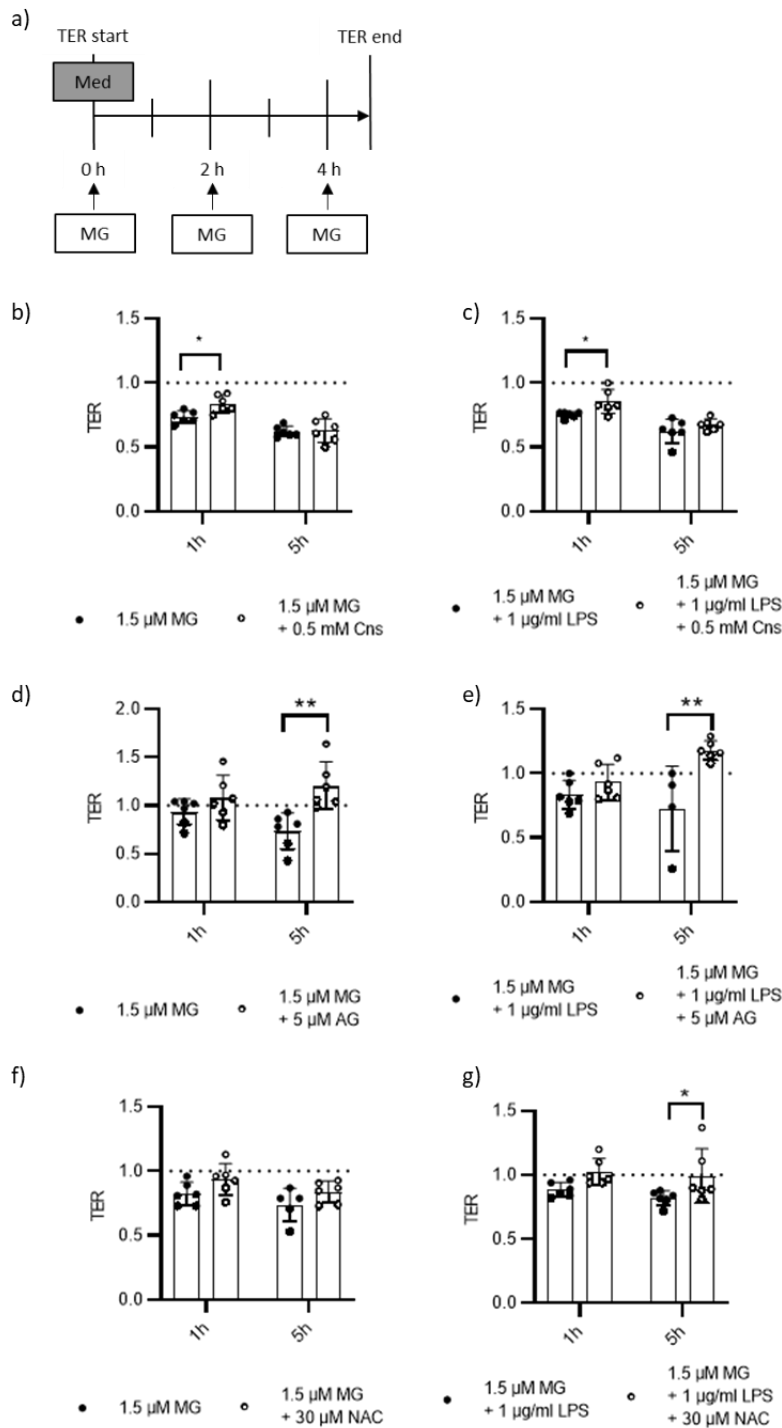


**Figure 9: MG-scavengers and antioxidants show moderate effects in MG-induced TER loss**

a) Scheme of substance administration for TER cotreatment measurements. The given MG concentration was generated in cell media. Every 2 h the desired concentration was restored in the apical compartment. b) Effect of repeated MG and single Cns cotreatment on the TER of a HUVEC polarized monolayer relative to MG-free control. c) Effect of a single LPS and a single Cns cotreatment on the TER of a HUVEC polarized monolayer relative to MG-free control. d) Effect of repeated MG, a single LPS and a single Cns cotreatment on the TER of a HUVEC polarized monolayer relative to MG-free control. e) Effect of repeated MG and a single AG cotreatment on the TER of a HUVEC polarized monolayer relative to MG-free control. f) Effect of a single LPS and a single AG cotreatment on the TER of a HUVEC polarized monolayer relative to MG-free control. g) Effect of repeated MG, a single LPS and a single AG cotreatment on the TER of a HUVEC polarized monolayer relative to MG-free control. h) Effect of repeated MG and a single NAC cotreatment on the TER of a HUVEC polarized monolayer relative to MG-free control. f) Effect of a single LPS and a single NAC cotreatment on the TER of a HUVEC polarized monolayer relative to MG-free control. g) Effect of repeated MG, a single LPS and a single NAC cotreatment on the TER of a HUVEC polarized monolayer relative to MG-free control. Concentrations as indicated. Mann-Whitney U test; concerning symbols: \*  $p \leq 0.05$ , \*  $p \leq 0.01$ . Data represent mean values of TER from  $n=6$  and SEM.

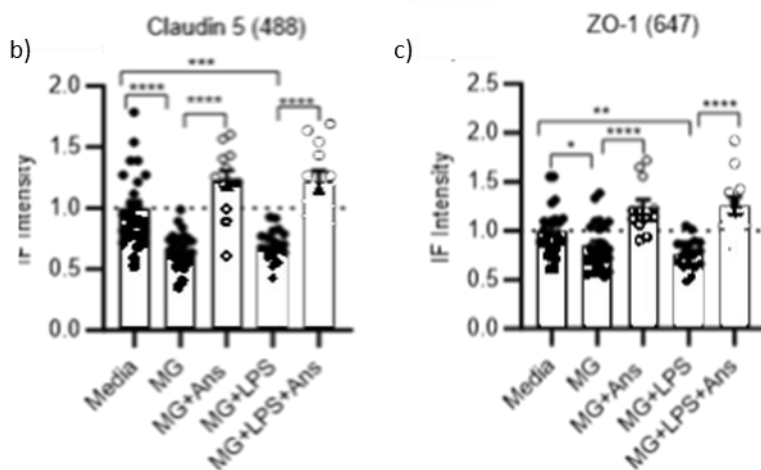
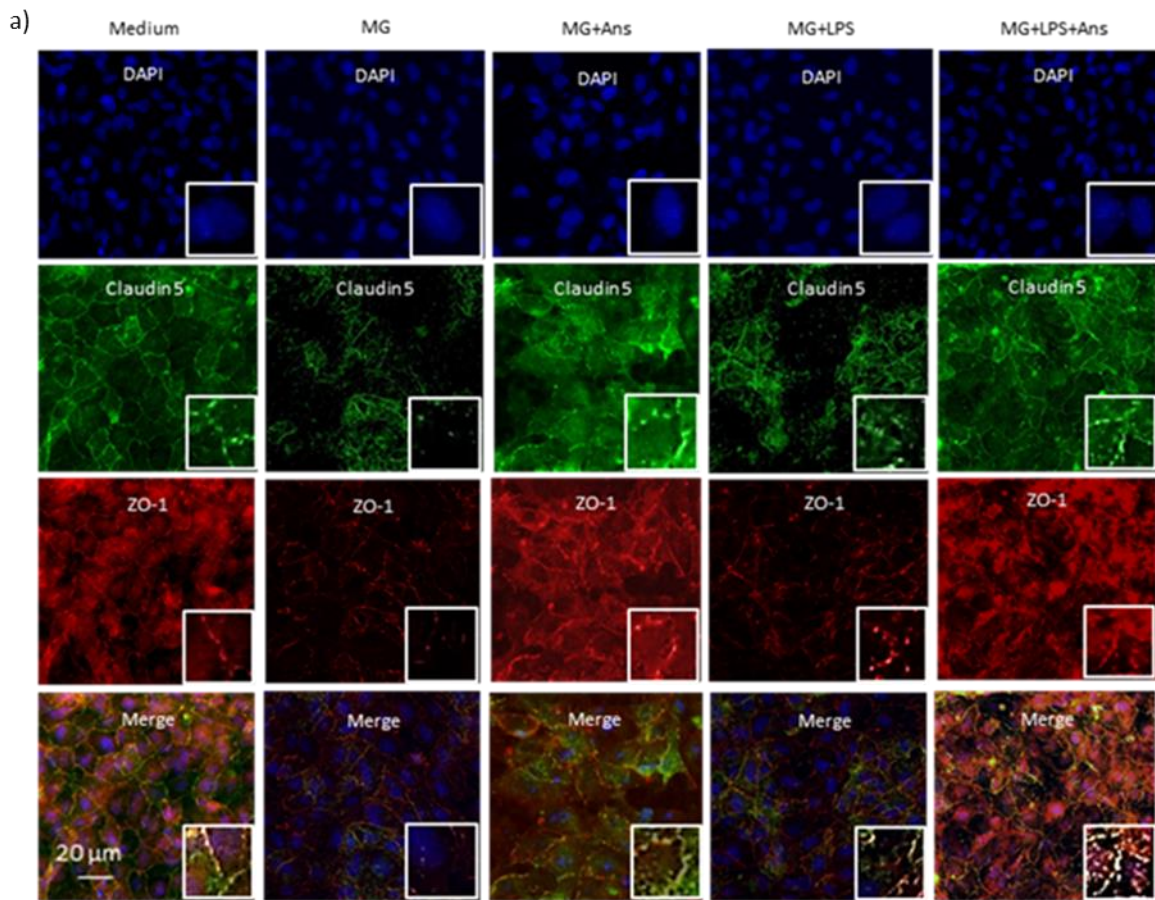


**Figure 10: MG leads to disruption of endothelial barrier forming proteins**

a) Representative immune fluorescence (IF) claudin 5 and ZO-1 stainings in HUVEC treated (from left to right) with media, 1.5  $\mu$ M MG, 1.5  $\mu$ M MG + 0,5 mM Ans, 1.5  $\mu$ M MG + 1  $\mu$ g/ml LPS or 1.5  $\mu$ M MG + 1  $\mu$ g/ml LPS + 0.5 mM Ans for 5 h. MG was administered every 2 h. Blue: DAPI, 488 green: Claudin 5, 555 red: ZO-1. b) Bar graph of relative IF intensity of HUVEC stained for claudin 5. c) Bar graph of relative IF intensity of HUVEC stained for ZO-1.

HUVEC were treated as indicated in a). Each bar represents mean IF intensity relative to media control. Pictures were taken in 20-fold magnification with an ACQUIFIER imaging system. Mann-Whitney U test, concerning symbols: \*  $p \leq 0.05$ ; \*\*  $p \leq 0.01$ ; \*\*\*\*  $p \leq 0.0001$ ; data represent mean and SEM; the experiment was repeated for 3 times. From every image, six randomly selected excerpts were further densitometrically analyzed for IF intensity on selected membrane areas in grey scales.

### 3.2 Anserine effects in a murine model of sepsis (*in vivo*)

As a proof of concept, the aforementioned *in vitro* findings were retranslated back into a mouse model of sepsis. Therefore, the animals were pretreated with Ans in a dosage of 1.500 mg/kg bw i.p. every 12 hours for 3 days (72 hours) before surgery. From wound closure on, Ans was then used as a posttreatment (after CLP) in a dosage of 1.500 mg/kg bw i.p. every 8 hours for a maximum of 36 hours for organ harvesting or 2 days (48 hours) for the survival analysis (Fig. 11a). For the survival analysis, the animals were monitored for 7 days after CLP. The Ans treatment significantly improved survival probability (60 % vs. 36.6 %, \*p = 0.04) in CLP-induced experimental sepsis in mice (Fig. 11b). In addition, the Ans-treated animals were significantly more stable in the clinical scoring and returned to a harmless range more quickly (data not shown). Ans concentrations in harvested organs were measured at 6 hours, 24 hours, and 36 hours after CLP via HPLC. In the kidneys, Ans concentration was continuously and significantly increased within 36 hours up to 40-fold compared to the vehicle group, which received 0.9% NaCl instead of Ans (Fig. 11c). Lung and heart concentrations were only measured at 6 and 24 hours. Ans concentration in the heart tissue was stably increased approximately 25-fold over 36 hours (Fig. 11d), in the lung at 6 hours after CLP Ans concentration was increased approximately 27-fold and after 36 hours still 17-fold compared to the vehicle group. (Fig. 11e). The measurement of the plasma concentration of Ans could only be measured at 6 hours and was 100-fold higher than in the control group (Fig. 11f). At 6 hours the Ans plasma concentration correlated with the tissue concentration of the heart (Fig. 11g) and the lung (Fig. 11h). For the same time points of 6 hours, 24 hours and 36 hours, the capillary leakage was determined through the i.v. injection of EB in the tail vein. Although not significantly, the data revealed that Ans treatment reduced the capillary leakage in the analyzed tissues at almost all time points (Fig. 12). The most prominent differences were observed at 6 and 24 hours in the lung, and small intestine (Fig. 12a, d) and at 36 hours in the kidney and heart (Fig. 12b, c), whereby the difference over 36 hours was most stable in the lung and small intestine. Representative images in Fig. 12g and 12h visualize septic mice following CLP injected with EB at the indicated time points.

Since the results of the investigations at the TJ level *in vitro* were relatively obvious, the lung and kidney tissue of the 24-hour animals were also examined for ZO-1 and claudin 5. Unfortunately, the same clear differences as in the cell culture could not be determined. Visually there was no difference in ZO-1 and claudin 5 distribution or quantity between the kidney tissues from Ans (Fig. 13a) and vehicle treated animals (Fig. 13b). However, the densitometric analysis in the kidney tissue of the 24 h CLP animals, a slightly higher tendency for ZO-1 of Ans-treated animals compared to the vehicle control could be determined (Fig. 13c, left panel), but for claudin 5 no difference appeared (Fig. 13c, right panel). The opposite could be observed in the lung tissue of the 24 h CLP animals. Visually there seemed to be slightly more claudin 5 in the Ans group (Fig. 13d), while there was no difference between

Ans and NaCl treated animals for ZO-1 (Fig. 13e), the difference after densitometric analysis for claudin 5 was more evident, but not significant (Fig. 13f, right panel). However, here too the optical differences between the Ans-treated group and the vehicle control group were only marginal and not comparable with the results generated from cell culture.

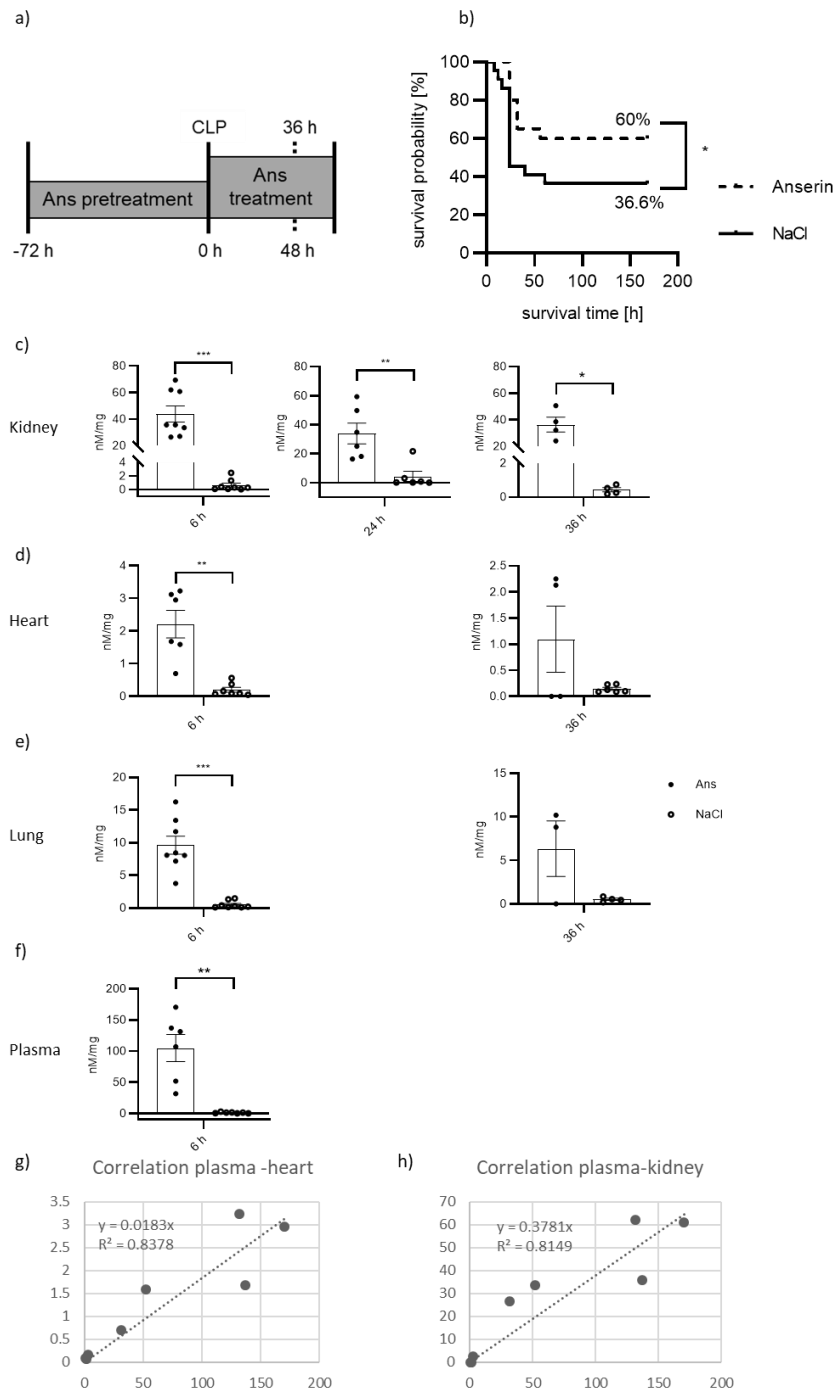


**Figure 11: Ans improves survival of septic mice by stably increasing Ans tissue concentrations**

a) Ans treatment regimen in a murine model of sepsis: C57/BL6 mice received an i.p. Ans pretreatment 72 h before CLP every 12 h and a posttreatment (1.500 mg/kg bw) from wound closure every 8 h until organ harvesting at 36h or until 48h. Controls received 0.9 % NaCl. b) Survival probability [%] of mice up to 168 h following CLP, which were pre- and post-treated with vehicle (n = 22) or Ans (n = 20). Gehan-Breslow-Wilcoxon test. c) Ans tissue concentrations in the kidney of Ans and vehicle treated animals. d) Ans tissue concentrations in the heart at 6 h of Ans and vehicle treated animals. e) Ans tissue concentrations in the lung at 6 h and 36 h of Ans and vehicle treated animals. f) Ans plasma concentrations at 6 h of Ans and vehicle treated animals. Mann-Whitney U test; concerning symbols: \* p ≤ 0.05, \*\* p ≤ 0.01, \*\*\* p ≤ 0.001.

$p \leq 0.001$ . Data represent mean values and SEM. g) 6 h correlation of Ans concentration from heart tissue and plasma samples. h) 6 h correlation of Ans concentration from kidney tissue and plasma samples.

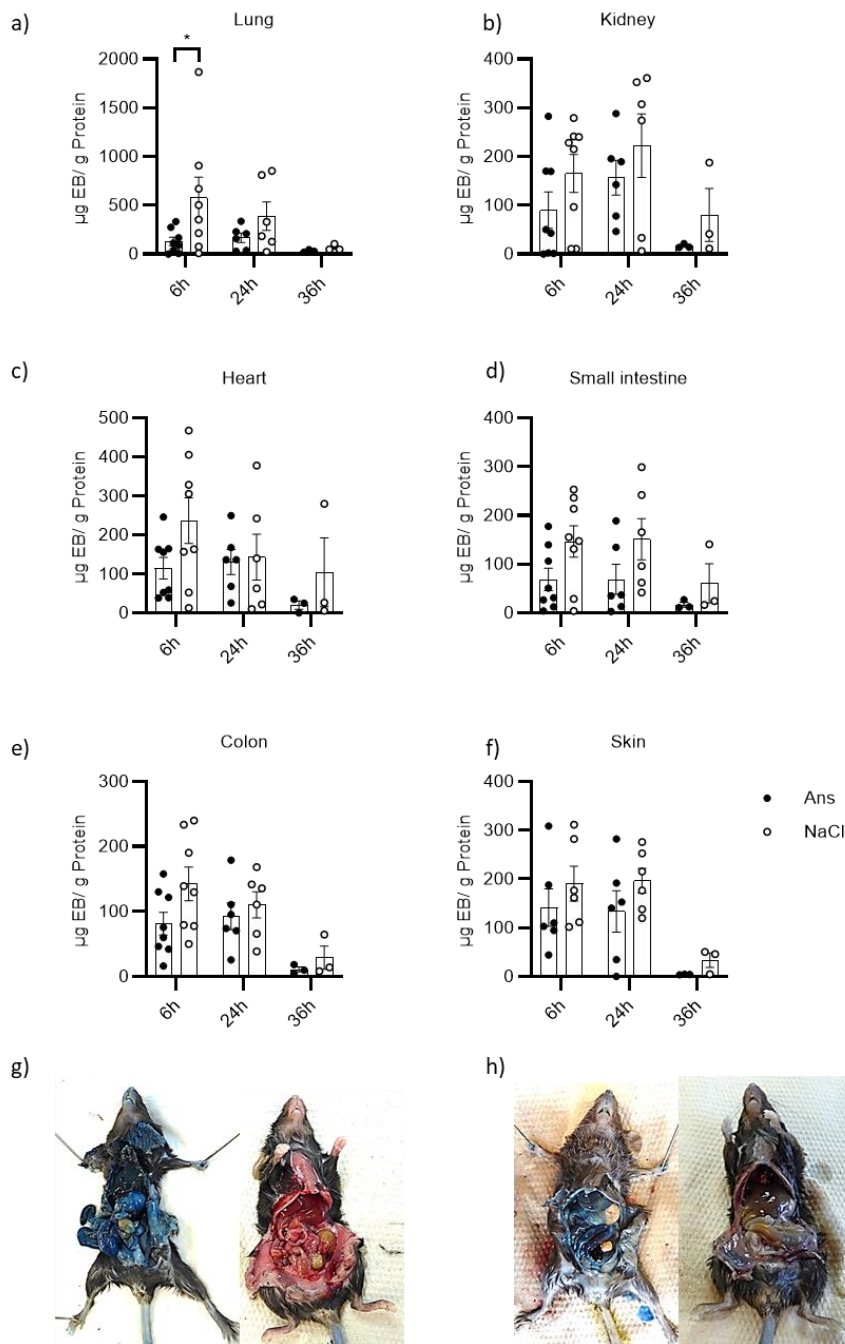


**Figure 12: Ans improves capillary leak of septic mice**

a) Overview of EB concentration in lung. b) Overview of EB concentration in kidney. c) Overview of EB concentration in heart. d) Overview of EB concentration in small intestine. e) Overview of EB concentration in colon. f) Overview of EB concentration in skin. g) Exemplary image of vehicle and Ans treated CLP mouse at 24 h. h) Overview of EB concentration in respective organs at 36 h. Treatment described in Fig. 8a Mann-Whitney U test; concerning symbols: \*  $p \leq 0.05$ . Data represent mean values and SEM.

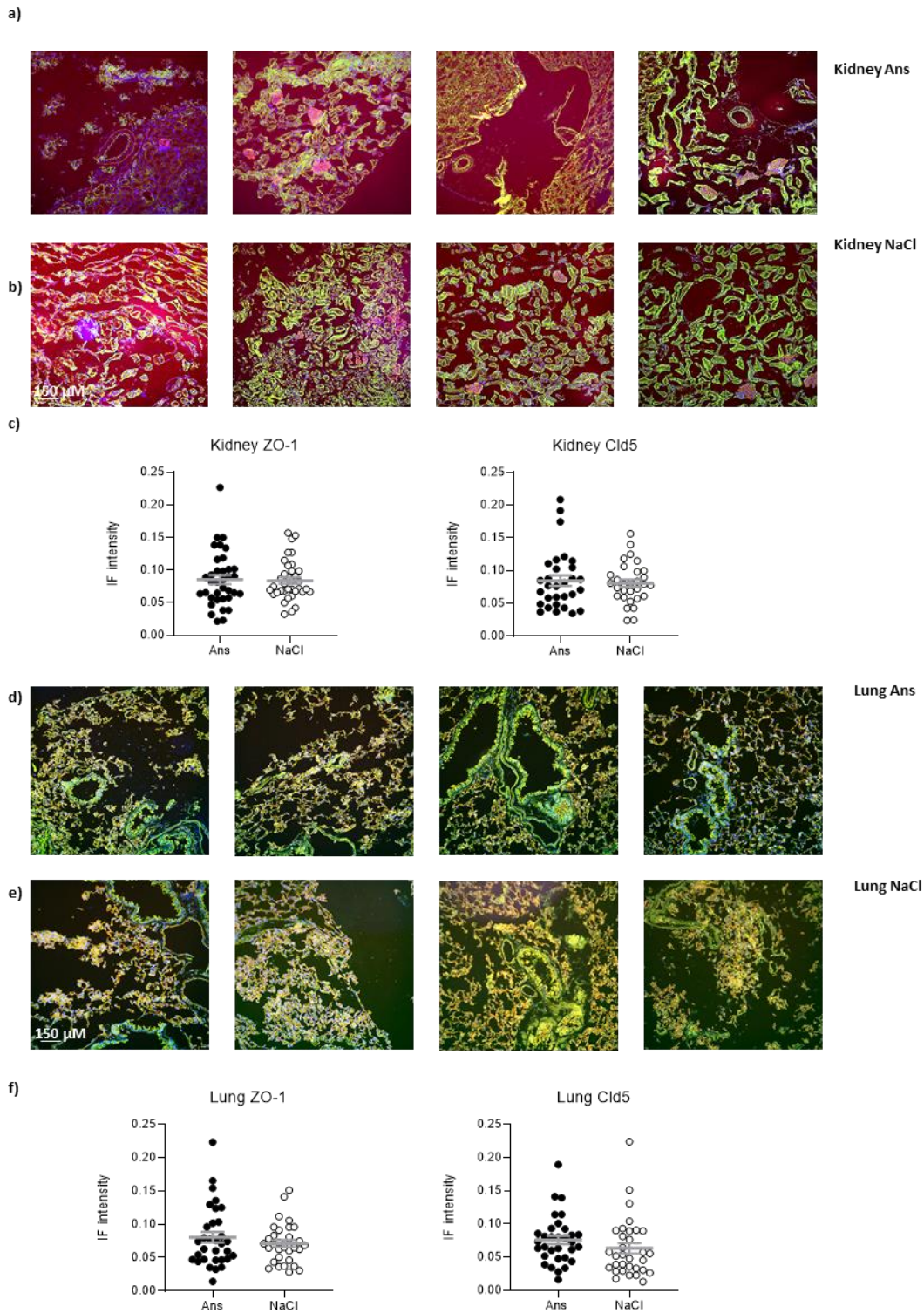


**Figure 13: Ans effect of barrier forming proteins *in vivo***

Representative IF claudin 5 and ZO-1 stainings in kidney tissue of 24 h CLP septic mice, either treated with a) Ans or b) with 0.9 % NaCl. Blue: DAPI, 488 green: Claudin 5, 555 red: ZO-1. c) Bar graph of relative IF intensity of kidney tissue of 24 h CLP septic mice, either treated with Ans or 0.9 % NaCl (n=6). Left panel: ZO-1; right panel claudin 5. Representative IF claudin 5 and ZO-1 stainings in lung tissue of 24 h CLP septic mice, either treated with d) Ans) or with e) 0.9 % NaCl. Blue: DAPI, 488 green: Claudin 5, 555 red: ZO-1. f) Bar graph of relative IF intensity of lung tissue of 24 h CLP septic mice, either treated with Ans or 0.9 % NaCl (n=6). Left panel: ZO-1; right panel claudin 5.

In order to investigate the effect of Ans as a MG-scavenger in tissue respectively *in vivo*, both the lungs and kidneys of the 24-hour CLP animals were examined for AGE distribution using immunohistochemical staining. In fact, there were visible differences in the lung tissues of Ans treated CLP-mice compared to the vehicle control groups (Fig. 14a). Correspondingly, immunohistochemical quantification detected significantly fewer AGEs in the lung tissue of the Ans treated animals (Fig. 14b). The visual trend could also be verified in comparison of the kidney tissue of the septic animals at the 24-hour time point (Fig. 14c) and the effect could even be proved to a significantly greater extent in immunohistochemical quantification (Fig. 14d).

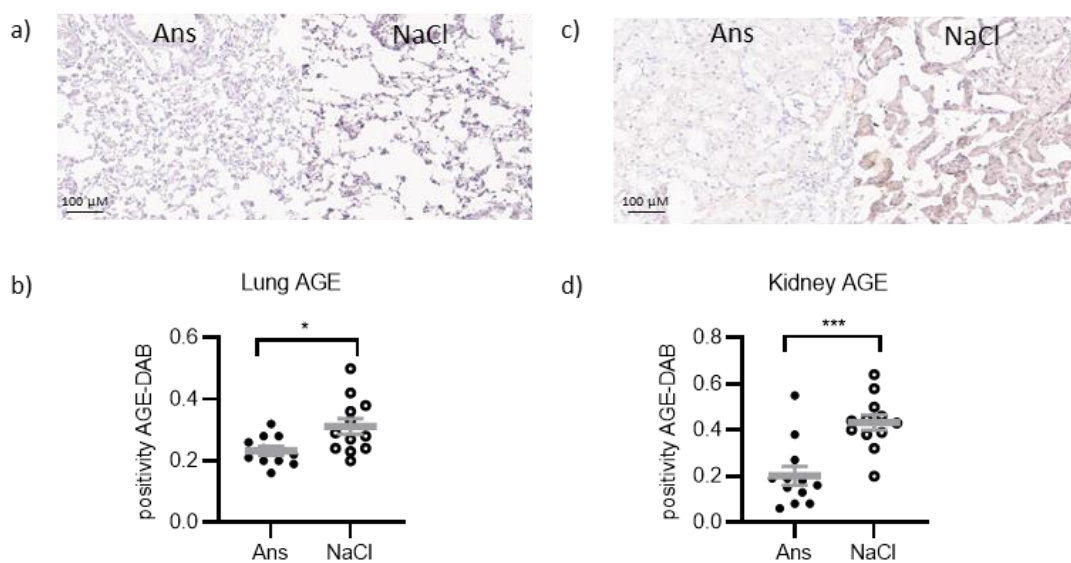


**Figure 14: Ans functions as an effective MG-scavenger *in vivo***

a) Representative images of AGE-DAB staining of lung tissue after 24 h CLP induced sepsis, treatment as indicated in Fig. 8a. b) immunohistochemical quantification of AGE-DAB staining of lung tissue after 24 h CLP induced sepsis, Mann-Whitney U test; Data represent mean values and SEM of n=6. c) Representative images of AGE-DAB staining of kidney tissue after 24 h CLP induced sepsis, treatment as indicated in Fig. 8a. d) immunohistochemical quantification of AGE-DAB staining of kidney tissue after 24 h CLP induced sepsis, Mann-Whitney U test; \* p<0.05, \*\*\* p<0.001. Data represent mean values and SEM of n=6.

### 3.3 Mechanisms of action of MG and Ans *in vitro*

#### 3.3.1 MG, Ans and the extracellular matrix

After an effect of MG and Ans on the barrier-forming proteins could be demonstrated *in vitro* and Ans improved capillary deficiencies *in vivo* as well as reduced AGE formation in lung and kidney tissues, possible mechanisms of action were investigated. First it was examined, whether the capillary leak, respectively the decrease of TER *in vitro* by MG was caused by a breakdown of the extracellular matrix by gelatinases (MMP2 and 9) or collagenases (MMP1 and 8). Therefore, HUVEC were pretreated for 2

hours with either gelatinase inhibitor (MMPi 2/9) or a collagenase inhibitor (MMPi 1/8). This was followed by the MG administration regimen as previously described, adjusting the MG concentration every 2 hours, and observing the TER for a total of 5 hours after MG administration. The MMPi 1/8 was able to reverse the loss of resistance up to a concentration of 150  $\mu$ M MG and maintained resistance at the level of the unstimulated, MG-free control. However, when the supraphysiological dosage of 500  $\mu$ M was applied, the effect did not sustain (Fig. 15a). Interestingly, increasing MG concentrations did not lead to reinforced shedding of the MMP1, but rather showed a reverse effect in MMP1 concentrations in the collected supernatants (Fig. 15b). The observed dose- and time dependent effect of MG in TER reduction was therefore not applicable to MMP1 activity. The pathophysiological dosage of 1.5  $\mu$ M MG resulted in the highest activation of MMP1, whereas increasing dosages did not show considerable effects on MMP1 activity in comparison to the MG-free control (Fig. 15c, left panel). Supraphysiological dosages of MG, as well as Ans treatment only halved MMP1 activity in HUVEC. Cotreatment of MG and Ans showed no difference in MMP1 activity, and also the combined treatment of MG and LPS seemed not to increase the enzyme activity in HUVEC. Curiously, the cotreatment of MG and LPS with Ans led to a significantly higher MMP1 activity and was comparable to that of MG alone or of MG and Ans, although Ans alone rather showed a decrease. LPS alone did not lead to an activation of MMP1 (Fig. 15c, right panel). Using the MMPi 2/9, the same TER tendency appeared as for the MMPi 1/8, except that the resistance did not break off only at the supraphysiological MG dose of 500  $\mu$ M, but already at 150  $\mu$ M (Fig. 15d). MMP2 concentrations did not alter with increasing MG dosages (data not shown). No difference in MMP2 concentration could be detected between the different treatment regimens, regardless of whether MG (with or without Ans), MG and LPS or LPS alone were administered. Only the cotreatment of MG, LPS and Ans seemed to fall below the control level (Fig. 15e). To examine MMP2 gelatinase activity, a zymography was performed from the concentrated supernatants of the TER experiments. There was a very weak gelatinase activity in all samples in general and no MG-titration effect in MMP2 activity. Only the supraphysiological dosage led to a complete inhibition of gelatinase activity (Fig. 15f, left panel). Ans cotreatment did not lead to a change in MMP2 or gelatinase activity in any of the cases, regardless of the MG treatment or in combination with LPS (Fig. 15f, right panel). MMP9 could not be detected in any case (data not shown).



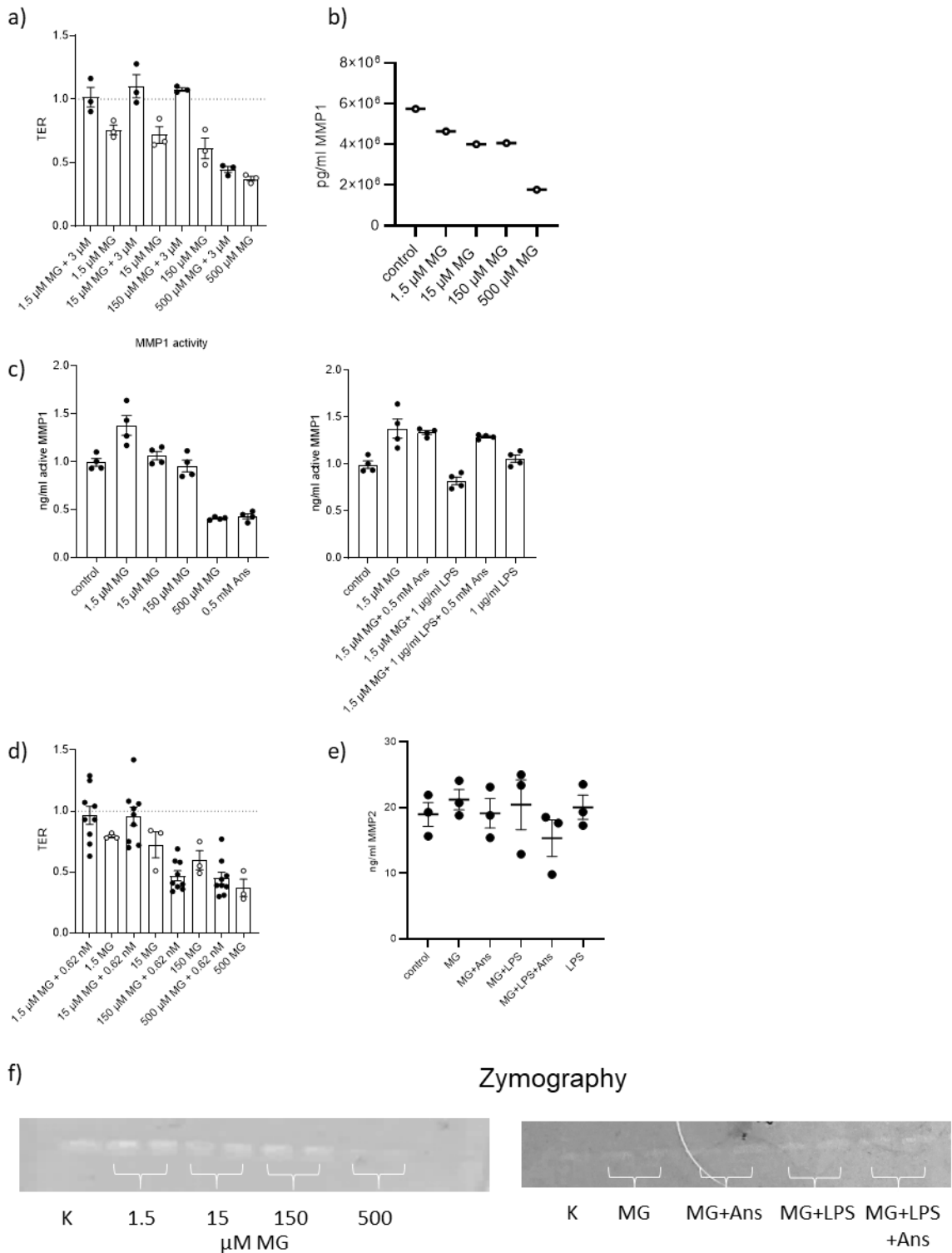
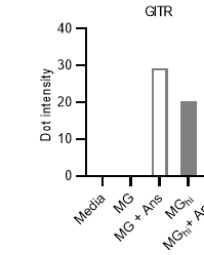
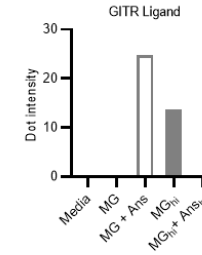
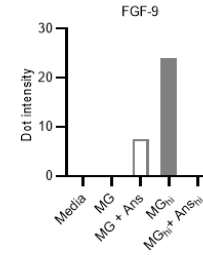
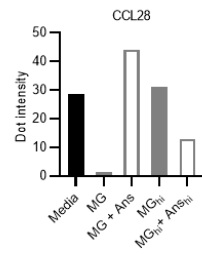
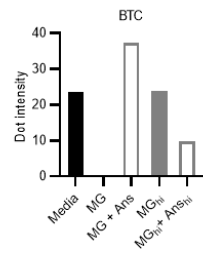
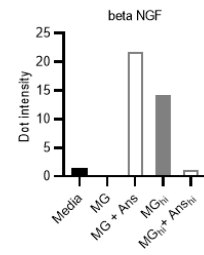
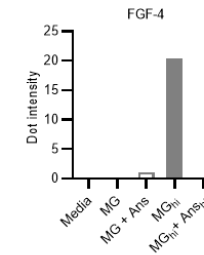
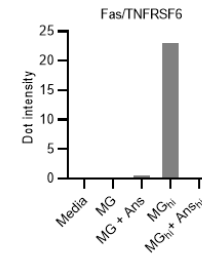
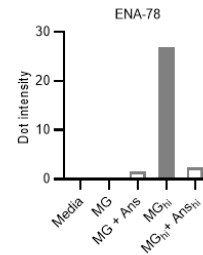
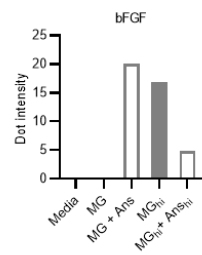
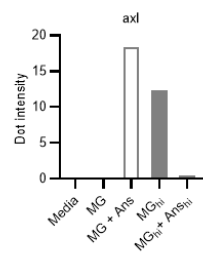
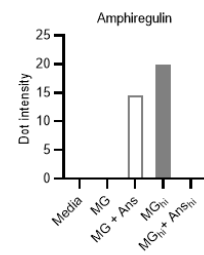
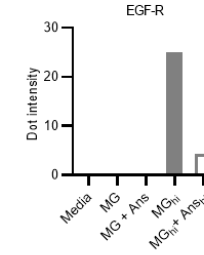
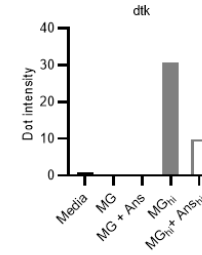
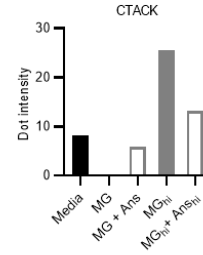
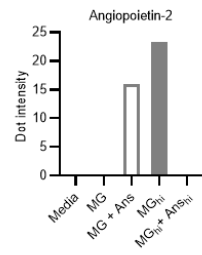
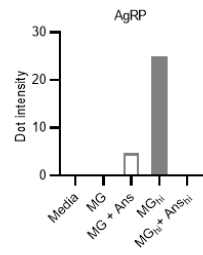
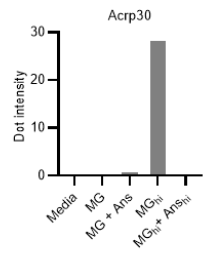


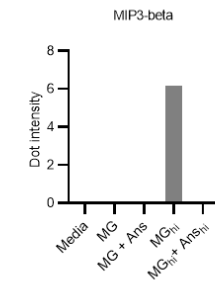
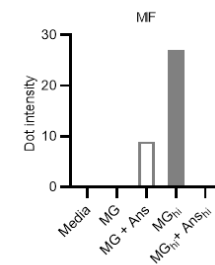
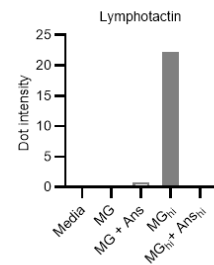
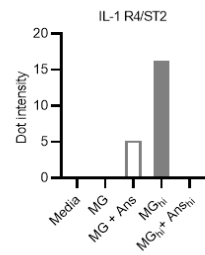
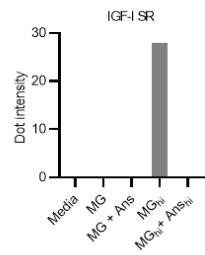
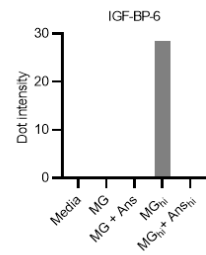
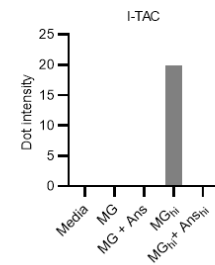
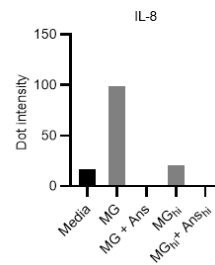
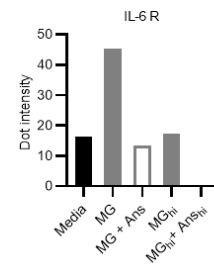
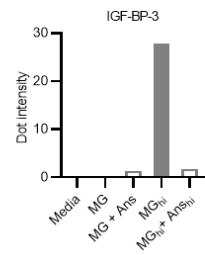
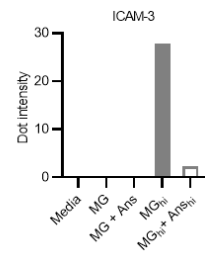
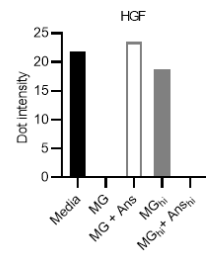
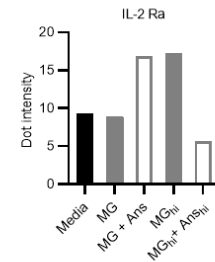
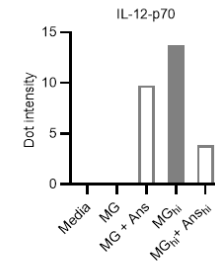
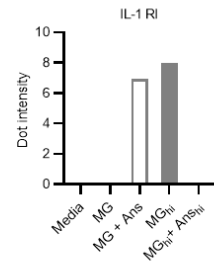
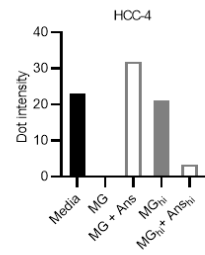
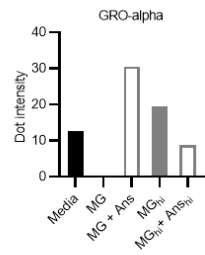
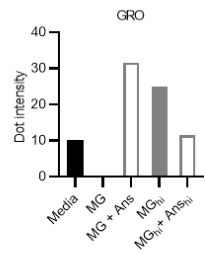
**Figure 15: MG in pathophysiological dosages activates MMP1**

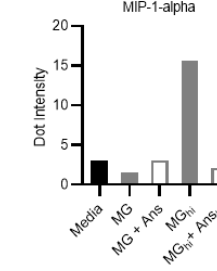
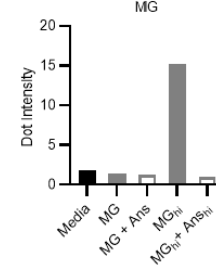
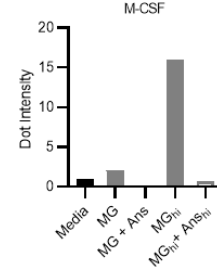
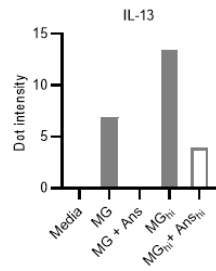
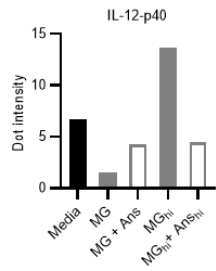
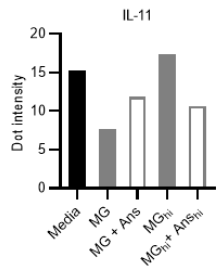
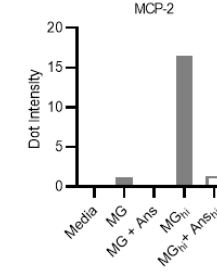
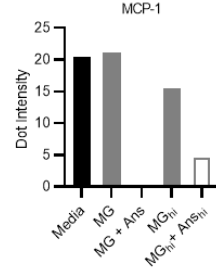
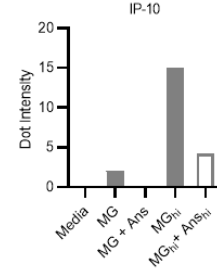
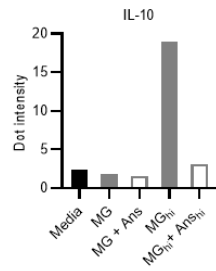
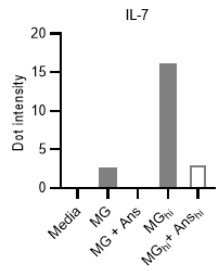
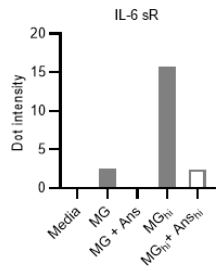
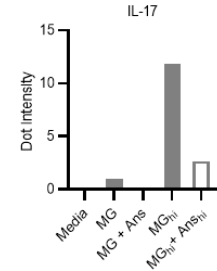
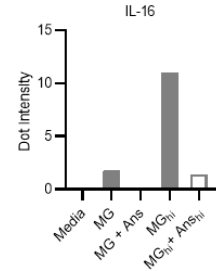
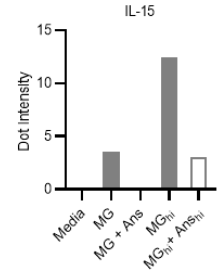
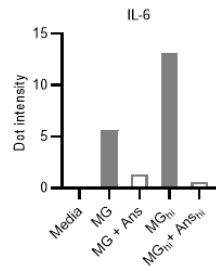
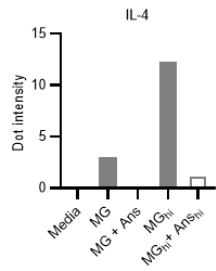
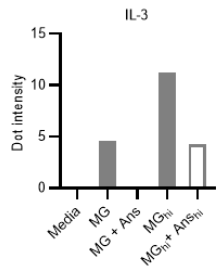
a) Effect of repeated and increasing MG dosages and a single MMP1/8 inhibitor 2 h pretreatment on the 5 h TER of a HUVEC polarized monolayer relative to MG-free control (n=6). b) MMP1 concentration from n=6 up-concentrated supernatants from MG dose titration. c) MMP1 enzyme activity from MG dose titration of up-concentrated supernatants (1:500, left panel) and pathophysiological MG dosages with indicated treatments (1:500, right panel), each n=3. d) Effect of repeated and increasing MG dosages and a single MMP2/9 inhibitor 2 h pretreatment on the 5 h TER of a HUVEC polarized monolayer relative to MG-free control (n=6). e) MMP2 concentration from n=6 supernatants from MG stimulation. Treatment: 1.5  $\mu$ M MG, 1.5  $\mu$ M MG + 0.5 mM Anis, 1.5  $\mu$ M MG + 1  $\mu$ g/ml LPS, 1.5  $\mu$ M MG + 1  $\mu$ g/ml LPS + 0.5 mM Anis, 1  $\mu$ g/ml LPS. Data represent mean values and SEM of n=6. f) Exemplary zymography of up-concentrated supernatants from n=6 MG dose titrations as indicated (left panel) or (from left to right) 1.5  $\mu$ M MG, 1.5  $\mu$ M MG + 0.5 mM Anis, 1.5  $\mu$ M MG + 1  $\mu$ g/ml LPS, 1.5  $\mu$ M MG + 1  $\mu$ g/ml LPS + 0.5 mM Anis. The experiment was repeated for 3 times.

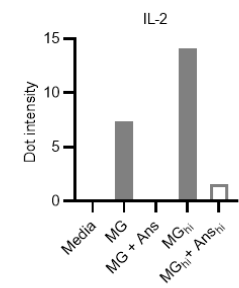
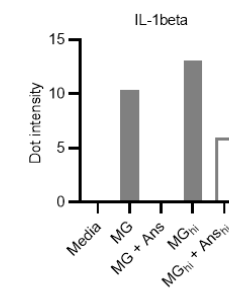
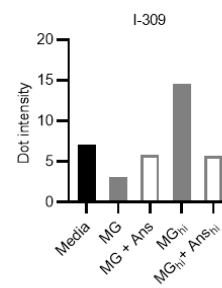
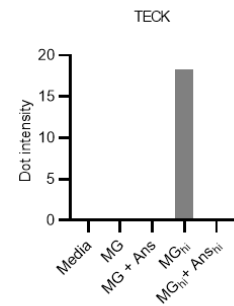
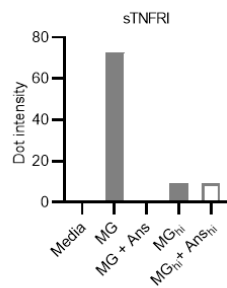
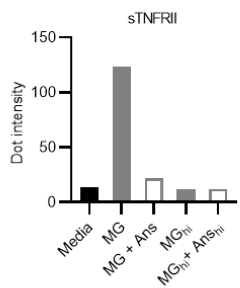
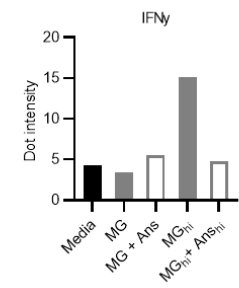
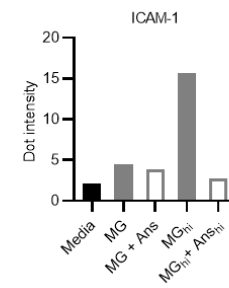
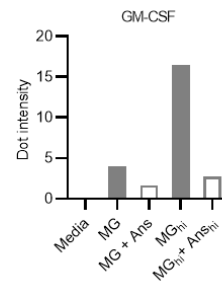
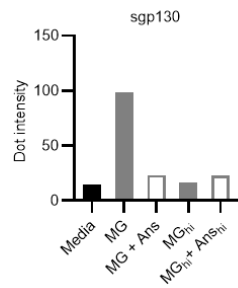
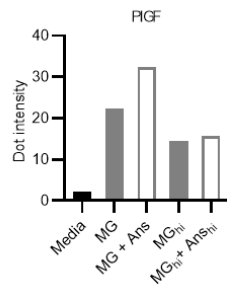
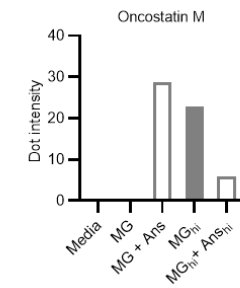
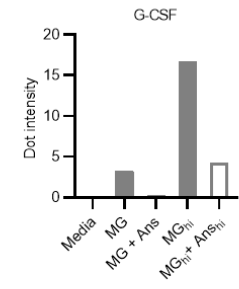
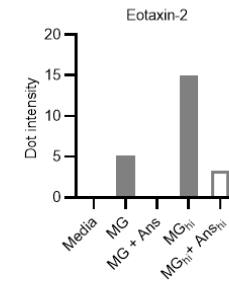
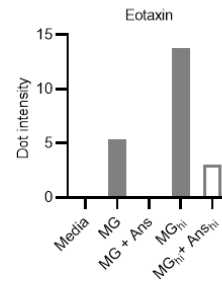
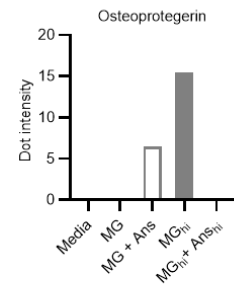
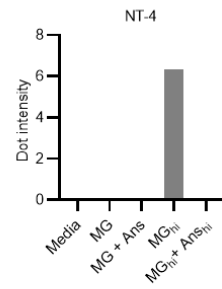
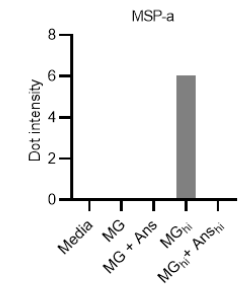
### 3.3.2 Immunological effects of MG

To examine the immunological effects of MG on endothelial cells, human cytokine antibody arrays were used to detect over 60 human proteins in the cell culture supernatants. Therefore, the pathophysiological dosage of MG (1.5  $\mu$ M) and the supraphysiological dosage of 500  $\mu$ M were used. Ans was placed in the same effective relationship. For the high MG dosage, an increased release was observed for almost all cytokines, which in almost all cases could be prevented by the co-treatment with Ans or showed lower values. For a wide range of interleukins, including IL-1 $\beta$ , IL-8 and IL-6, which are particularly associated with endothelial inflammation, the pathophysiological dosage was already sufficient to trigger a cytokine release. A similar picture emerged for various soluble receptors, including soluble TNF receptors (sTNFR), soluble and membrane-bound IL-6rs and eotaxins, as well as granulocyte colony-stimulating factor (G-CSF), granulocyte colony-stimulating factor (GM-CSF) and ICAM-1. However, with the pathophysiological MG dosage, Ans cotreatment did not always show an “anti-inflammatory” effect but raised in some cases the cytokine secretion up to the levels of the supraphysiological MG dose. In some cases, MG even showed a decreased cytokine expression compared to the MG-free control (Fig. 16). In summary, no clear general statement can be made about MG and inflammatory cytokines. There is no clear dosage-dependent effect on inflammatory cytokines and there is also no clear anti-inflammatory spectrum of action for Ans. However, the meaningful results of the pathophysiological MG dosage in relation to IL-1 $\beta$  were further investigated because of their importance within the context of sepsis. Because of the presence of IL-1 $\beta$  after MG treatment, the caspase-1 activity, respectively activation of the NLRP3 inflammasome was determined. In this case, because of the method handling, MG, and/or if indicated LPS with and without Ans was added once and the activity was observed over 3 hours. Already after 30 min MG was able to activate caspase-1 to a comparable extent as LPS and rose to a plateau after 90 min, which was maintained over the rest of the 3 hours (Fig. 17a). The combination of MG and LPS was also on the same level and no additional effect of the two stimulants could be seen (Fig. 17a). The addition of Ans to MG had an almost imperceptible effect on caspase-1 activity (Fig. 17b). The Ans effect as cotreatment for MG and LPS combined was larger than that of MG and Ans alone, but also not of great magnitude (Fig. 17c). MG treatment did not lead to cell death, even in supraphysiological doses, as confirmed by the vitality staining (Fig. 17d). Besides the MG increased IL-1 $\beta$  values (Fig. 16) and the increased caspase-1 activity, it was determined if the precursor of IL-1 $\beta$  was also more secreted through MG. The pathophysiological dosage of 1.5  $\mu$ M lead to an almost no noticeable difference compared to the MG-free media control. However, with increasing MG dosages, a dose titration effect could be observed, which broke again with the supraphysiological dosage (Fig. 18a). The addition of Ans in the pathophysiological effective spectrum tended to fall below the level of the unstimulated or MG-free media control but showed no clear perceptible effect (Fig. 18b).









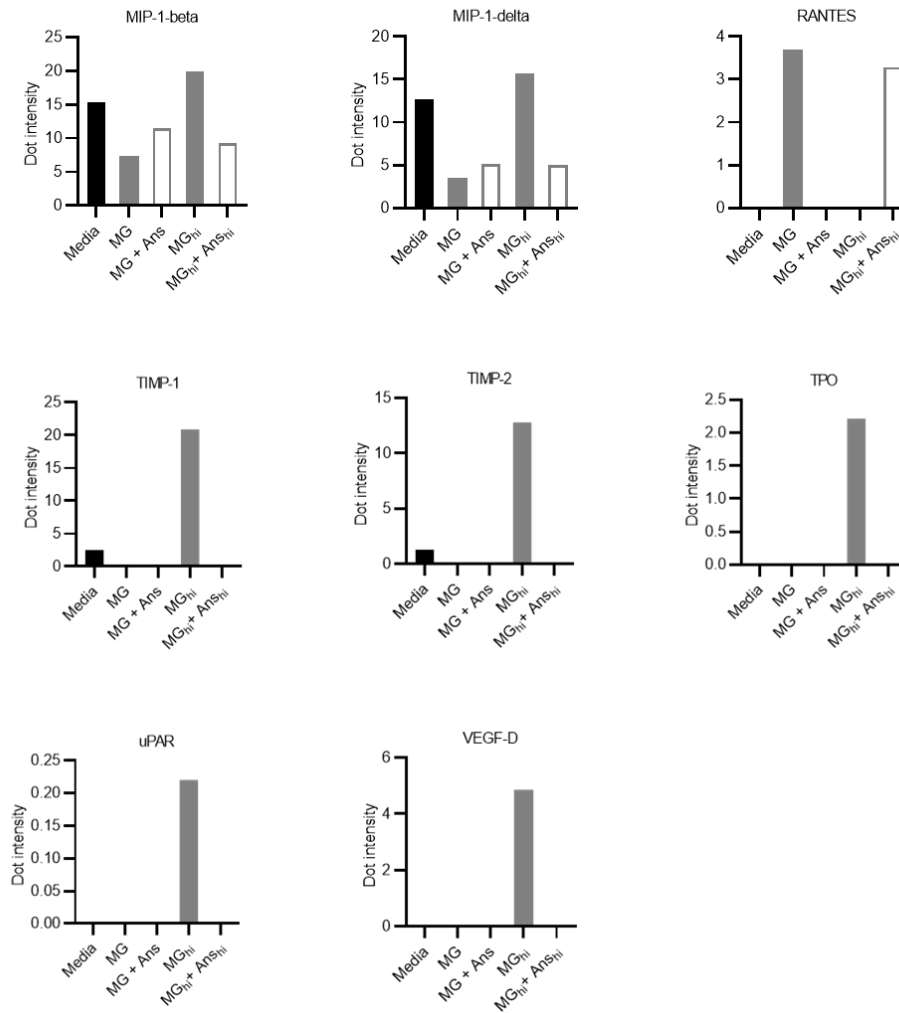


**Figure 16: Inflammatory cytokine profile from MG- and Ans stimulated HUVEC**

Inflammation-, apoptosis-, and angiogenic-related cytokines, excreted from HUVEC monolayer after incubation with MG (1.5  $\mu$ M MG), MG+Ans (1.5  $\mu$ M MG+0.5 mM Ans), MG<sub>hi</sub> (500  $\mu$ M MG), MG<sub>hi</sub>+Ans<sub>hi</sub> (500  $\mu$ M MG+170 mM Ans) for 5 h in comparison to MG-free media control. In pathophysiological dosages MG was administered every 2 h. In supraphysiological (hi) dosages, MG as well as Ans were administered every 2 h. Bar graphs represent values of batched supernatants from n=4 experiments.

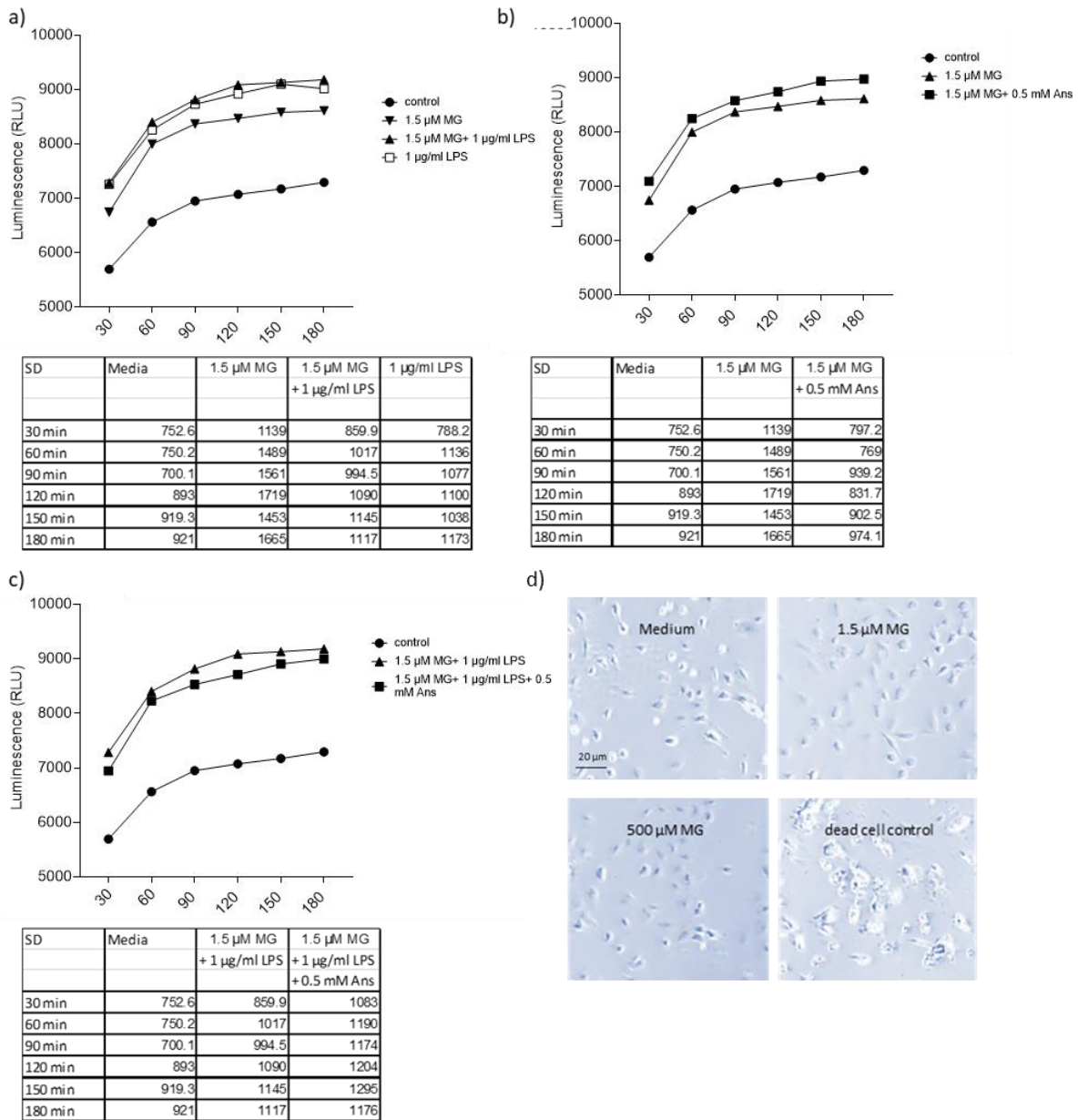


**Figure 17: MG leads to caspase-1 activation in HUVEC independent of cell death.**

a) Mean values of HUVEC caspase-1 activity of MG, LPS or MG and LPS combined in a time course of 3 h. SDs below. b) Mean values of HUVEC caspase-1 activity of MG with and without Ans cotreatment in a time course of 3 h. SDs below. c) Mean values of HUVEC caspase-1 activity of MG and LPS with and without Ans cotreatment in a time course of 3 h. SDs below. d) Examples of HUVEC in situ Trypan blue vitality staining of patho- and supraphysiological MG stimulation after 5 h in comparison to MG-free media and dead cells treated with 100 % EtOH. The experiment was repeated 3 times. RLU: relative luminescence units. Data represent mean values and SEM of n=3.

In order to check whether all these effects were possibly mediated by the PRR RAGE, the TER system was returned to. It was found here that a two-hour pretreatment of the HUVEC with the RAGE inhibitor FPSZM-1 completely prevented the complete drop in TER up to 15  $\mu$ M MG and at least increased the resistance up to the supraphysiological dose of 500  $\mu$ M. A MG dose-dependent effect was observed with and without FPSZM-1 (Fig. 19).



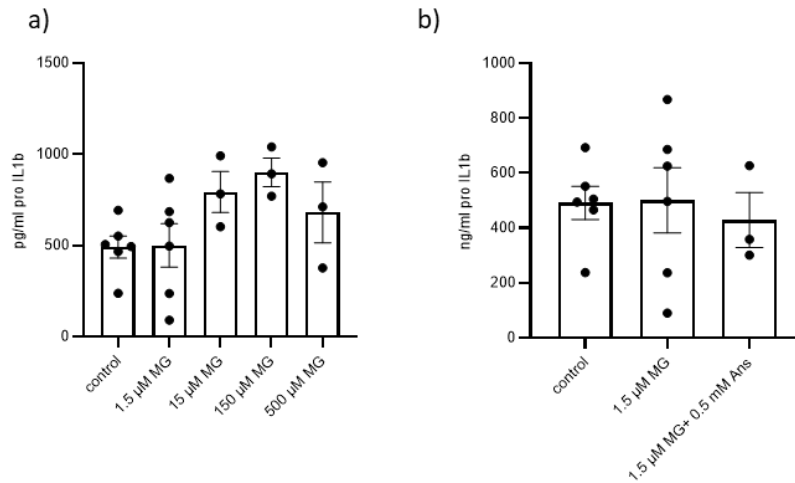


**Figure 18: MG dose-dependently increases human pro IL-1beta secretion from HUVEC.**

a) Human pro IL-1beta concentration of MG dose titration from HUVEC cell lysate. b) Human pro IL-1beta concentration of MG and Ans cotreatment from HUVEC cell lysate. Cell lysates were created after 5 h with the indicated treatments. Data represent mean values and SEM of n=6.

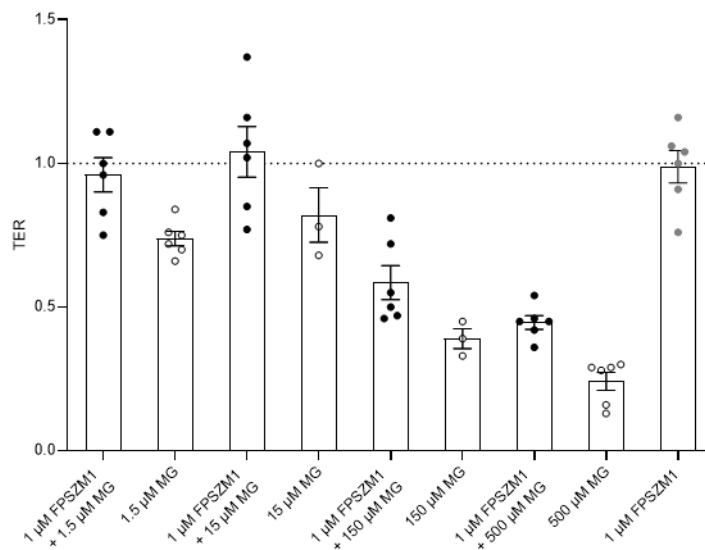


**Figure 19: The MG effect on TER is RAGE-dependent**

Effect of repeated and increasing MG dosages and a single RAGE inhibitory 2 h pretreatment with FPSZM-1 on the 5 h TER of a HUVEC polarized monolayer relative to MG-free control. Data represent mean values and SEM of n=6.

The activation or ligand binding of RAGE can lead to the activation of various signaling pathways or transcription factors. Some of these signaling pathways were examined in the next step under the treatment of MG in FACS. TNF was used as a positive control in all cases. Contrary to expectations, a reduced phosphorylation of the NF-κB subunit p65 could be observed for increasing MG dosages. TNF, on the other hand, led to an increased phosphorylation of p65 after 30 minutes (Fig. 20a). Next it was

investigated whether MG was able to activate protein kinase B (Akt) (essential part of the PI3K (phosphatidylinositol 3-kinase) pathway). However, after 30 minutes even the signal for the positive control seemed to appear weak. MG was not really capable to induce a noticeable activation of Akt but showed a similar trend for the increasing MG dosages, namely rather a decrease in Akt-phosphorylation (Fig. 20b).

Then the activation or phosphorylation of MAPK by MG was examined. Here p38 and JNK (c-Jun) were chosen. After just 15 minutes, TNF almost doubled p38 phosphorylation compared to the untreated control. MG again showed a slight titration effect. With a dosage of 150  $\mu$ M, an increase in p38 phosphorylation comparable to that of TNF could be achieved in the same period of 15 minutes. Increasing to the supraphysiological MG dosage showed no difference (Fig. 20c). The same tendency could be shown for the phosphorylation of c-Jun. Here, after 30 min, TNF led to a more than twice as high phosphorylation of c-Jun compared to the untreated control, and here, too, 150  $\mu$ M MG and the supraphysiological dose of 500  $\mu$ M were able to activate c-Jun to a comparable extent (Fig. 20d).

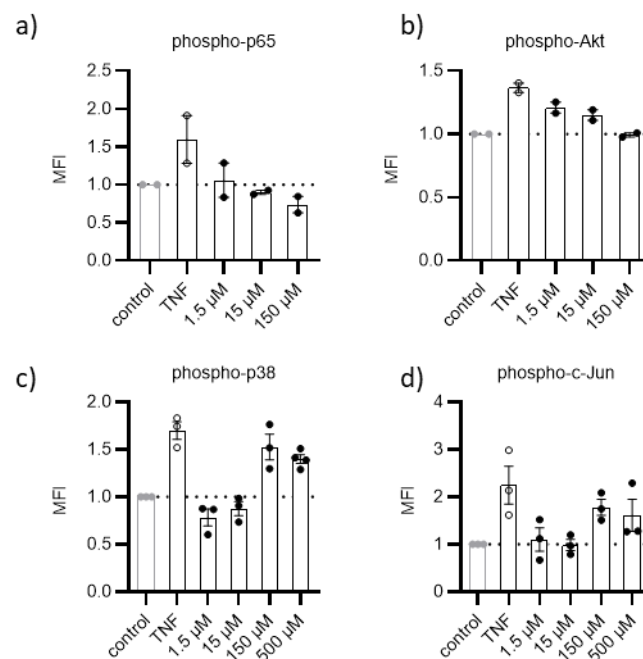


**Figure 20: MG activates MAPK but not the NF- $\kappa$ B subunit or Akt kinase**

a) Mean fluorescence Intensity (MFI) of MG treatment as indicated and 50 ng/ml TNF for phosphorylation of p65 after 30 min. b) MFI of MG treatment as indicated and 50 ng/ml TNF for phosphorylation of Akt after 30 min. c) MFI of MG treatment as indicated and 50 ng/ml TNF for phosphorylation of p38 after 15 min. d) MFI of MG treatment as indicated and 50 ng/ml TNF for phosphorylation of c-Jun after 30 min. Data represent mean values and SEM of n=3.

It was further investigated whether the observed Ans effects in TER were related to these signaling pathways. Therefore, the previously described Ans cotreatment and the 2 hours Ans pretreatment

were transferred to flow cytometric experiments. The Ans cotreatment was adjusted to the original effectiveness and added once, MG was added once. Ans cotreatment did neither prevent p38 phosphorylation (Fig. 21a), nor phosphorylation of c-Jun (Fig. 20b). Unfortunately, the effect was also not available in the Ans pretreatment setting, neither for p38 phosphorylation (Fig. 21c), nor for phosphorylation of c-Jun (Fig. 21d).

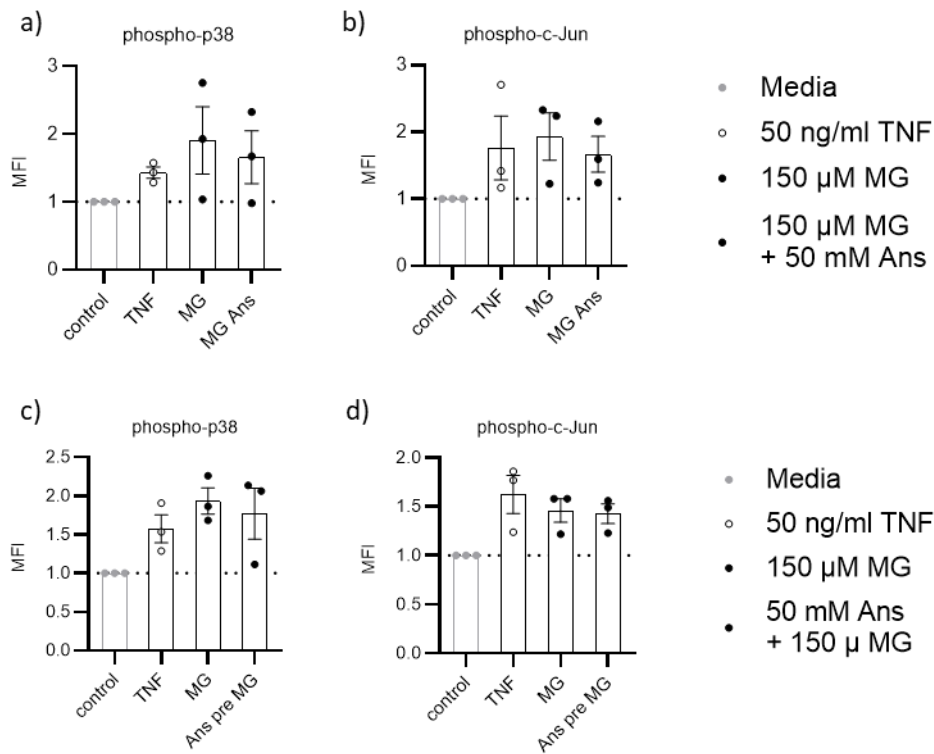


**Figure 21: Ans does not exert effects on MG-induced p38- or c-Jun phosphorylation**

a) MFI of MG treatment alone or as cotreatment with Ans as indicated and TNF for phosphorylation of p38 after 15 min. b) MFI of MG treatment alone or as cotreatment with Ans as indicated and TNF for phosphorylation of c-Jun after 30 min. c) MFI of MG treatment alone or as a 2 h pretreatment with Ans as indicated and TNF for phosphorylation of p38 after 15 min. d) MFI of MG treatment alone or as a 2 h pretreatment with Ans as indicated and TNF for phosphorylation of c-Jun after 30 min. Data represent mean values and SEM of n=3.

To determine whether the MG induced p38 and c-Jun phosphorylation was RAGE dependent, the cells were pretreated with FPSZM-1 for 2 hours and then treated for the respective time period with 150  $\mu$ M MG and analyzed for p-38 or c-Jun phosphorylation. Interestingly, MG induced phosphorylation of p38 did not seem to be RAGE-dependent (Fig. 22a), however c-Jun phosphorylation of MG could successfully be prevented by using the RAGE inhibitor FPSZM-1 (Fig. 22b).

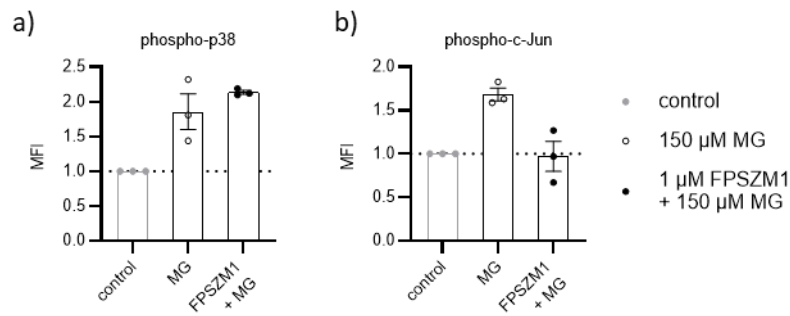


**Figure 22: c-Jun but not p38 phosphorylation by MG is RAGE dependent**

a) MFI of MG treatment alone or pretreated with FPSZM-1 of phosphorylation of p38 after 15 min. b) MFI of MG treatment alone or pretreated with FPSZM-1 of phosphorylation of c-Jun after 30 min. Data represent mean values and SEM of n=3.

## 4. Discussion

In many pathological contexts such as diabetes (Rohlenova et al., 2018, Schalkwijk and Stehouwer, 2005), atherosclerosis (Mäkinen et al., 2014, Stratmann et al., 2016, Brownlee, 2001) or high blood pressure (Prasad and Mishra, 2017), a harmful effect on the endothelium or on vascular cells is attributed to MG, even if the underlying molecular and biochemical functions have not been fully investigated. In the context of increased vascular permeability in sepsis or septic shock, however, there is no data available at all. Therefore, this work investigated how MG affects EC *in vitro* and how to influence MG-induced damage *in vitro* and in an *in vivo* model of murine sepsis.

### 4.1 Ans shows protective and restoring effects against MG induced endothelial damage *in vitro*

The *in vitro* MG effects were investigated by using resistance and transport measurements, as well as antibody-based assays, vitality staining and flow cytometry. These experiments were able to show that pathophysiological dosages of MG lead to a reduction in the TER HUVEC monolayer in a dose- and time-dependent manner and at the same time to an increased paracellular leakage. This effect could be explained *in vitro* by the visualization of damage or by a restructuring of the barrier-forming proteins claudin 5 and ZO-1.

Apparently, the effects of MG seem to be extremely cell-type specific, since, for example, in human brain microvascular endothelial cells supraphysiological MG dosages induced TER loss which correlated with occludin-glycation (Li et al., 2015). In immortalized mouse brain endothelial cells, 750 and 1000  $\mu$ M MG reduced the protein levels of occludin, claudin 5 and ZO-1, which was accompanied by an

increased paracellular leakage with a decreased TER (Kim et al., 2020). In line with that, exposure of brain micro vessels to hyperglycemic conditions or AGEs *ex vivo* resulted in significant abnormalities in membranous distribution of occludin and claudin 5 (Rom et al., 2020). Contrariwise, in mouse cardiac endothelial cells (MCEC) supraphysiological MG stimulation was found to impair barrier functions by non-significantly reducing TER and not affecting permeability to large molecular compounds (Fleming et al., 2022). However, these studies lack of clinical or translational relevance of the used MG concentrations and were investigated in the context of diabetes mellitus. The concentration of MG used in these studies was up to 1.000  $\mu$ M, which is approximately 200-fold higher than the plasma concentration observed in patients with diabetes (Li et al., 2015). In the context of sepsis and septic shock, the HUVEC model is physiologically representative for the human vascular endothelium, allowing to investigate the physiological and pathological effects of different stimuli (Maciag et al., 1981). This model has already been chosen for a broad range of biological processes and diseases, such as inflammation (Onat et al., 2011), cancer (Rhim et al., 1998) and regenerative medicine (Bachetti and Morbidelli, 2000). Furthermore, in this investigation, for the most part, the pathophysiological MG concentrations measured in septic patients (Brenner et al., 2014) were used. Also, in a diabetic context, Ans has been described to have protective effects on epithelial cells (Peters et al., 2018). In a hyperuricaemic mouse model, anti-hyperuricaemic and anti-inflammatory effects on the intestinal epithelium were described for Ans (Han et al., 2021). However, in the context of inflammation, data is limited. E.g., in a double-blinded randomized controlled trial, analysis of peripheral blood mononuclear cells (PBMCs) showed decreased expression of C-C Motif Chemokine Ligand 24 (CCL24) after oral intake of 300 mg Ans in elderly people (Katakura et al., 2017). However, Ans has never been studied in the context of sepsis or septic shock and endothelium. In this study carried out here, not only a stable protective, prophylactic as well as rescuing effect of Ans against MG-induced damage to the endothelium could be shown, but also for the first time ever a long-lasting, protective effect against LPS-induced damage. Over time, other MG-scavengers and antioxidants could not achieve a comparable stable effect as Ans for either MG or LPS. Also, at the level of the barrier-forming proteins, the Ans treatment led not only to a preservation of the proteins but even to an increase, despite MG and/or LPS treatment. These results suggest that Ans may exert vascular strengthening effects via increased membrane accumulation of these proteins.

#### 4.2 Ans reduces MG-induced endothelial leak, tissue AGE formation and improves survival in septic mice (*in vivo*)

Since Ans showed a protective effect on the endothelium in the cell culture experiments, its application using a CLP-induced mouse model of sepsis with a focus on capillary leakage, lungs and kidneys is

absolutely reasonable, since these organs are particularly affected by the after-effects of increased vascular permeability and subsequent organ failure. Here, too, it should be emphasized that the data collected are unique and an application of Ans in a septic context has never been investigated before. Furthermore, in several mice trials, Ans was administered over a long period of time via food or water (Sakano et al., 2022) and mostly investigated in the diabetic context (Everaert et al., 2021). Intraperitoneal Ans administration has only been investigated in a neuronal context over a longer period of time (Kubomura et al., 2010, Min et al., 2008). In the here presented study, mice received a three-day i.p. pretreatment and a posttreatment for two days after CLP and were then observed for survival for seven days. The Ans-treated mice showed a survival advantage of almost 25 % and were significantly better in clinical scoring. This effect could be related to an accumulation and thus greater availability of Ans in the various tissues or rather a resulting increase in antioxidant or scavenging activity. For organ harvesting, the animals were pretreated i.p. for 3 days and posttreated with Ans for a maximum of 36 hours following CLP. Over 36 hours the Ans concentration in the kidney was significantly increased, being in line with previously published data from diabetes research (Peters et al., 2012). As already published in other contexts, Ans accumulation can also be found in the heart muscle (Blancquaert et al., 2016) and in the kidneys (Peters et al., 2018). The increased plasma concentrations of Ans in correlation with that of the tissues indicate an adequate distribution of the active ingredient despite ongoing sepsis. The accumulation in the lungs and kidneys could be of greater relevance, since these organs are known to be particularly affected by multiple organ failure in sepsis or septic shock (Caraballo and Jaimes, 2019). Since Ans had obviously strengthened the barrier-forming proteins of the endothelial cells in the previous *in-vitro* studies, the capillary leakage of the CLP-induced septic animals was examined in the acute model up to 36 hours. There was less capillary leakage, especially in organs where the Ans concentrations had previously been elevated. The effect in the lungs and kidneys was again particularly pronounced. In the heart, however, the effect seemed to fluctuate at 24 hours, but stabilized again at 36 hours, which could indicate that an ongoing administration over 36 hours could be beneficial for the cardiovascular system. A similar effect was also observed in the colon, while in other organs such as the small intestine the effect over 36 hours showed the same stable tendency on capillary leakage. This suggests that the effects of Ans are organ specific. Furthermore, Ans was administered i.p. and therefore a stable effect in the area of the abdominal cavity had to be expected due to the high resorption power. Unfortunately, the vascular strengthening effect could not be explained by clustering of ZO-1 or claudin 5 since there was no difference between the Ans-treated and vehicle-treated for ZO-1 in the lungs and kidneys in the *in vivo* model. For claudin 5 there was also no visible difference, although there was a tendency for claudin 5 to increase in the lungs of Ans-treated animals. In principle, the results can be explained by the fact that work is carried out very isolated *in vitro* and a direct effect of MG or MG and LPS was shown. However, sepsis or septic

shock is systemic. Another possibility is that the capillary vessels are not visible due to the slice size and an effect cannot be visualized. Furthermore, there are 27 different claudins alone (Günzel and Yu, 2013). In addition to claudins, ZO-1 also interacts with occludins (Pummi et al., 2004), which were not further investigated in this setting. In another mouse CLP model of sepsis, it was demonstrated that occludin and claudins were displaced from raft fractions to non-raft fractions membrane microdomains and redistribution of claudins in epithelial cells of the colon lead to alteration of TJ architecture and barrier dysfunction during the development of polymicrobial sepsis (Li et al., 2009). In a rat CLP model sepsis-induced intestinal epithelial permeability changes were caused by damage of the intestinal mucosa including TJ disruption and of ZO-1, claudin 1 and occludin (Zhang et al., 2015). In a comparative sepsis experiment using CLP and *Pseudomonas aeruginosa* pneumonia, the intestinal permeability was examined. It was determined that claudin 5 and occludin were decreased in both sepsis models. Alterations in occludin were detectable as early as 1 hour after CLP. Pneumonia also had a marked decrease in ZO-1 not seen in CLP. The TJ changes in CLP and pneumonia are similar but not entirely identical. This suggests that most TJ changes are common in critical illness, although there appear to be components that are model-specific (Yoseph et al., 2016). A systematic evaluation in brain samples from septic patients showed that positive occludin, ZO-1 and claudin 5 staining were absent from the endothelial cells and that high organ failure scores and biomarkers of systemic inflammation were associated with a loss of TJ proteins (Erikson et al., 2020). However, the majority of studies examine either the intestinal barrier or the blood-brain barrier in sepsis or investigate the barriers *in vitro* (Ni et al., 2019). Recently in a rat CLP model with acute kidney injury, they found the positive expression level of ZO-1 in kidney tissue to be significantly reduced (Yang et al., 2020). Here, too, the various damages seem to be extremely specific to the organ, model, and time. As a result, it remains a challenge even today of transferring such results from bench to bedside (Fernández-Sarmiento et al., 2022). In contrast to the immunofluorescence staining of the TJs of the lungs and kidneys, a clear effect on AGE accumulation in the tissues mentioned could be shown for Ans in the histopathological investigations. This effect is most likely related to previously measured Ans concentrations in the respective tissues. Furthermore, they support the data on capillary leakage, since it has been shown several times that AGEs are able to damage the endothelium or contribute to endothelial dysfunction (de la Cruz-Ares et al., 2020, Krishnasamy et al., 2020).

### 4.3 MG does not increase MMP shedding or activity in HUVEC *in vitro*

To further understand the mechanistic actions of MG and Ans, respectively proof of principles, the *in vitro* model was returned to. LPS, ROS and pro-inflammatory cytokines are described to be involved in activated MMP shedding (Chappell et al., 2009, Goligorsky and Sun, 2020, Uchimido et al., 2019, Cao et al., 2019b). In different models, it has been described that RCS respectively AGEs lead to activation of MMP. In kidney proximal epithelial cells MG derived AGEs induced activation of MMP-2 and MMP-9 via an AGE-RAGE interaction (Jeong et al., 2020, Nam et al., 2021). In intravitreally injection experiments with mice, MG activated retinal MMP-2 and MMP-9 (Kim et al., 2012). Another study with rats came to similar results, in which MG injection into the vitreous cavity of one eye led to a general activation of the MMPs (unspecified) (Kamiya et al., 2023). In the context of sepsis, endothelium and MMPs, the gelatinases (MMP2 and 9) or collagenases (MMP1 and 8) have been described to be associated with severity, coagulation state, circulating cytokine levels and mortality (Lorente et al., 2014, Opal and van der Poll, 2015, Fang et al., 2022, de Souza et al., 2015). In the TER measurements of the here presented study, both collagenase and gelatinase inhibitors were able to limit the loss of resistance up to a certain concentration. Surprisingly, a negative dose dependency for MG was found for MMP1 shedding, which was also confirmed in a similar way for enzyme activity. The pathophysiological dose, which was also measured in septic patients (1.5  $\mu$ M) (Brenner et al., 2014), induced the highest enzyme activity, comparable to LPS. However, Ans showed no effect, so that the mechanism of action of Ans runs via other pathways as an inhibition of the MMPs. Supraphysiological doses led to a kind of standby mode of the cells, which still showed signs of vitality but no longer had any relevant enzyme activity. The MMP2 concentration shows no relevant increase by MG and no significant change by the administration of Ans. An activity measurement in the form of zymography showed, that escalating MG dosages caused no changes in enzyme activity. As with MMP1, the supraphysiological dose led to the arrest of enzymatic activity. Ans could not change the enzyme activity in this case either. Based on the TER results with the MMP inhibitors, one would have expected that more MG would lead to more shedding of the MMPs, and that the loss of resistance could be explained by this. However, other pathways must at least be interposed or involved, since a sole effect of MG on MMP concentration and enzyme activity was ruled out. This phenomenon can possibly be explained by the short test duration of 5 hours, since other studies used much longer treatment times and higher concentrations of MG. However, sepsis and septic shock are acute, and death can occur within hours (Cao et al., 2019a).



#### 4.4 MG induces inflammation by activating the NLRP3 inflammasome *in vitro*

It is known from diabetes that high TNF and IL-6 levels are associated with high plasma MG levels (Lu et al., 2011) and that MG formed AGEs stimulated IL-6 and IL-8 production in mesothelial cells (Welten et al., 2003). In non-diabetic individuals, MG stimulated cytokine production in neutrophils (Wang et al., 2007). Increased levels of IL-1 $\beta$  and IL-6 were found in blood samples from MG-treated mice (Prantner et al., 2021). However, here too there is no unequivocal data to answer the question of which cytokines are released from the endothelium after stimulation with free MG. In many cases there is only data describing the effects of MG-AGEs or AGEs in general *in vitro* (Zhou et al., 2019). The pathophysiological MG dosage induced an increase in the protein expression of the IL-6/IL-6R/IL6sR axis. Binding of IL-6 to membrane-bound IL-6R induces classic signaling via gp130 (interleukin-6 signal-transducer), whereas binding of IL-6 to sIL-6R induces trans-signaling, i.e., via gp130. IL-6 classic signaling induces the acute-phase response (Rose-John, 2017). In fact, it has been described that endothelial cells produce gp130 but not transmembrane IL-6R (Kang et al., 2020). However, this axis has never been studied before under MG influence on the endothelium. In the setting described no increase in TNF per se could be confirmed, but the increase in soluble TNFRs. The soluble TNFR variants are described to inhibit TNF by competing with the cellular receptor species for TNF binding, but possibly also by acting as dominant-negative molecules (Chan et al., 2000). However, this would also explain why no increase of plasmatic TNF itself could be measured and there is no comparable data or study results. For a number of proinflammatory cytokines (Justiz Vaillant and Qurie, 2023), , including IL-1 $\beta$ , IL-2, IL-3, IL-7, IL-8, IL-13, IL-15, IL-16 and IL-17 MG stimulation was able to achieve an increase of plasma concentrations with a pathophysiological dose. In this context, there is no data for MG and its effect on the endothelium in the literature. In almost all cases, Ans had an anti-inflammatory effect and lead to less or non-cytokine expression. An increase was also found for the colony stimulating factors M-CSF and GM-CSF which could possibly be related to the increased IL-3 production (Young et al., 1990, Donahue et al., 1988). A finding which further needs to be investigated is the relation of eotaxin, IL-8 and G-CSF upon MG stimulation. Eotaxin is described to suppress IL-8 secretion from microvascular endothelial cells (Cheng et al., 2002). However, MG induced a robust elevation in IL-8 as well as in G-CSF; IL-8 promotes chemotaxis of neutrophils (Baggiolini et al., 1994), whereas G-CSF stimulates survival and proliferation of immature granulocytes (Tigue et al., 2007). Neutrophils play a critical role in controlling infection under normal conditions, and their migration and antimicrobial activity are thought to be impaired during sepsis, contributing to the dysregulation of immune responses. Furthermore, interactions or effects of MG on neutrophils have already been described (Gawlowski et al., 2007, Wang et al., 2007, Ward and McLeish, 2004). Anti-inflammatory cytokines like IL-4, IL-10, and IL-11, as well as IL-12 with both pro- and anti-inflammatory properties were

downregulated by MG stimulation in the present study. There is no MG-related data in the literature for endothelial cells. The present study shows that MG had the capacity to elevate the ICAM expression from HUVEC, in line with previous publications describing that MG increased ICAM-1 expression in hypertensive rat vascular smooth muscle cells (Wu and Juurlink, 2002), MG-elicited ICAM-1 upregulation in murine endothelial cell lines (Su et al., 2014) and intravitreally MG injection in mice induced an upregulation of ICAM-1 (Lin et al., 2014). This is interesting for further studies because ICAM-1 has an important pathophysiological role in the context of polymicrobial sepsis (Hildebrand et al., 2005) and was recently described to regulate neutrophil adhesion *in vitro* and septic lung injury *in vivo* (Du et al., 2022). For the sepsis relevant cytokines IL-1beta, IL-6 and IL-8, a robust elevation in cytokine levels could be detected after MG stimulation with pathophysiological doses. At the time of diagnosis, serum IL-1beta, IL-6, IL-8 levels of culture-proven sepsis are observed to be significantly elevated in septic patients (Kurt et al., 2007). IL-6 and IL-8 are also described to accurately diagnose the hyperinflammatory state and to increase diagnostic specificity (Zeng et al., 2022). IL-1beta possesses a broad spectrum of biological properties. IL-1beta induces hemodynamic shock in experimental animals; the infusion of IL-1beta produces tissue damage and metabolic derangements similar to those associated with injury and sepsis in humans (Okusawa et al., 1988, Tredget et al., 1988, Movat et al., 1987). Furthermore, serum IL-1beta levels are elevated in patients with gram-negative bacteremia and correlate with the severity of sepsis (Okusawa et al., 1988, Tredget et al., 1988, Cannon et al., 1988, Cannon et al., 1990b, Cannon et al., 1990a). Therefore, a working hypothesis for the role of IL-1beta in sepsis is that it is produced during infection as well as trauma and induces the subsequent effector molecules of the shock syndrome (Dinarello et al., 1992). IL-1beta is released by the NLRP3 inflammasome and its role in the pathophysiology of sepsis may be ambivalent. Although it may protect against sepsis when moderately activated after initial infection, over-activation of the NLRP3 inflammasome can trigger dysregulated inflammation leading to multiple organ failure and death during the acute phase of sepsis. Furthermore, this activation could become exhausted and contribute to post-septic immunosuppression and dysfunction of innate and adaptive immune cells (Vigneron et al., 2023). In the previously presented experiments, Ans also showed an influence or an anti-inflammatory effect on IL-1beta production, and RAGE has also already been described in connection with inflammation and IL-1beta (Ito et al., 2012). This axis, in relation to the NLRP3 inflammasome and IL-1beta release, or caspase-1, was examined in more detail in the next step. Therefore, the pathophysiological MG dose, LPS or combined with or without Ans was applied to HUVEC and the activation of the NLRP3 inflammasome was investigated via the activation of caspase-1. Caspase-1 activation was monitored for 3 hours. Indeed, MG was able to activate caspase-1 in the same manner as LPS, however combining both agents did not lead to differences. The addition of Ans to MG did not lead to any changes. Surprisingly, there was a visible effect when adding Ans to the MG/LPS

combination. This inhibitory effect may be due to the antioxidative capacity (Aldini et al., 2021, Boldyrev et al., 2013) of Ans and therefore only acts on the LPS-generated caspase activation. However, this would have to be verified again in a follow-up experiment, since this study was intended to refer to the possible inflammatory effects of MG or the anti-inflammatory effects of Ans. The present findings after MG stimulation cannot be attributed to an increase in pyroptosis since the loss of TER was not associated with an increased cell death. The vitality staining also showed no apoptotic cells as in the dead cell control, even after administering the supraphysiological dose. It is a fact that many cell types secrete cytokines even though they show absolutely no signs of pyroptosis. It has often been debated whether the mode of action of cell death can be separated from IL-1 $\beta$  secretion. Several cell death-regulating proteins can interact directly with the inflammasome, and IL-1 $\beta$ -containing protein complexes are able to modulate their function, which would support this hypothesis. Although a close association between caspase-1 killing and IL-1 $\beta$  has been described, there is a growing body of genetic and biochemical data suggesting that, in at least some cell types, these two events are separable (Vince and Silke, 2016). It is known that caspase-1 does not necessarily play a central role in cell death (Wang and Lenardo, 2000), since Casp1 knockout mice, for example, did not show any obvious defect in apoptosis. Casp1-deficient macrophages and thymocytes retained the ability to undergo apoptosis in response to multiple stimuli. However, these mice are resistant to lethal doses of endotoxin/lipopolysaccharide (LPS) and have an acute defect in their ability to convert pro IL-1 $\beta$  to its mature form (Li et al., 1995). These features indicate rather a more important role for caspase-1 in processes associated with inflammation than in apoptotic cell death.

The next step was to investigate whether MG generally increases the amount of pro IL-1 $\beta$  (p35), the inactive IL-1 $\beta$  precursor (Dinarello, 1998), and thus provokes increased caspase activity, and whether the anti-inflammatory effect of Ans on IL-1 $\beta$  is related to this, since no difference existed in caspase-1 activation with Ans. It was observed that increasing MG doses lead to elevated pro IL-1 $\beta$  levels which in turn collapsed with the supraphysiological dose, which in turn underpins the previously described "standby mode" of the cell. The trend in pro IL-1 $\beta$  levels suggested a dose-dependency of MG. However, again, the addition of Ans made no difference, indicating that the mode of action of Ans occurs at a different site during inflammation.

#### 4.5 MG activates MAPKs via RAGE-dependent and -independent pathways *in vitro*

In order to check whether all these effects were possibly mediated by RAGE, often referred to as PRR, the MG dose titration TER experiment was repeated with a RAGE inhibitor (FPSZM1). The same concentration of the RAGE inhibitor was able to prevent the MG induced TER loss from the pathophysiological dose up to 15  $\mu$ M; in 100-fold and a supraphysiological dosage, FPSZM1 still tended to ameliorate TER. This suggests that MG influences the TJs or barrier-forming proteins via RAGE. Unfortunately, there is not enough comparable literature on this, but for example in brain endothelial cells, an increase of permeability was observed by interaction with RAGE, caused by a downregulation of ZO-1, occludin, and claudin 5 and stimulation of oxidative stress pathways (Kook et al., 2012). In human brain endothelial cells RAGE binding induced ROS production, which ultimately lead to disruption of TJs and loss of blood brain barrier (BBB) integrity (Carrano et al., 2011). After its activation, RAGE acts via three different downstream pathways: 1) the I $\kappa$ B signalosome dependent phosphorylation of NF- $\kappa$ B inhibitors (I $\kappa$ B inhibitors), and thus the activation of the NF- $\kappa$ B pathway, subsequently inducing the synthesis of pro-inflammatory cytokines (Hofmann et al., 1999, Henkel et al., 1993), 2) the PI3K/ Akt pathway, and 3) the activation of MAPK, including JNK, p38, and extracellular signal-regulated kinases (ERK) (Leclerc et al., 2007, Li et al., 2004, Stern et al., 2002, Taguchi et al., 2000). Therefore, the subsequent investigations were based on these pathways. Phosphorylation of subunit p65 plays a key role in regulating NF- $\kappa$ B activation and function (Zhong et al., 1998). Stimulus signals, including LPS and AGEs, lead to the phosphorylation of I $\kappa$ B $\alpha$ , thus liberating NF- $\kappa$ B and enabling it to translocate into the nucleus, where it binds to specific response elements in DNA and activates the expression of inflammatory cytokines (Pradère et al., 2016). It is reported that an AGE-RAGE interaction initiates the phosphorylation of MAPKs, which subsequently lead to the aberrant activation of NF- $\kappa$ B. Furthermore, the activation of NF- $\kappa$ B in return induces the expression of RAGE, resulting in a vicious cycle upregulating inflammatory responses (Davis et al., 2016). However, in the present study MG failed to induce phosphorylation of p65 in HUVEC. A trend towards less p65 phosphorylation was even observed with increasing MG concentrations. In endothelial cells, PI3K/Akt signaling mostly acts as a positive regulator of eNOS and Akt activation which promote cell survival (Ho et al., 2006). The PI3K/Akt/eNOS pathway plays a pivotal role in the process of endothelial cell mobilization, migration, and homing (Everaert et al., 2010). However, in line with pre-published data (Chu et al., 2017, Lee et al., 2020) treatment of HUVEC with MG inhibited the phosphorylation of Akt. MAPKs are involved in directing cellular responses to various stimuli, such as mitogens, osmotic stress, heat shock and proinflammatory cytokines (Pearson et al., 2001). The mammalian MAPK family includes ERKs, JNKs and p38s (Yu et al., 2020, Shi and Sun, 2018). ERKs are activated by growth factors and mitogens, whereas cellular stresses and inflammatory cytokines rather activate JNKs and p38s (Yu et al., 2020).

p38 is activated by a variety of cellular stresses including osmotic shock, inflammatory cytokines, LPS, ultraviolet light, and growth factors (Bachstetter et al., 2011). Additionally, p38 has been identified as a key downstream effector of RAGE binding (Yeh et al., 2001, Wang et al., 2022) and seems to be involved in TJ damages of the intestinal mucosal barrier (Ouyang et al., 2016). Inflammatory signals, changes in ROS levels, ultraviolet radiation, protein synthesis inhibitors, and a variety of stress stimuli can activate JNK. Specific phosphatases normally inhibit the activity of JNK itself and the activity of proteins, which are linked to JNK activation (Vlahopoulos and Zoumpourlis, 2004). In epithelial cells, JNK is largely involved in the regulation of TJs (Kojima et al., 2010). In the present study, acute increasing MG concentrations lead indeed to an activation respectively phosphorylation of the MAPKs p38 and c-Jun which were comparable to that of the inflammatory stimulus by TNF within 15 or 30 minutes. These data are consistent with results in the context of diabetes, also derived from HUVEC reporting activation of JNK and p38 MAPK but not NF- $\kappa$ B after 20 min of acute MG stimulation, with MG being identified as a stimulant for vascular inflammatory responses (Yamawaki et al., 2008). In order to check whether the beneficial effects of Ans in the TER experiments occur on the MAPK level, the most effective MG dose of 150  $\mu$ M was chosen for further experiments. This can be explained by the fact that it is a relatively short period of time for the stimulation. The MG-Ans effect ratio, which had previously proven to be effective, was retained for further experiments. Unfortunately, Ans did not exert effects on MG-induced p38- or c-Jun phosphorylation, which could possibly also be due to the very short time span. Therefore, the HUVEC were again pre-treated with Ans for 2 hours before receiving the MG stimulation. And again, Ans showed no effect in this setting, even as a pretreatment. The beneficial effect of Ans on maintenance of resistance is therefore likely to be found elsewhere. To determine whether the MG induced p38 and c-Jun phosphorylation was RAGE dependent in the present HUVEC model, the inhibitor experiments were transferred into flow cytometry. Cells were pretreated with the RAGE inhibitor FPSZM-1 for 2 hours and then treated for the respective period with 150  $\mu$ M MG and analyzed for p38 or c-Jun phosphorylation. The inhibitor showed no difference to MG on the phosphorylation of p38, so no RAGE dependency could be determined for p38 activation. Interestingly, the phosphorylation of c-Jun however was distinctly RAGE dependent, since FPSZM1 pretreated HUVEC exerted the same phosphorylation levels as the untreated media control. p38 and c-jun were recently shown to decrease the expression of TJ proteins via a NLRP3 inflammasome activation (Kang et al., 2022, Chu et al., 2021). In the present project, the identification respectively, the activation of the MG-AGE/RAGE axis is associated with a loss of the TER and the endothelial barrier binding proteins, providing a novel, important contributor to endothelial barrier damage in sepsis. It should be noted, that, unlike in the literature mentioned above (Kang et al., 2022, Chu et al., 2021), these effects were independent of NF- $\kappa$ B, an important inflammatory driver in sepsis (Böhler et al.,

1997, Hofmann et al., 1999) but in line with a more recent investigation by Yamayaki et al. (Yamawaki et al., 2008).

The finding that MG activates both p38 and c-Jun MAPKs, but only c-Jun in a RAGE dependent way, points out that MG is able to activate p38 MAPK via another receptor, pathway or a direct, as yet unknown effect. Furthermore, the effect upstream of the MAPK could be explained by the activation of different MAPK kinases (MKKs). MKK 4 and 7 activate c-Jun, MKK 3 and 6 activate p38. Upstream of the MKKs are the MKK kinases (MKKKs) e.g., mixed-lineage kinases (MLKs). All the MLK family members have been shown to activate the JNK pathway (Fanger et al., 1997). MLK3 and dual-leucine-zipper-bearing kinase (DLK) have also been shown to activate the p38 MAPK pathway, but it is not known whether other MLKs can also activate p38 (Tibbles et al., 1996, Gotoh et al., 2001). The different regulatory properties predicted for the different MLKs would allow integration of JNK and p38 activation with different cellular responses (Gallo and Johnson, 2002). Overexpression of these MKKKs leads to activation of both p38 and JNK pathways which is one possible explanation why these two pathways are often co-activated (Ogura and Kitamura, 1998). To date there is no data explaining the observations from the present study, how or even whether the MKKKs eventually interact with upstream RAGE signaling. Despite everything, one returns to the thesis that the effects of RCS or RCS-AGEs are very organ- or even cell-specific and differ under certain pathological conditions such as chronic diabetes or, as here, acute sepsis. As an example, a study on mesangial cells in the context of diabetes should be presented here: AGEs have been shown to activate ERK and PI3K pathways, whereas JNK and p38 MAPK in turn are not activated in these cells (Xu and Kyriakis, 2003). Of course, the cell-specific effects of AGEs make it difficult to focus on a specific clue in systemic diseases such as sepsis. Nonetheless, the data from the current study demonstrate an impact of MG on the endothelium and its specific barrier-forming proteins, and that pathways of the same class are induced by MG in different ways. Using a translational approach, it was shown that sepsis is linked to MG-induced carbonyl stress, which has a causal effect on outcome. Furthermore, Ans was able to prevent and restore MG-induced endothelial barrier damage and improve the outcome in experimental sepsis. Therefore, Ans could be an innovative therapeutic option for the treatment of sepsis and septic shock. Therefore, to evaluate the efficacy and safety of Ans in a clinical context, clinical trials are the next step. It will also be helpful to go further into the mechanisms of action of MG in sepsis and to identify the exact effect or target of Ans. If these are known, the area of application of Ans could also be extended to other RCS-related diseases.

## 4.6 Limitations of the study

Since sepsis is a systemic disease and no suitable cell models exists, individual stress parameters such as inflammation, endotoxins or oxidative, nitrosative or carbonyl stress can only be simulated to a limited extent on a cell- or organ-specific basis. In this context, these only give an overview of the physiological effects of MG or Ans. Furthermore, only female mice were used for the present animal experiments, which can be viewed critically with regard to sepsis, since the influence of gender on the development and course of the disease is relevant and the majority of septic patients are male (Angele et al., 2014). These data provide the first evidence that not ROS or RNS, but the RCS MG via MG-AGE (otherwise RAGE would not be involved) causes capillary leakage. Since blocking MG-AGE formation also prevents leakage and mortality, this finding provides evidence for the role of MG-AGE-mediated capillary leakage. For a complete proof one would have to show that Ans has no effect in RAGE-/- mouse. There is also a lack of histological data on the fact that the signaling pathway MG/MG-AGE/RAGE/TJ/Leakage is suppressed after Ans treatment in wild-type and e.g., in RAGE -/- mice. This is important since there is also data that MG eventually cannot bind covalently to proteins and change functions (Rodnick et al., 2017) contrary to the popular belief (Murata-Kamiya and Kamiya, 2001, Thornalley, 2008, Eberhardt et al., 2012, Polykretis et al., 2020, Lai et al., 2022).

## 4.7 Outlook

The here presented results for the first time show a causal influence of MG on the hyperacute status or on the increased vascular permeability in sepsis. On the other hand, it becomes clear that increased Ans concentrations in organ tissues and plasma exert protective effects *in vivo*. The positive effects observed from the Ans application cannot be clearly defined in terms of one body compartment, but a broad spectrum of effects on the metabolism can be assumed here. A large number of other bioactive dipeptides are now also coming into focus. This underlines that this is a hitherto underestimated and insufficiently researched field and that other dipeptides besides Ans could also be of therapeutic or diagnostic value. Studies on the influence of MG (or Ans) and a possible shift of the general dipeptide profile beyond the cell culture model under septic conditions are planned. Through the modification of organ-specific dipeptide profiles, innovative therapeutic approaches e.g., for septic acute kidney injury could be pursued. A characterization and proof of the pathway MG/MG-AGE/RAGE/TJ/leakage in the septic RAGE-/- mouse, as well as the transfer to an endotoxin model in pigs, should provide more clarity. However, these additional experiments were no longer possible at the end of the here presented work.

## 5. Summary

Therapeutic options for the treatment of sepsis/septic shock are still limited and mortality remains unacceptably high. Besides autonomic, endocrine, hematological, and immunological alteration in the septic patient, many metabolic changes occur as a result of inflammation, which lead to the release of reactive compounds such as reactive carbonyl species. The reactive carbonyl metabolite and advanced glycation end-product precursor methylglyoxal was identified as an early biomarker for the diagnosis and outcome prediction in sepsis. The extent to which increases in methylglyoxal play a role in the course of the disease in sepsis and septic shock is not known yet. In order to test a potential adjuvant therapy that has already been shown to reduce advanced glycation end-products, oxidative stress and glucose homeostasis-regulating properties associated with diabetic damage, the histidine-rich dipeptide anserine was applied in the septic context. Within the here presented approach, methylglyoxal-derived carbonyl stress was identified as a major contributor to the disruption respectively reconstruction of the endothelial barrier forming proteins claudin 5 and zonula occludens-1 in a cell culture model, comparable to inflammatory insults following lipopolysaccharide and tumor necrosis factor administration. Methylglyoxal leads to a disturbed cell integrity as well as to an increased paracellular leakage of small and big molecules. These effects were not dependent on matrix metalloproteinase cleavage of the extracellular matrix. Anserine was able to prevent and to restore methylglyoxal-induced damage *in vitro* and showed a protective effect on the level of barrier forming proteins claudin 5 and zonula occludens-1. In an *in vivo* mouse model of sepsis, anserine accumulated stably for 36 h in several organs and showed protective effects via reducing methylglyoxal - advanced glycation end-product formation in lungs as well as kidneys and reduced capillary leakage and mortality. Furthermore, anserine improved survival probability to 60 % compared to vehicle controls (36.6 %) and improved the clinical outcome of the animals. On the immunological base, methylglyoxal leads to non-apoptotic and non-pyroptotic nucleotide-binding oligomerization domain-like receptor containing pyrin domain 3 inflammasome assembly, as well as an increase of the interleukin-1 $\beta$  precursor and proinflammatory cytokines like interleukin-1 $\beta$ , interleukin-6 and interleukin-8 *in vitro*. Methylglyoxal did not activate nuclear factor  $\kappa$ -light-chain-enhancer of activated B cells subunit p65 assembly or the protein kinase B pathway, but rather activated mitogen-activated protein kinases c-Jun and p38 via different pathways. C-Jun-N-terminal kinase activation by methylglyoxal could be identified as receptor of advanced glycation end-product dependent, whereas p38 activation by methylglyoxal could persist even when the receptor of advanced glycation end-products was inhibited. The results propose a pathway in addition to direct toxic effects of methylglyoxal, by which methylglyoxal might causally contribute to the development as well as the severity of septic shock via an methylglyoxal - advanced glycation end-product/ receptor of advanced glycation end-product/ mitogen-activated protein kinase pathway functionally resulting in the activation of the nucleotide-



binding oligomerization domain-like receptor containing pyrin domain 3 inflammasome with a subsequent release of proinflammatory cytokines as well as a loss of tight junctions alongside. In summary, using a translational approach, sepsis was shown to be associated with methylglyoxal-derived carbonyl stress causally impacting outcome. Moreover, anserine was able to prevent and restore methylglyoxal-induced damages of the endothelial barrier and improved outcome in experimental sepsis. Therefore, anserine might be an innovative therapeutic option for the treatment of sepsis and septic shock.

## 6. Zusammenfassung

Die therapeutischen Möglichkeiten zur Behandlung der Sepsis/des septischen Schocks sind nach wie vor begrenzt, und die Sterblichkeitsrate ist nach wie vor unannehmbar hoch. Neben autonomen, endokrinen, hämatologischen und immunologischen Veränderungen beim septischen Patienten treten infolge der Entzündung zahlreiche Stoffwechseleränderungen auf, die zur Freisetzung reaktiver Verbindungen wie reaktiver Carbonylspezies führen. Der reaktive Carbonyl-Metabolit und *advanced glycation end-product* Vorläufer Methylglyoxal wurde als früher Biomarker für die Diagnose und Ergebnisvorhersage bei Sepsis identifiziert. Inwieweit Erhöhungen von Methylglyoxal eine Rolle für den Krankheitsverlauf bei Sepsis und septischem Schock spielen, ist noch nicht bekannt. Um eine potenzielle adjuvante Therapie zu testen, die bereits gezeigt hat, dass sie *advanced glycation end-products*, oxidativen Stress und die Glukosehomöostase regulierende Eigenschaften, die mit diabetischen Schäden verbunden sind, reduziert, wurde das histidinreiche Dipeptid Anserin im septischen Kontext eingesetzt. Im Rahmen des hier vorgestellten Ansatzes wurde Methylglyoxal-abgeleiteter Carbonylstress als ein Hauptfaktor für die Störung bzw. den Umbau der endothelialen Barriere bildenden Proteine Claudin 5 und zonula occludens-1 in einem Zellkulturmodell identifiziert, vergleichbar mit entzündlichen Schäden nach Verabreichung von Lipopolysaccharid und Tumor-Nekrosefaktor. Methylglyoxal führt zu einer gestörten Zellintegrität sowie zu einem erhöhten parazellulären Austritt von kleinen und großen Molekülen. Diese Effekte waren nicht von der Matrix-Metalloproteinase-Spaltung der extrazellulären Matrix abhängig. Anserin war in der Lage, Methylglyoxal-induzierte Schäden *in vitro* zu verhindern und wiederherzustellen und zeigte eine schützende Wirkung auf der Basis der Barriere bildenden Proteine Claudin 5 und zonula occludens-1. In einem In-vivo-Mausmodell der Sepsis akkumulierte sich Anserin 36 Stunden lang stabil in mehreren Organen und zeigte schützende Effekte, indem es die Bildung von Methylglyoxal und *advanced glycation end-products* in der Lunge und in den Nieren verringerte und die Kapillarleckage als auch die Sterblichkeit reduzierte. Darüber hinaus erhöhte Anserin die Überlebenschancen auf 60 % im Vergleich zur Vehikelkontrolle (36,6 %) und verbesserte den klinischen Verlauf der Tiere. Auf immunologischer Ebene führte Methylglyoxal zu einer nicht-apoptischen und nicht-pyoptischen Nukleotid-bindenden Oligomerisierungsdomänen-ähnlichen Rezeptor-enthaltenden Pyrin-Domäne 3-Inflammasom-Assemblierung sowie zu einem Anstieg des Interleukin-1beta-Vorläufers und proinflammatorischer Zytokine wie Interleukin-1beta, Interleukin-6 und Interleukin-8 *in vitro*. Methylglyoxal aktivierte weder den Zusammenbau der Untereinheit p65 des nukleären Faktors kappaB, noch den Weg der Proteinkinase B (Akt), sondern aktivierte über verschiedene Wege die mitogen-aktivierten Proteinkinasen c-Jun und p38. Die Aktivierung der c-Jun-N-terminalen Kinase durch Methylglyoxal konnte als rezeptorabhängig für *advanced glycation end-products* identifiziert werden, während die p38-Aktivierung durch Methylglyoxal auch dann bestehen blieb, wenn der

Rezeptor *advanced glycation end-products* gehemmt wurde. Die Ergebnisse legen nahe, dass es neben den direkten toxischen Wirkungen von Methylglyoxal einen weiteren Weg gibt, über den Methylglyoxal kausal zur Entwicklung und zum Schweregrad des septischen Schocks beitragen könnte, und zwar über einen Methylglyoxal - *advanced glycation end-product*/ Rezeptor für *advanced glycation end-products*/ mitogen-aktivierten Proteinkinase- Pfadweg, der funktionell zur Aktivierung des Nukleotid-bindenden Oligomerisierungsdomänen-ähnlichen Rezeptor-enthaltenden Pyrin-Domäne 3-Inflammasoms mit anschließender Freisetzung von proinflammatorischen Zytokinen sowie einem Verlust der *tight junctions* führt. Zusammenfassend wurde mithilfe eines translationalen Ansatzes gezeigt, dass Sepsis mit Methylglyoxal-abgeleitetem Carbonylstress assoziiert ist, der sich kausal auf das Ergebnis auswirkt. Darüber hinaus war Anserin in der Lage, die durch Methylglyoxal verursachten Schäden an der Endothelbarriere zu verhindern und wiederherzustellen und das Ergebnis der experimentellen Sepsis zu verbessern. Daher könnte Anserin eine innovative therapeutische Option für die Behandlung von Sepsis und septischem Schock sein.

## 7. References

- ABORDO, E. A., MINHAS, H. S. & THORNALLEY, P. J. 1999. Accumulation of alpha-oxoaldehydes during oxidative stress: a role in cytotoxicity. *Biochem Pharmacol*, 58, 641-8.
- ABORDO, E. A., WESTWOOD, M. E. & THORNALLEY, P. J. 1996. Synthesis and secretion of macrophage colony stimulating factor by mature human monocytes and human monocytic THP-1 cells induced by human serum albumin derivatives modified with methylglyoxal and glucose-derived advanced glycation endproducts. *Immunology Letters*, 53, 7-13.
- AHMED, N. & THORNALLEY, P. J. 2005. Peptide mapping of human serum albumin modified minimally by methylglyoxal in vitro and in vivo. *Ann N Y Acad Sci*, 1043, 260-6.
- AKHAND, A. A., HOSSAIN, K., KATO, M., MIYATA, T., DU, J., SUZUKI, H., KUROKAWA, K. & NAKASHIMA, I. 2001. Glyoxal and methylglyoxal induce lyoxal and methyglyoxal induce aggergation and inactivation of ERK in human endothelial cells. *Free Radical Biology and Medicine*, 31, 1228-1235.
- ALDINI, G., DE COURTEN, B., REGAZZONI, L., GILARDONI, E., FERRARIO, G., BARON, G., ALTOMARE, A., D'AMATO, A., VISTOLI, G. & CARINI, M. 2021. Understanding the antioxidant and carbonyl sequestering activity of carnosine: direct and indirect mechanisms. *Free Radic Res*, 55, 321-330.
- ALDINI, G., ORIOLI, M., ROSSONI, G., SAVI, F., BRAIDOTTI, P., VISTOLI, G., YEUM, K. -J., NEGRISOLI, G. & CARINI, M. 2011. The carbonyl scavenger carnosine ameliorates dyslipidaemia and renal function in Zucker obese rats. 15, 1339-1354.
- ALLAMAN, I., BÉLANGER, M. & MAGISTRETTI, P. J. 2015. Methylglyoxal, the dark side of glycolysis. *Front Neurosci*, 9, 23.
- ALLINGHAM, M. J., VAN BUUL, J. D. & BURRIDGE, K. 2007. ICAM-1-mediated, Src- and Pyk2-dependent vascular endothelial cadherin tyrosine phosphorylation is required for leukocyte transendothelial migration. *J Immunol*, 179, 4053-64.
- AMICARELLI, F., COLAFARINA, S., CATTANI, F., CIMINI, A., DI ILIO, C., CERU, M. P. & MIRANDA, M. 2003. Scavenging system efficiency is crucial for cell resistance to ROS-mediated methylglyoxal injury. *Free Radical Biology and Medicine*, 35, 856-871.
- ANDERSON, E. J., VISTOLI, G., KATUNGA, L. A., FUNAI, K., REGAZZONI, L., MONROE, T. B., GILARDONI, E., CANNIZZARO, L., COLZANI, M., DE MADDIS, D., ROSSONI, G., CANEVOTTI, R., GAGLIARDI, S., CARINI, M. & ALDINI, G. 2018. A carnosine analog mitigates metabolic disorders of obesity by reducing carbonyl stress. *The Journal of Clinical Investigation*, 128, 5280-5293.
- ANGELE, M. K., PRATSCHKE, S., HUBBARD, W. J. & CHAUDRY, I. H. 2014. Gender differences in sepsis: cardiovascular and immunological aspects. *Virulence*, 5, 12-9.
- ARULKUMARAN, N., DEUTSCHMAN, C. S., PINSKY, M. R., ZUCKERBRAUN, B., SCHUMACKER, P. T., GOMEZ, H., GOMEZ, A., MURRAY, P. & KELLUM, J. A. 2016. MITOCHONDRIAL FUNCTION IN SEPSIS. *Shock*, 45, 271-81.
- ASLAN, M. & OZBEN, T. 2003. Oxidants in receptor tyrosine kinase signal transduction pathways. *Antioxid Redox Signal*, 5, 781-8.
- BABIOR, B. M. 2000. Phagocytes and oxidative stress. *Am J Med*, 109, 33-44.
- BACHETTI, T. & MORBIDELLI, L. J. P. R. 2000. Endothelial cells in culture: a model for studying vascular functions. 42, 9-19.
- BACHSTETTER, A. D., XING, B., DE ALMEIDA, L., DIMAYUGA, E. R., WATTERSON, D. M. & VAN ELDIK, L. J. 2011. Microglial p38 $\alpha$  MAPK is a key regulator of proinflammatory cytokine up-regulation induced by toll-like receptor (TLR) ligands or beta-amyloid (A $\beta$ ). *J Neuroinflammation*, 8, 79.
- BAGGIOLINI, M., DEWALD, B. & MOSER, B. 1994. Interleukin-8 and related chemotactic cytokines—CXC and CC chemokines. *Adv Immunol*, 55, 97-179.
- BALDRIDGE, C. W. & GERARD, R. W. 1932. THE EXTRA RESPIRATION OF PHAGOCYTOSIS. 103, 235-236.
- BARSKI, O. A., TIPPARAJU, S. M. & BHATNAGAR, A. 2008. The aldo-keto reductase superfamily and its role in drug metabolism and detoxification. *Drug metabolism reviews*, 40, 553-624.
- BARTOSOVA, M., HERZOG, R., RIDINGER, D., LEVAI, E., JENEI, H., ZHANG, C., GONZÁLEZ MATEO, G. T., MARINOVIC, I., HACKERT, T., BESTVATER, F., HAUSMANN, M., LÓPEZ CABRERA, M.,

- KRATOCHWILL, K., ZAROGIANNIS, S. G. & SCHMITT, C. P. 2020. Alanyl-Glutamine Restores Tight Junction Organization after Disruption by a Conventional Peritoneal Dialysis Fluid. *Biomolecules*, 10.
- BASKARAN, S., RAJAN, D. P. & BALASUBRAMANIAN, K. A. 1989. Formation of methylglyoxal by bacteria isolated from human faeces. *J Med Microbiol*, 28, 211-5.
- BECK, F. X., NEUHOFER, W. & MÜLLER, E. 2000. Molecular chaperones in the kidney: distribution, putative roles, and regulation. *Am J Physiol Renal Physiol*, 279, F203-15.
- BEIER, U. H., ANGELIN, A., AKIMOVA, T., WANG, L., LIU, Y., XIAO, H., KOIKE, M. A., HANCOCK, S. A., BHATTI, T. R., HAN, R., JIAO, J., VEASEY, S. C., SIMS, C. A., BAUR, J. A., WALLACE, D. C. & HANCOCK, W. W. 2015. Essential role of mitochondrial energy metabolism in Foxp3<sup>+</sup> T-regulatory cell function and allograft survival. *Faseb j*, 29, 2315-26.
- BEISSWENGER, P. J., DRUMMOND, K. S., NELSON, R. G., HOWELL, S. K., SZWERGOLD, B. S. & MAUER, M. 2005. Susceptibility to Diabetic Nephropathy Is Related to Dicarbonyl and Oxidative Stress. *Diabetes*, 54, 3274-3281.
- BEISSWENGER, P. J., HOWELL, S. K., NELSON, R. G., MAUER, M. & SZWERGOLD, B. S. 2003. Alpha-oxoaldehyde metabolism and diabetic complications. *Biochem Soc Trans*, 31, 1358-63.
- BEISSWENGER, P. J., HOWELL, S. K., TOUCHETTE, A. D., LAL, S. & SZWERGOLD, B. S. 1999. Metformin reduces systemic methylglyoxal levels in type 2 diabetes. *Diabetes*, 48, 198-202.
- BELLAHCÈNE, A., NOKIN, M.-J., CASTRONOVO, V. & SCHALKWIJK, C. 2018. Methylglyoxal-derived stress: An emerging biological factor involved in the onset and progression of cancer. *Seminars in Cancer Biology*, 49, 64-74.
- BELLIA, F., VECCHIO, G., CUZZOCREA, S., CALABRESE, V. & RIZZARELLI, E. 2011. Neuroprotective features of carnosine in oxidative driven diseases. *Mol Aspects Med*, 32, 258-66.
- BELTRÁN, B., ORSI, A., CLEMENTI, E. & MONCADA, S. 2000. Oxidative stress and S-nitrosylation of proteins in cells. *Br J Pharmacol*, 129, 953-60.
- BERLANGA, J., CIBRIAN, D., GUILLEN, I., FREYRE, F., ALBA, JOSÉ S., LOPEZ-SAURA, P., MERINO, N., ALDAMA, A., QUINTELA, ANA M., TRIANA, MARIA E., MONTEQUIN, JOSE F., AJAMIEH, H., URQUIZA, D., AHMED, N. & THORNALLEY, PAUL J. 2005. Methylglyoxal administration induces diabetes-like microvascular changes and perturbs the healing process of cutaneous wounds. *Clinical Science*, 109, 83-95.
- BIERHAUS, A., FLEMING, T., STOYANOV, S., LEFFLER, A., BABES, A., NEACSU, C., SAUER, S. K., EBERHARDT, M., SCHNÖLZER, M., LASITSCHKA, F., NEUHUBER, W. L., KICHKO, T. I., KONRADE, I., ELVERT, R., MIER, W., PIRAGS, V., LUKIC, I. K., MORCOS, M., DEHMER, T., RABBANI, N., THORNALLEY, P. J., EDELSTEIN, D., NAU, C., FORBES, J., HUMPERT, P. M., SCHWANINGER, M., ZIEGLER, D., STERN, D. M., COOPER, M. E., HABERKORN, U., BROWNLEE, M., REEH, P. W. & NAWROTH, P. P. 2012. Methylglyoxal modification of Nav1.8 facilitates nociceptive neuron firing and causes hyperalgesia in diabetic neuropathy. *Nat Med*, 18, 926-33.
- BIERHAUS, A., ILLMER, T., KASPER, M., LUTHER, T., QUEHENBERGER, P., TRITSCHLER, H., WAHL, P., ZIEGLER, R., MÜLLER, M. & NAWROTH, P. P. 1997. Advanced glycation end product (AGE)-mediated induction of tissue factor in cultured endothelial cells is dependent on RAGE. *Circulation*, 96, 2262-71.
- BIERHAUS, A., STOYANOV, S., HAAG, G.-M., KONRADE, I., HUMPERT, P. M., THORNALLEY, P., THORPE, S. R. & NAWROTH, P. P. RAGE-deficiency reduces diabetes-associated impairment of glyoxalase-1 in neuronal cells. *Diabetes*, 2006. AMER DIABETES ASSOC 1701 N BEAUREGARD ST, ALEXANDRIA, VA 22311-1717 USA, A511-A511.
- BLANCQUAERT, L., BABA, S. P., KWIATKOWSKI, S., STAUTEMAS, J., STEGEN, S., BARBARESI, S., CHUNG, W., BOAKYE, A. A., HOETKER, J. D., BHATNAGAR, A., DELANGHE, J., VANHEEL, B., VEIGA-DACUNHA, M., DERAIVE, W. & EVERAERT, I. 2016. Carnosine and anserine homeostasis in skeletal muscle and heart is controlled by  $\beta$ -alanine transamination. *J Physiol*, 594, 4849-63.
- BÖHRER, H., QIU, F., ZIMMERMANN, T., ZHANG, Y., JLLMER, T., MÄNNEL, D., BÖTTIGER, B. W., STERN, D. M., WALDHERR, R., SAEGER, H. D., ZIEGLER, R., BIERHAUS, A., MARTIN, E. & NAWROTH, P. P. 1997. Role of NFkappaB in the mortality of sepsis. *J Clin Invest*, 100, 972-85.

- BOLDYREV, A., BULYGINA, E., LEINSOO, T., PETRUSHANKO, I., TSUBONE, S. & ABE, H. 2004. Protection of neuronal cells against reactive oxygen species by carnosine and related compounds. *Comp Biochem Physiol B Biochem Mol Biol*, 137, 81-8.
- BOLDYREV, A. A., ALDINI, G. & DERAVE, W. 2013. Physiology and pathophysiology of carnosine. *Physiol Rev*, 93, 1803-45.
- BOLTON, W. K., CATTRAN, D. C., WILLIAMS, M. E., ADLER, S. G., APPEL, G. B., CARTWRIGHT, K., FOILES, P. G., FREEDMAN, B. I., RASKIN, P., RATNER, R. E., SPINOWITZ, B. S., WHITTIER, F. C., WUERTH, J. P. & FOR THE ACTION I INVESTIGATOR GROUP, F. 2004. Randomized Trial of an Inhibitor of Formation of Advanced Glycation End Products in Diabetic Nephropathy. *American Journal of Nephrology*, 24, 32-40.
- BONE, R. C., BALK, R. A., CERRA, F. B., DELLINGER, R. P., FEIN, A. M., KNAUS, W. A., SCHEIN, R. M. & SIBBALD, W. J. 1992. Definitions for sepsis and organ failure and guidelines for the use of innovative therapies in sepsis. The ACCP/SCCM Consensus Conference Committee. American College of Chest Physicians/Society of Critical Care Medicine. *Chest*, 101, 1644-55.
- BONE, R. C., GRODZIN, C. J. & BALK, R. A. 1997. Sepsis: a new hypothesis for pathogenesis of the disease process. *Chest*, 112, 235-43.
- BOOTH, I. R., FERGUSON, G. P., MILLER, S., LI, C., GUNASEKERA, B. & KINGHORN, S. 2003. Bacterial production of methylglyoxal: a survival strategy or death by misadventure? *Biochem Soc Trans*, 31, 1406-8.
- BORGONETTI, V., PRESSI, G., BERTAIOLA, O., GUARNERIO, C., MANDRONE, M., CHIOCCHIO, I. & GALEOTTI, N. 2022. Attenuation of neuroinflammation in microglia cells by extracts with high content of rosmarinic acid from in vitro cultured *Melissa officinalis* L. cells. *J Pharm Biomed Anal*, 220, 114969.
- BOULOS, M., ASTIZ, M. E., BARUA, R. S. & OSMAN, M. 2003. Impaired mitochondrial function induced by serum from septic shock patients is attenuated by inhibition of nitric oxide synthase and poly(ADP-ribose) synthase. *Crit Care Med*, 31, 353-8.
- BREALEY, D., BRAND, M., HARGREAVES, I., HEALES, S., LAND, J., SMOLENSKI, R., DAVIES, N. A., COOPER, C. E. & SINGER, M. 2002. Association between mitochondrial dysfunction and severity and outcome of septic shock. *Lancet*, 360, 219-23.
- BREALEY, D., KARYAMPUDI, S., JACQUES, T. S., NOVELLI, M., STIDWILL, R., TAYLOR, V., SMOLENSKI, R. T. & SINGER, M. 2004. Mitochondrial dysfunction in a long-term rodent model of sepsis and organ failure. *Am J Physiol Regul Integr Comp Physiol*, 286, R491-7.
- BRENNER, T., FLEMING, T., UHLE, F., SILAFF, S., SCHMITT, F., SALGADO, E., ULRICH, A., ZIMMERMANN, S., BRUCKNER, T., MARTIN, E., BIERHAUS, A., NAWROTH, P. P., WEIGAND, M. A. & HOFER, S. 2014. Methylglyoxal as a new biomarker in patients with septic shock: an observational clinical study. *Crit Care*, 18, 683.
- BRENNER, T., FLEMING, T. H., SPRANZ, D., SCHEMMER, P., BRUCKNER, T., UHLE, F., MARTIN, E. O., WEIGAND, M. A. & HOFER, S. 2013. Reactive metabolites and AGE-RAGE-mediated inflammation in patients following liver transplantation. *Mediators Inflamm*, 2013, 501430.
- BRINGS, S., FLEMING, T., DE BUHR, S., BEIJER, B., LINDNER, T., WISCHNJOW, A., KENDER, Z., PETERS, V., KOPF, S., HABERKORN, U., MIER, W. & NAWROTH, P. P. 2017. A scavenger peptide prevents methylglyoxal induced pain in mice. *Biochimica et Biophysica Acta (BBA) - Molecular Basis of Disease*, 1863, 654-662.
- BROUWERS, O., NIESSEN, P. M., FERREIRA, I., MIYATA, T., SCHEFFER, P. G., TEERLINK, T., SCHRAUWEN, P., BROWNLEE, M., STEHOUWER, C. D. & SCHALKWIJK, C. G. 2011. Overexpression of Glyoxalase-I Reduces Hyperglycemia-induced Levels of Advanced Glycation End Products and Oxidative Stress in Diabetic Rats\*. *Journal of Biological Chemistry*, 286, 1374-1380.
- BROUWERS, O., NIESSEN, P. M., HAENEN, G., MIYATA, T., BROWNLEE, M., STEHOUWER, C. D., DE MEY, J. G. & SCHALKWIJK, C. G. 2010. Hyperglycaemia-induced impairment of endothelium-dependent vasorelaxation in rat mesenteric arteries is mediated by intracellular methylglyoxal levels in a pathway dependent on oxidative stress. *Diabetologia*, 53, 989-1000.

- BROUWERS, O., NIESSEN, P. M. G., MIYATA, T., ØSTERGAARD, J. A., FLYVBJERG, A., PEUTZ-KOOTSTRA, C. J., SIEBER, J., MUNDEL, P. H., BROWNLEE, M., JANSSEN, B. J. A., DE MEY, J. G. R., STEHOUWER, C. D. A. & SCHALKWIJK, C. G. 2014. Glyoxalase-1 overexpression reduces endothelial dysfunction and attenuates early renal impairment in a rat model of diabetes. *Diabetologia*, 57, 224-235.
- BROUWERS, O., VOS-HOUBEN, J. M. J. D., NIESSEN, P. M. G., MIYATA, T., NIEUWENHOVEN, F. V., JANSSEN, B. J. A., HAGEMAN, G., STEHOUWER, C. D. A. & SCHALKWIJK, C. G. 2013. Mild Oxidative Damage in the Diabetic Rat Heart Is Attenuated by Glyoxalase-1 Overexpression. 14, 15724-15739.
- BROWN, B. E., DEAN, R. T. & DAVIES, M. J. 2005. Glycation of low-density lipoproteins by methylglyoxal and glycolaldehyde gives rise to the in vitro formation of lipid-laden cells. *Diabetologia*, 48, 361-369.
- BROWNLEE, M. 2001. Biochemistry and molecular cell biology of diabetic complications. *Nature*, 414, 813-20.
- BROWNLEE, M., VLASSARA, H., KOONEY, A., ULRICH, P. & CERAMI, A. 1986. Aminoguanidine Prevents Diabetes-Induced Arterial Wall Protein Cross-Linking. 232, 1629-1632.
- CAI, H. & HARRISON, D. G. 2000. Endothelial dysfunction in cardiovascular diseases: the role of oxidant stress. *Circ Res*, 87, 840-4.
- CANNON, J., GELFAND, J., TOMPKINS, R., HEGARTY, M., BURKE, J., DINARELLO, C. J. T. P. & PATHOLOGICALEFFECTS OF CYTOKINES, E. B. D. C., KLUGER MJ, POWANDA MC, OPPENHEIM JJ, NEW YORK, WILEY-LISS 1990a. Plasma IL-1b and TNFa levels in humans following cutaneous injury. 301-306.
- CANNON, J. G., TOMPKINS, R. G., GELFAND, J. A., MICHIE, H. R., STANFORD, G. G., VAN DER MEER, J. W., ENDRES, S., LONNEMANN, G., CORSETTI, J. & CHERNOW, B. J. J. O. I. D. 1990b. Circulating interleukin-1 and tumor necrosis factor in septic shock and experimental endotoxin fever. 161, 79-84.
- CANNON, J. G., VAN DER MEER, J. W., KWIATKOWSKI, D., ENDRES, S., LONNEMANN, G., BURKE, J. F. & DINARELLO, C. A. 1988. Interleukin-1beta in human plasma: optimization of blood collection, plasma extraction, and radioimmunoassay methods. *Lymphokine Res*, 7, 457-67.
- CAO, C., YU, M. & CHAI, Y. 2019a. Pathological alteration and therapeutic implications of sepsis-induced immune cell apoptosis. *Cell Death & Disease*, 10, 782.
- CAO, R. N., TANG, L., XIA, Z. Y. & XIA, R. 2019b. Endothelial glycocalyx as a potential therapeutic target in organ injuries. *Chin Med J (Engl)*, 132, 963-975.
- CAPES, S. E., HUNT, D., MALMBERG, K. & GERSTEIN, H. C. 2000. Stress hyperglycaemia and increased risk of death after myocardial infarction in patients with and without diabetes: a systematic overview. *Lancet*, 355, 773-8.
- CARABALLO, C. & JAIMES, F. 2019. Organ Dysfunction in Sepsis: An Ominous Trajectory From Infection To Death. *Yale J Biol Med*, 92, 629-640.
- CARRANO, A., HOOZEMANS, J. J., VAN DER VIES, S. M., ROZEMULLER, A. J., VAN HORSSSEN, J. & DE VRIES, H. E. 2011. Amyloid Beta induces oxidative stress-mediated blood-brain barrier changes in capillary amyloid angiopathy. *Antioxid Redox Signal*, 15, 1167-78.
- CARRÉ, J. E. & SINGER, M. 2008. Cellular energetic metabolism in sepsis: the need for a systems approach. *Biochim Biophys Acta*, 1777, 763-71.
- CEPINSKAS, G. & WILSON, J. X. 2008. Inflammatory response in microvascular endothelium in sepsis: role of oxidants. *J Clin Biochem Nutr*, 42, 175-84.
- CHAKRABORTY, R. K. & BURNS, B. 2023. Systemic Inflammatory Response Syndrome. *StatPearls*. Treasure Island (FL): StatPearls Publishing Copyright © 2023, StatPearls Publishing LLC.
- CHAN, F. K.-M., CHUN, H. J., ZHENG, L., SIEGEL, R. M., BUI, K. L. & LENARDO, M. J. J. S. 2000. A domain in TNF receptors that mediates ligand-independent receptor assembly and signaling. 288, 2351-2354.

- CHAN, W. H., WU, H. J. & SHIAO, N. H. 2007. Apoptotic signaling in methylglyoxal-treated human osteoblasts involves oxidative stress, c-Jun N-terminal kinase, caspase-3, and p21-activated kinase 2. *J Cell Biochem*, 100, 1056-69.
- CHAPPELL, D., WESTPHAL, M. & JACOB, M. 2009. The impact of the glycocalyx on microcirculatory oxygen distribution in critical illness. *Curr Opin Anaesthesiol*, 22, 155-62.
- CHEBOTAREVA, N., BOBKOVA, I. & SHILOV, E. 2017. Heat shock proteins and kidney disease: perspectives of HSP therapy. *Cell Stress Chaperones*, 22, 319-343.
- CHELAZZI, C., VILLA, G., MANCINELLI, P., DE GAUDIO, A. R. & ADEMBRI, C. 2015. Glycocalyx and sepsis-induced alterations in vascular permeability. *Crit Care*, 19, 26.
- CHENG, S. S., LUKACS, N. W. & KUNKEL, S. L. 2002. Eotaxin/CCL11 suppresses IL-8/CXCL8 secretion from human dermal microvascular endothelial cells. *J Immunol*, 168, 2887-94.
- CHU, P., HAN, G., AHSAN, A., SUN, Z., LIU, S., ZHANG, Z., SUN, B., SONG, Y., LIN, Y., PENG, J. & TANG, Z. 2017. Phosphocreatine protects endothelial cells from Methylglyoxal induced oxidative stress and apoptosis via the regulation of PI3K/Akt/eNOS and NF- $\kappa$ B pathway. *Vascular Pharmacology*, 91, 26-35.
- CHU, X., WANG, C., WU, Z., FAN, L., TAO, C., LIN, J., CHEN, S., LIN, Y. & GE, Y. 2021. JNK/c-Jun-driven NLRP3 inflammasome activation in microglia contributed to retinal ganglion cells degeneration induced by indirect traumatic optic neuropathy. *Exp Eye Res*, 202, 108335.
- CLARK, P. R., KIM, R. K., POBER, J. S. & KLUGER, M. S. 2015. Tumor necrosis factor disrupts claudin-5 endothelial tight junction barriers in two distinct NF- $\kappa$ B-dependent phases. *PLoS One*, 10, e0120075.
- COLZANI, M., DE MADDIS, D., CASALI, G., CARINI, M., VISTOLI, G. & ALDINI, G. 2016. Reactivity, Selectivity, and Reaction Mechanisms of Aminoguanidine, Hydralazine, Pyridoxamine, and Carnosine as Sequestering Agents of Reactive Carbonyl Species: A Comparative Study. 11, 1778-1789.
- COOPER, R. A. 1984. Metabolism of methylglyoxal in microorganisms. *Annu Rev Microbiol*, 38, 49-68.
- CRAIGE, S. M., KANT, S. & KEANEY, J. F., JR. 2015. Reactive oxygen species in endothelial function - from disease to adaptation. *Circ J*, 79, 1145-55.
- CROUSER, E. D., JULIAN, M. W. & DORINSKY, P. M. 1999. Ileal VO<sub>2</sub>-O<sub>2</sub> alterations induced by endotoxin correlate with severity of mitochondrial injury. *Am J Respir Crit Care Med*, 160, 1347-53.
- CULLUM, N. A., MAHON, J., STRINGER, K. & MCLEAN, W. G. 1991. Glycation of rat sciatic nerve tubulin in experimental diabetes mellitus. *Diabetologia*, 34, 387-389.
- CUZZOCREA, S., MAZZON, E., DI PAOLA, R., ESPOSITO, E., MACARTHUR, H., MATUSCHAK, G. M. & SALVEMINI, D. 2006. A role for nitric oxide-mediated peroxynitrite formation in a model of endotoxin-induced shock. *J Pharmacol Exp Ther*, 319, 73-81.
- DAHLGREN, C. & KARLSSON, A. 1999. Respiratory burst in human neutrophils. *J Immunol Methods*, 232, 3-14.
- DAVIS, K. E., PRASAD, C., VIJAYAGOPAL, P., JUMA, S., IMRHAN, V. J. C. R. I. F. S. & NUTRITION 2016. Advanced glycation end products, inflammation, and chronic metabolic diseases: links in a chain? 56, 989-998.
- DE COURTEN, B., JAKUBOVA, M., DE COURTEN, M. P., KUKUROVA, I. J., VALLOVA, S., KRUMPOLEC, P., VALKOVIC, L., KURDIOVA, T., GARZON, D., BARBARESI, S., TEEDE, H. J., DERAIVE, W., KRSSAK, M., ALDINI, G., UKROPEC, J. & UKROPCOVA, B. 2016. Effects of carnosine supplementation on glucose metabolism: Pilot clinical trial. 24, 1027-1034.
- DE LA CRUZ-ARES, S., CARDELO, M. P., GUTIÉRREZ-MARISCAL, F. M., TORRES-PEÑA, J. D., GARCÍA-RIOS, A., KATSIKI, N., MALAGÓN, M. M., LÓPEZ-MIRANDA, J., PÉREZ-MARTÍNEZ, P. & YUBERO-SERRANO, E. M. 2020. Endothelial Dysfunction and Advanced Glycation End Products in Patients with Newly Diagnosed Versus Established Diabetes: From the CORDIOPREV Study. *Nutrients*, 12.



- DE SOUZA, P., SCHULZ, R. & DA SILVA-SANTOS, J. E. 2015. Matrix metalloproteinase inhibitors prevent sepsis-induced refractoriness to vasoconstrictors in the cecal ligation and puncture model in rats. *European Journal of Pharmacology*, 765, 164-170.
- DHAR, A., DHAR, I., DESAI, K. M. & WU, L. 2010. Methylglyoxal scavengers attenuate endothelial dysfunction induced by methylglyoxal and high concentrations of glucose. *British Journal of Pharmacology*, 161, 1843-1856.
- DÍAZ-CORÁNGUEZ, M., RAMOS, C. & ANTONETTI, D. A. 2017. The inner blood-retinal barrier: Cellular basis and development. *Vision Research*, 139, 123-137.
- DINARELLO, C. A. 1998. Interleukin-1 beta, interleukin-18, and the interleukin-1 beta converting enzyme. *Ann NY Acad Sci*, 856, 1-11.
- DINARELLO, C. A. 2007. Historical insights into cytokines. *Eur J Immunol*, 37 Suppl 1, S34-45.
- DINARELLO, C. A., AIURA, K. & GELFAND, J. A. The Role of Interleukin-1 in Septic Shock. In: VINCENT, J.-L., ed. Yearbook of Intensive Care and Emergency Medicine 1992, 1992// 1992 Berlin, Heidelberg. Springer Berlin Heidelberg, 25-35.
- DING, J. & LIU, Q. 2019. Toll-like receptor 4: A promising therapeutic target for pneumonia caused by Gram-negative bacteria. *J Cell Mol Med*, 23, 5868-5875.
- DOBLER, D., AHMED, N., SONG, L., EBOIGBODIN, K. E. & THORNALLEY, P. J. 2006. Increased dicarbonyl metabolism in endothelial cells in hyperglycemia induces anoikis and impairs angiogenesis by RGD and GFOGER motif modification. *Diabetes*, 55, 1961-1969.
- DONAHUE, R. E., SEEHRA, J., METZGER, M., LEFEBVRE, D., ROCK, B., CARBONE, S., NATHAN, D. G., GARNICK, M., SEHGAL, P. K., LASTON, D., LAVALLIE, E., MCCOY, J., SCHENDEL, P. F., NORTON, C., TURNER, K., YANG, Y.-C. & CLARK, S. C. 1988. Human IL-3 and GM-CSF Act Synergistically in Stimulating Hematopoiesis in Primates. *Science*, 241, 1820-1823.
- DONNELLY, R. P., LOFTUS, R. M., KEATING, S. E., LIOU, K. T., BIRON, C. A., GARDINER, C. M. & FINLAY, D. K. 2014. mTORC1-dependent metabolic reprogramming is a prerequisite for NK cell effector function. *J Immunol*, 193, 4477-84.
- DOUGHTY, C. A., BLEIMAN, B. F., WAGNER, D. J., DUFORT, F. J., MATARAZA, J. M., ROBERTS, M. F. & CHILES, T. C. 2006. Antigen receptor-mediated changes in glucose metabolism in B lymphocytes: role of phosphatidylinositol 3-kinase signaling in the glycolytic control of growth. *Blood*, 107, 4458-65.
- DRIESSEN, R. G. H., KIERS, D., SCHALKWIJK, C. G., SCHEIJEN, J., GERRETSSEN, J., PICKKERS, P., VAN DE POLL, M. C. G., VAN DER HORST, I. C. C., BERGMANS, D., KOX, M. & VAN BUSSEL, B. C. T. 2021. Systemic inflammation down-regulates glyoxalase-1 expression: an experimental study in healthy males. *Biosci Rep*, 41.
- DU, F., HAWEZ, A., DING, Z., WANG, Y., RÖNNOW, C. F., RAHMAN, M. & THORLACIUS, H. 2022. E3 Ubiquitin Ligase Midline 1 Regulates Endothelial Cell ICAM-1 Expression and Neutrophil Adhesion in Abdominal Sepsis. *Int J Mol Sci*, 24.
- DU, J., ZENG, J., OU, X., REN, X. & CAI, S. 2006. Methylglyoxal downregulates Raf-1 protein through a ubiquitination-mediated mechanism. *Int J Biochem Cell Biol*, 38, 1084-91.
- DUNGAN, K. M., BRAITHWAITE, S. S. & PREISER, J. C. 2009. Stress hyperglycaemia. *Lancet*, 373, 1798-807.
- EBERHARDT, M. J., FILIPOVIC, M. R., LEFFLER, A., DE LA ROCHE, J., KISTNER, K., FISCHER, M. J., FLEMING, T., ZIMMERMANN, K., IVANOVIC-BURMAZOVIC, I., NAWROTH, P. P., BIERHAUS, A., REEH, P. W. & SAUER, S. K. 2012. Methylglyoxal activates nociceptors through transient receptor potential channel A1 (TRPA1): a possible mechanism of metabolic neuropathies. *J Biol Chem*, 287, 28291-306.
- ECHEVERRI-RUIZ, N., HAYNES, T., LANDERS, J., WOODS, J., GEMMA, M. J., HUGHES, M. & DEL RIO-TSONIS, K. 2018. A biochemical basis for induction of retina regeneration by antioxidants. *Dev Biol*, 433, 394-403.
- EMRE, Y., HURTAUD, C., NÜBEL, T., CRISCUOLO, F., RICQUIER, D. & CASSARD-DOULCIER, A. M. 2007. Mitochondria contribute to LPS-induced MAPK activation via uncoupling protein UCP2 in macrophages. *Biochem J*, 402, 271-8.

- ENGVALL, E. & PERLMANN, P. 1971. Enzyme-linked immunosorbent assay (ELISA). Quantitative assay of immunoglobulin G. *Immunochemistry*, 8, 871-4.
- ERIKSON, K., TUOMINEN, H., VAKKALA, M., LIISANANTTI, J. H., KARTTUNEN, T., SYRJÄLÄ, H. & ALAKOKKO, T. I. 2020. Brain tight junction protein expression in sepsis in an autopsy series. *Critical Care*, 24, 385.
- ERINGA, E. C., SERNE, E. H., MEIJER, R. I., SCHALKWIJK, C. G., HOUBEN, A. J. H. M., STEHOUWER, C. D. A., SMULDERS, Y. M. & VAN HINSBERGH, V. W. M. 2013. Endothelial dysfunction in (pre)diabetes: Characteristics, causative mechanisms and pathogenic role in type 2 diabetes. *Reviews in Endocrine and Metabolic Disorders*, 14, 39-48.
- EVERAERT, B. R., VAN CRAENENBROECK, E. M., HOYMANS, V. Y., HAINE, S. E., VAN NASSAUW, L., CONRAADS, V. M., TIMMERMANS, J. P. & VRINTS, C. J. 2010. Current perspective of pathophysiological and interventional effects on endothelial progenitor cell biology: focus on PI3K/AKT/eNOS pathway. *Int J Cardiol*, 144, 350-66.
- EVERAERT, I., BARON, G., BARBARESI, S., GILARDONI, E., COPPA, C., CARINI, M., VISTOLI, G., BEX, T., STAUTEMAS, J., BLANCQUAERT, L., DRAVE, W., ALDINI, G. & REGAZZONI, L. 2019. Development and validation of a sensitive LC-MS/MS assay for the quantification of anserine in human plasma and urine and its application to pharmacokinetic study. *Amino Acids*, 51, 103-114.
- EVERAERT, I., VAN DER STEDE, T., STAUTEMAS, J., HANSENS, M., VAN AANHOLD, C., BAELE, H., VANHAECKE, L. & DRAVE, W. 2021. Oral anserine supplementation does not attenuate type-2 diabetes or diabetic nephropathy in BTBR ob/ob mice. *Amino Acids*, 53, 1269-1277.
- FANG, X., DUAN, S. F., HU, Z. Y., WANG, J. J., QIU, L., WANG, F. & CHEN, X. L. 2022. Inhibition of Matrix Metalloproteinase-8 Protects Against Sepsis Serum Mediated Leukocyte Adhesion. *Front Med (Lausanne)*, 9, 814890.
- FANGER, G. R., GERWINS, P., WIDMANN, C., JARPE, M. B. & JOHNSON, G. L. 1997. MEKKs, GCKs, MLKs, PAKs, TAKs, and tkls: upstream regulators of the c-Jun amino-terminal kinases? *Curr Opin Genet Dev*, 7, 67-74.
- FERGUSON, G. P., TÖTEMEYER, S., MACLEAN, M. J. & BOOTH, I. R. 1998. Methylglyoxal production in bacteria: suicide or survival? *Arch Microbiol*, 170, 209-18.
- FERNÁNDEZ-SARMIENTO, J., SCHLAPBACH, L. J., ACEVEDO, L., SANTANA, C. R., ACOSTA, Y., DIANA, A., MONSALVE, M. & CARCILLO, J. A. 2022. Endothelial Damage in Sepsis: The Importance of Systems Biology. *Front Pediatr*, 10, 828968.
- FERRO, T., NEUMANN, P., GERTZBERG, N., CLEMENTS, R. & JOHNSON, A. 2000. Protein kinase C- $\alpha$  mediates endothelial barrier dysfunction induced by TNF- $\alpha$ . *Am J Physiol Lung Cell Mol Physiol*, 278, L1107-17.
- FESSEL, G., LI, Y., DIEDERICH, V., GUIZAR-SICAÍROS, M., SCHNEIDER, P., SELL, D. R., MONNIER, V. M. & SNEDEKER, J. G. 2014. Advanced glycation end-products reduce collagen molecular sliding to affect collagen fibril damage mechanisms but not stiffness. *PLoS One*, 9, e110948.
- FINK, M. P. 2001. Cytopathic hypoxia. Mitochondrial dysfunction as mechanism contributing to organ dysfunction in sepsis. *Crit Care Clin*, 17, 219-37.
- FINK, M. P. 2015. Cytopathic hypoxia and sepsis: is mitochondrial dysfunction pathophysiologically important or just an epiphenomenon. *Pediatr Crit Care Med*, 16, 89-91.
- FIORY, F., LOMBARDI, A., MIELE, C., GIUDICELLI, J., BEGUINOT, F. & VAN OBBERGHEN, E. 2011. Methylglyoxal impairs insulin signalling and insulin action on glucose-induced insulin secretion in the pancreatic beta cell line INS-1E. *Diabetologia*, 54, 2941-2952.
- FISHER, A. B., DODIA, C., CHATTERJEE, S. & FEINSTEIN, S. I. 2020. Correction: Fisher, Aron B., et al. A Peptide Inhibitor of NADPH Oxidase (NOX2) Activation Markedly Decreases Mouse Lung Injury and Mortality Following Administration of Lipopolysaccharide (LPS). *Int. J. Mol. Sci.* 2019, 20, 2395. *Int J Mol Sci*, 21.
- FLEMING, T., VON NETTELBLADT, B., MORGENSTERN, J., CAMPOS, M., LE MAROIS, M., BARTOSOVA, M., HAUSSER, I., SCHWAB, C., FISCHER, A., NAWROTH, P. P., SZENDRÖDI, J. & HERZIG, S. 2022.

- Methylglyoxal Induces Endothelial Dysfunction via a Stunning-like Phenotype. *Diabetologie und Stoffwechsel*, 17, P 039.
- FREEDMAN, B. I., WUERTH, J.-P., CARTWRIGHT, K., BAIN, R. P., DIPPE, S., HERSHON, K., MOORADIAN, A. D. & SPINOWITZ, B. S. 1999. Design and Baseline Characteristics for the Aminoguanidine Clinical Trial in Overt Type 2 Diabetic Nephropathy (ACTION II). *Controlled Clinical Trials*, 20, 493-510.
- FUKUNAGA, M., MIYATA, S., LIU, B. F., MIYAZAKI, H., HIROTA, Y., HIGO, S., HAMADA, Y., UEYAMA, S. & KASUGA, M. 2004. Methylglyoxal induces apoptosis through activation of p38 MAPK in rat Schwann cells. *Biochemical and Biophysical Research Communications*, 320, 689-695.
- GABOURY, J. P., ANDERSON, D. C. & KUBES, P. 1994. Molecular mechanisms involved in superoxide-induced leukocyte-endothelial cell interactions in vivo. *Am J Physiol*, 266, H637-42.
- GALE, S. C., SICOUTRIS, C., REILLY, P. M., SCHWAB, C. W. & GRACIAS, V. H. 2007. Poor glycemic control is associated with increased mortality in critically ill trauma patients. *Am Surg*, 73, 454-60.
- GALLO, K. A. & JOHNSON, G. L. 2002. Mixed-lineage kinase control of JNK and p38 MAPK pathways. *Nature Reviews Molecular Cell Biology*, 3, 663-672.
- GARRETT RH, G. C. 2012. *Biochemistry (5th ed.)*, Cengage Learning.
- GAUTIERI, A., PASSINI, F. S., SILVÁN, U., GUIZAR-SICAIROS, M., CARIMATI, G., VOLPI, P., MORETTI, M., SCHOENHUBER, H., REDAELLI, A., BERLI, M. & SNEDEKER, J. G. 2017. Advanced glycation end-products: Mechanics of aged collagen from molecule to tissue. *Matrix Biology*, 59, 95-108.
- GAWLOWSKI, T., STRATMANN, B., STIRBAN, A. O., NEGREAN, M. & TSCHOEPE, D. 2007. AGEs and methylglyoxal induce apoptosis and expression of Mac-1 on neutrophils resulting in platelet—neutrophil aggregation. *Thrombosis Research*, 121, 117-126.
- GENESTRA, M. 2007. Oxy radicals, redox-sensitive signalling cascades and antioxidants. *Cell Signal*, 19, 1807-19.
- GERRIETS, V. A., KISHTON, R. J., NICHOLS, A. G., MACINTYRE, A. N., INOUE, M., ILKAYEVA, O., WINTER, P. S., LIU, X., PRIYADHARSHINI, B., SLAWINSKA, M. E., HAEBERLI, L., HUCK, C., TURKA, L. A., WOOD, K. C., HALE, L. P., SMITH, P. A., SCHNEIDER, M. A., MACIVER, N. J., LOCASALE, J. W., NEWGARD, C. B., SHINOHARA, M. L. & RATHMELL, J. C. 2015. Metabolic programming and PDHK1 control CD4+ T cell subsets and inflammation. *J Clin Invest*, 125, 194-207.
- GHIRLANDA, G., DI LEO, M. A., CAPUTO, S., CERCONE, S. & GRECO, A. V. 1997. From functional to microvascular abnormalities in early diabetic retinopathy. *Diabetes Metab Rev*, 13, 15-35.
- GHOSH, A., BERA, S., RAY, S., BANERJEE, T. & RAY, M. 2011. Methylglyoxal induces mitochondria-dependent apoptosis in sarcoma. *Biochemistry (Moscow)*, 76, 1164-1171.
- GIACCO, F., DU, X., D'AGATI, V. D., MILNE, R., SUI, G., GEOFFRION, M. & BROWNLEE, M. 2013. Knockdown of Glyoxalase 1 Mimics Diabetic Nephropathy in Nondiabetic Mice. *Diabetes*, 63, 291-299.
- GOLDIN, A., BECKMAN, J. A., SCHMIDT, A. M. & CREAGER, M. A. 2006. Advanced glycation end products: sparking the development of diabetic vascular injury. *Circulation*, 114, 597-605.
- GOLIGORSKY, M. S. & SUN, D. 2020. Glycocalyx in Endotoxemia and Sepsis. *Am J Pathol*, 190, 791-798.
- GOTOH, I., ADACHI, M. & NISHIDA, E. 2001. Identification and characterization of a novel MAP kinase kinase kinase, MLTK. *J Biol Chem*, 276, 4276-86.
- GÜNZEL, D. & YU, A. S. 2013. Claudins and the modulation of tight junction permeability. *Physiol Rev*, 93, 525-69.
- GUTTERIDGE, J. M. & MITCHELL, J. 1999. Redox imbalance in the critically ill. *Br Med Bull*, 55, 49-75.
- HACK, C. E. & ZEERLEDER, S. 2001. The endothelium in sepsis: source of and a target for inflammation. *Crit Care Med*, 29, S21-7.
- HAIK, G. M., LO, T. W. C. & THORNALLEY, P. J. 1994. Methylglyoxal Concentration and Glyoxalase Activities in the Human Lens. *Experimental Eye Research*, 59, 497-500.
- HAMMES, H. P., MARTIN, S., FEDERLIN, K., GEISEN, K. & BROWNLEE, M. 1991. Aminoguanidine treatment inhibits the development of experimental diabetic retinopathy. *Proc Natl Acad Sci U S A*, 88, 11555-8.

- HAN, J., WANG, Z., LU, C., ZHOU, J., LI, Y., MING, T., ZHANG, Z., WANG, Z. J. & SU, X. 2021. The gut microbiota mediates the protective effects of anserine supplementation on hyperuricaemia and associated renal inflammation. *Food & Function*, 12, 9030-9042.
- HAN, Y. J., KWON, Y. G., CHUNG, H. T., LEE, S. K., SIMMONS, R. L., BILLIAR, T. R. & KIM, Y. M. 2001. Antioxidant enzymes suppress nitric oxide production through the inhibition of NF-kappa B activation: role of H<sub>2</sub>O<sub>2</sub> and nitric oxide in inducible nitric oxide synthase expression in macrophages. *Nitric Oxide*, 5, 504-13.
- HANSEN, N. M., BEULENS, J. W., VAN DIEREN, S., SCHEIJEN, J. L., VAN DER, A. D., SPIJKERMAN, A. M., VAN DER SCHOUW, Y. T., STEHOUWER, C. D. & SCHALKWIJK, C. G. 2015. Plasma advanced glycation end products are associated with incident cardiovascular events in individuals with type 2 diabetes: a case-cohort study with a mean follow-up of 10 years (EPIC-NL). *Diabetes*, 64, 257-65.
- HANSEN, N. M. J., BEULENS, J. W. J., VAN DIEREN, S., SCHEIJEN, J. L. J. M., VAN DER A, D. L., SPIJKERMAN, A. M. W., VAN DER SCHOUW, Y. T., STEHOUWER, C. D. A. & SCHALKWIJK, C. G. 2014a. Plasma Advanced Glycation End Products Are Associated With Incident Cardiovascular Events in Individuals With Type 2 Diabetes: A Case-Cohort Study With a Mean Follow-up of 10 Years (EPIC-NL). *Diabetes*, 64, 257-265.
- HANSEN, N. M. J., SCHEIJEN, J. L. J. M., JORSAL, A., PARVING, H.-H., TARNOW, L., ROSSING, P., STEHOUWER, C. D. A. & SCHALKWIJK, C. G. 2017. Higher Plasma Methylglyoxal Levels Are Associated With Incident Cardiovascular Disease in Individuals With Type 1 Diabetes: A 12-Year Follow-up Study. *Diabetes*, 66, 2278-2283.
- HANSEN, NORDIN M. J., STEHOUWER, COEN D. A. & SCHALKWIJK, CASPER G. 2014b. Methylglyoxal and glyoxalase I in atherosclerosis. *Biochemical Society Transactions*, 42, 443-449.
- HANSEN, N. M. J., STEHOUWER, C. D. A. & SCHALKWIJK, C. G. 2019. Methylglyoxal stress, the glyoxalase system, and diabetic chronic kidney disease. 28, 26-33.
- HANSEN, N. M. J., TERA, M., SCHEIJEN, J. L. J. M., VAN DE WAARENBURG, M., GREMMELS, H., STEHOUWER, C. D. A., VERHAAR, M. C. & SCHALKWIJK, C. G. 2020. Plasma Methylglyoxal Levels Are Associated With Amputations and Mortality in Severe Limb Ischemia Patients With and Without Diabetes. *Diabetes Care*, 44, 157-163.
- HANSEN, N. M. J., WESTERINK, J., SCHEIJEN, J. L. J. M., VAN DER GRAAF, Y., STEHOUWER, C. D. A., SCHALKWIJK, C. G. & GROUP, S. S. 2018. Higher Plasma Methylglyoxal Levels Are Associated With Incident Cardiovascular Disease and Mortality in Individuals With Type 2 Diabetes. *Diabetes Care*, 41, 1689-1695.
- HAORAH, J., SCHALL, K., RAMIREZ, S. H. & PERSIDSKY, Y. 2008. Activation of protein tyrosine kinases and matrix metalloproteinases causes blood-brain barrier injury: Novel mechanism for neurodegeneration associated with alcohol abuse. *Glia*, 56, 78-88.
- HE, Y., YUAN, X., ZUO, H., SUN, Y. & FENG, A. 2018. Berberine Exerts a Protective Effect on Gut-Vascular Barrier via the Modulation of the Wnt/Beta-Catenin Signaling Pathway During Sepsis. *Cell Physiol Biochem*, 49, 1342-1351.
- HENKEL, T., MACHLEIDT, T., ALKALAY, I., KRÖNKE, M., BEN-NERIAH, Y. & BAEUERLE, P. A. 1993. Rapid proteolysis of I kappa B-alpha is necessary for activation of transcription factor NF-kappa B. *Nature*, 365, 182-5.
- HENNIG, P., GARSTKIEWICZ, M., GROSSI, S., DI FILIPPO, M., FRENCH, L. & BEER, H.-D. 2018. The Crosstalk between Nrf2 and Inflammasomes. *International Journal of Molecular Sciences*, 19, 562.
- HENSLEY, K., ROBINSON, K. A., GABBITA, S. P., SALSMAN, S. & FLOYD, R. A. 2000. Reactive oxygen species, cell signaling, and cell injury. *Free Radic Biol Med*, 28, 1456-62.
- HERNANDES, M. S., D'AVILA, J. C., TREVELIN, S. C., REIS, P. A., KINJO, E. R., LOPES, L. R., CASTRO-FARIANETO, H. C., CUNHA, F. Q., BRITTO, L. R. & BOZZA, F. A. 2014. The role of Nox2-derived ROS in the development of cognitive impairment after sepsis. *J Neuroinflammation*, 11, 36.

- HILDEBRAND, F., PAPE, H. C., HARWOOD, P., MÜLLER, K., HOEVEL, P., PÜTZ, C., SIEMANN, A., KRETTEK, C. & VAN GRIENSVEN, M. 2005. Role of adhesion molecule ICAM in the pathogenesis of polymicrobial sepsis. *Exp Toxicol Pathol*, 56, 281-90.
- HO, F. M., LIN, W. W., CHEN, B. C., CHAO, C. M., YANG, C.-R., LIN, L. Y., LAI, C. C., LIU, S. H. & LIAU, C. S. 2006. High glucose-induced apoptosis in human vascular endothelial cells is mediated through NF- $\kappa$ B and c-Jun NH2-terminal kinase pathway and prevented by PI3K/Akt/eNOS pathway. 18, 391-399.
- HOBART, L. J., SEIBEL, I., YEARGANS, G. S. & SEIDLER, N. W. 2004. Anti-crosslinking properties of carnosine: significance of histidine. *Life Sci*, 75, 1379-89.
- HOFER, S., UHLE, F., FLEMING, T., HELL, C., SCHMOCH, T., BRUCKNER, T., WEIGAND, M. A. & BRENNER, T. 2016. RAGE-mediated inflammation in patients with septic shock. *J Surg Res*, 202, 315-27.
- HOFMANN, M. A., DRURY, S., FU, C., QU, W., TAGUCHI, A., LU, Y., AVILA, C., KAMBHAM, N., BIERHAUS, A., NAWROTH, P., NEURATH, M. F., SLATTERY, T., BEACH, D., MCCLARY, J., NAGASHIMA, M., MORSER, J., STERN, D. & SCHMIDT, A. M. 1999. RAGE mediates a novel proinflammatory axis: a central cell surface receptor for S100/calgranulin polypeptides. *Cell*, 97, 889-901.
- HOON, S., GEBBIA, M., COSTANZO, M., DAVIS, R. W., GIAEVER, G. & NISLOW, C. 2011. A global perspective of the genetic basis for carbonyl stress resistance. *G3 (Bethesda)*, 1, 219-31.
- HOSODA, F., ARAI, Y., OKADA, N., SHIMIZU, H., MIYAMOTO, M., KITAGAWA, N., KATAI, H., TANIGUCHI, H., YANAGIHARA, K., IMOTO, I., INAZAWA, J., OHKI, M. & SHIBATA, T. 2015. Integrated genomic and functional analyses reveal glyoxalase I as a novel metabolic oncogene in human gastric cancer. *Oncogene*, 34, 1196-1206.
- HOTCHKISS, R. S. & KARL, I. E. 2003. The pathophysiology and treatment of sepsis. *N Engl J Med*, 348, 138-50.
- HYSLOP, P. A., HINSHAW, D. B., HALSEY, W. A., JR., SCHRAUFSTÄTTER, I. U., SAUERHEBER, R. D., SPRAGG, R. G., JACKSON, J. H. & COCHRANE, C. G. 1988. Mechanisms of oxidant-mediated cell injury. The glycolytic and mitochondrial pathways of ADP phosphorylation are major intracellular targets inactivated by hydrogen peroxide. *J Biol Chem*, 263, 1665-75.
- IBA, T., LEVY, J. H., RAJ, A. & WARKENTIN, T. E. 2019. Advance in the Management of Sepsis-Induced Coagulopathy and Disseminated Intravascular Coagulation. *J Clin Med*, 8.
- INCE, C., MAYEUX, P. R., NGUYEN, T., GOMEZ, H., KELLUM, J. A., OSPINA-TASCÓN, G. A., HERNANDEZ, G., MURRAY, P. & DE BACKER, D. 2016. THE ENDOTHELIUM IN SEPSIS. *Shock*, 45, 259-70.
- ITO, Y., BHAWAL, U. K., SASAHIRA, T., TOYAMA, T., SATO, T., MATSUDA, D., NISHIKIORI, H., KOBAYASHI, M., SUGIYAMA, M., HAMADA, N., ARAKAWA, H. & KUNIYASU, H. 2012. Involvement of HMGB1 and RAGE in IL-1 $\beta$ -induced gingival inflammation. *Arch Oral Biol*, 57, 73-80.
- JALBOUT, A. F., ABUL HAIDER SHIPAR, M. D., TRZASKOWSKI, B. & ADAMOWICZ, L. 2007. Formation of glyoxal in hydroxyacetaldehyde and glycine nonenzymatic browning Maillard reaction: A computational study. *Food Chemistry*, 103, 359-368.
- JANDIAL, R., NEMAN, J., LIM, P. P., TAMAE, D., KOWOLIK, C. M., WUENSCHHELL, G. E., SHUCK, S. C., CIMINERA, A. K., DE JESUS, L. R., OUYANG, C., CHEN, M. Y. & TERMINI, J. 2018. Inhibition of GLO1 in Glioblastoma Multiforme Increases DNA-AGEs, Stimulates RAGE Expression, and Inhibits Brain Tumor Growth in Orthotopic Mouse Models. 19, 406.
- JENSEN, T. M., VISTISEN, D., FLEMING, T., NAWROTH, P. P., ROSSING, P., JØRGENSEN, M. E., LAURITZEN, T., SANDBÆK, A. & WITTE, D. R. 2016. Methylglyoxal is associated with changes in kidney function among individuals with screen-detected Type 2 diabetes mellitus. 33, 1625-1631.
- JEONG, S. R., PARK, H. Y., KIM, Y. & LEE, K. W. 2020. Methylglyoxal-derived advanced glycation end products induce matrix metalloproteinases through activation of ERK/JNK/NF- $\kappa$ B pathway in kidney proximal epithelial cells. *Food Sci Biotechnol*, 29, 675-682.
- JHA, A. K., HUANG, S. C., SERGUSHICHEV, A., LAMPROPOULOU, V., IVANOVA, Y., LOGINICHEVA, E., CHMIELEWSKI, K., STEWART, K. M., ASHALL, J., EVERTS, B., PEARCE, E. J., DRIGGERS, E. M. & ARTYOMOV, M. N. 2015. Network integration of parallel metabolic and transcriptional data reveals metabolic modules that regulate macrophage polarization. *Immunity*, 42, 419-30.

- JO, S. H. 2011. N-acetylcysteine for Prevention of Contrast-Induced Nephropathy: A Narrative Review. *Korean Circ J*, 41, 695-702.
- JOSEPH, L. C., KOKKINAKI, D., VALENTI, M. C., KIM, G. J., BARCA, E., TOMAR, D., HOFFMAN, N. E., SUBRAMANYAM, P., COLECRAFT, H. M., HIRANO, M., RATNER, A. J., MADESH, M., DROSATOS, K. & MORROW, J. P. 2017. Inhibition of NADPH oxidase 2 (NOX2) prevents sepsis-induced cardiomyopathy by improving calcium handling and mitochondrial function. *JCI Insight*, 2.
- JUSTIZ VAILLANT, A. A. & QURIE, A. 2023. Interleukin. *StatPearls*. Treasure Island (FL): StatPearls Publishing
- Copyright © 2023, StatPearls Publishing LLC.
- KALAPOUS, M. P. 2008. The tandem of free radicals and methylglyoxal. *Chem Biol Interact*, 171, 251-71.
- KAMIYA, E., MORITA, A., MORI, A., SAKAMOTO, K. & NAKAHARA, T. 2023. The process of methylglyoxal-induced retinal capillary endothelial cell degeneration in rats. *Microvascular Research*, 146, 104455.
- KANEKO, J., ENYA, A., ENOMOTO, K., DING, Q. & HISATSUNE, T. 2017. Anserine (beta-alanyl-3-methyl-L-histidine) improves neurovascular-unit dysfunction and spatial memory in aged AβPPswe/PSEN1dE9 Alzheimer's-model mice. *Sci Rep*, 7, 12571.
- KANG, J., ZHOU, Y., ZHU, C., REN, T., ZHANG, Y., XIAO, L. & FANG, B. 2022. Ginsenoside Rg1 Mitigates Porcine Intestinal Tight Junction Disruptions Induced by LPS through the p38 MAPK/NLRP3 Inflammasome Pathway. *Toxics*, 10.
- KANG, S., TANAKA, T., INOUE, H., ONO, C., HASHIMOTO, S., KIOI, Y., MATSUMOTO, H., MATSUURA, H., MATSUBARA, T., SHIMIZU, K., OGURA, H., MATSUURA, Y. & KISHIMOTO, T. 2020. IL-6 trans-signaling induces plasminogen activator inhibitor-1 from vascular endothelial cells in cytokine release syndrome. 117, 22351-22356.
- KANWAR, M. & KOWLURU, R. A. 2009. Role of glyceraldehyde 3-phosphate dehydrogenase in the development and progression of diabetic retinopathy. *Diabetes*, 58, 227-34.
- KÁSA, A., CSORTOS, C. & VERIN, A. D. 2015. Cytoskeletal mechanisms regulating vascular endothelial barrier function in response to acute lung injury. *Tissue Barriers*, 3, e974448.
- KATAKURA, Y., TOTSUKA, M., IMABAYASHI, E., MATSUDA, H. & HISATSUNE, T. 2017. Anserine/Carnosine Supplementation Suppresses the Expression of the Inflammatory Chemokine CCL24 in Peripheral Blood Mononuclear Cells from Elderly People. *Nutrients*, 9.
- KEMPE, D. S., AKEL, A., LANG, P. A., HERMLE, T., BISWAS, R., MURESANU, J., FRIEDRICH, B., DREISCHER, P., WOLZ, C., SCHUMACHER, U., PESCHEL, A., GÖTZ, F., DÖRING, G., WIEDER, T., GULBINS, E. & LANG, F. 2007. Suicidal erythrocyte death in sepsis. *J Mol Med (Berl)*, 85, 273-81.
- KEVIL, C. G., OSHIMA, T., ALEXANDER, B., COE, L. L. & ALEXANDER, J. S. 2000. H(2)O(2)-mediated permeability: role of MAPK and occludin. *Am J Physiol Cell Physiol*, 279, C21-30.
- KIHARA, M., SCHMELZER, J. D., PODUSLO, J. F., CURRAN, G. L., NICKANDER, K. K. & LOW, P. A. 1991. Aminoguanidine effects on nerve blood flow, vascular permeability, electrophysiology, and oxygen free radicals. *Proc Natl Acad Sci U S A*, 88, 6107-11.
- KIM, D., KIM, K. A., KIM, J. H., KIM, E. H. & BAE, O. N. 2020. Methylglyoxal-Induced Dysfunction in Brain Endothelial Cells via the Suppression of Akt/HIF-1α Pathway and Activation of Mitophagy Associated with Increased Reactive Oxygen Species. *Antioxidants (Basel)*, 9.
- KIM, J., KIM, C.-S., LEE, Y. M., JO, K., SHIN, S. D. & KIM, J. S. 2012. Methylglyoxal induces hyperpermeability of the blood-retinal barrier via the loss of tight junction proteins and the activation of matrix metalloproteinases. *Graefe's Archive for Clinical and Experimental Ophthalmology*, 250, 691-697.
- KING, C. J., TYTGAT, S., DELUDE, R. L. & FINK, M. P. 1999. Ileal mucosal oxygen consumption is decreased in endotoxemic rats but is restored toward normal by treatment with aminoguanidine. *Crit Care Med*, 27, 2518-24.
- KOHEN, R., YAMAMOTO, Y., CUNDY, K. C. & AMES, B. N. 1988. Antioxidant activity of carnosine, homocarnosine, and anserine present in muscle and brain. *Proc Natl Acad Sci U S A*, 85, 3175-9.

- KOJIMA, T., FUCHIMOTO, J., YAMAGUCHI, H., ITO, T., TAKASAWA, A., NINOMIYA, T., KIKUCHI, S., OGASAWARA, N., OHKUNI, T., MASAKI, T., HIRATA, K., HIMI, T. & SAWADA, N. 2010. c-Jun N-terminal kinase is largely involved in the regulation of tricellular tight junctions via tricellulin in human pancreatic duct epithelial cells. *J Cell Physiol*, 225, 720-33.
- KOOK, S. Y., HONG, H. S., MOON, M., HA, C. M., CHANG, S. & MOOK-JUNG, I. 2012. A $\beta_{1-42}$ -RAGE interaction disrupts tight junctions of the blood-brain barrier via Ca<sup>2+</sup>-calcineurin signaling. *J Neurosci*, 32, 8845-54.
- KRAWCZYK, C. M., HOLOWKA, T., SUN, J., BLAGIH, J., AMIEL, E., DEBERARDINIS, R. J., CROSS, J. R., JUNG, E., THOMPSON, C. B., JONES, R. G. & PEARCE, E. J. 2010. Toll-like receptor-induced changes in glycolytic metabolism regulate dendritic cell activation. *Blood*, 115, 4742-9.
- KRINSLEY, J. S. 2003. Association between hyperglycemia and increased hospital mortality in a heterogeneous population of critically ill patients. *Mayo Clin Proc*, 78, 1471-8.
- KRISHNASAMY, S., RAJARAMAN, B., RAVI, V., RAJAGOPAL, R., GANESHPRASAD, A., KUPPUSWAMY, A. A., PATHAK, A., DHEVASENA, C. S., SWAMINATHAN, K., SUNDARESAN, M., RAMADAS, N. & VEDANTHAM, S. 2020. Association of advanced glycation end products (AGEs) with endothelial dysfunction, oxidative stress in gestational diabetes mellitus (GDM). *International Journal of Diabetes in Developing Countries*, 40, 276-282.
- KUBOMURA, D., MATAHIRA, Y., NAGAI, K. & NIIJIMA, A. 2010. Effect of anserine ingestion on the hyperglycemia and autonomic nerves in rats and humans. *Nutr Neurosci*, 13, 123-8.
- KUMAR, H., KAWAI, T. & AKIRA, S. 2011. Pathogen recognition by the innate immune system. *Int Rev Immunol*, 30, 16-34.
- KURT, A. N., AYGUN, A. D., GODEKMERDAN, A., KURT, A., DOGAN, Y. & YILMAZ, E. 2007. Serum IL-1beta, IL-6, IL-8, and TNF-alpha levels in early diagnosis and management of neonatal sepsis. *Mediators Inflamm*, 2007, 31397.
- KUZMICH, N. N., SIVAK, K. V., CHUBAREV, V. N., POROZOV, Y. B., SAVATEEVA-LYUBIMOVA, T. N. & PERI, F. 2017. TLR4 Signaling Pathway Modulators as Potential Therapeutics in Inflammation and Sepsis. *Vaccines (Basel)*, 5.
- LAI, S. W. T., LOPEZ GONZALEZ, E. D. J., ZOUKARI, T., KI, P. & SHUCK, S. C. 2022. Methylglyoxal and Its Adducts: Induction, Repair, and Association with Disease. *Chemical Research in Toxicology*, 35, 1720-1746.
- LANDER, H. M. 1997. An essential role for free radicals and derived species in signal transduction. *Faseb j*, 11, 118-24.
- LANDER, H. M., TAURAS, J. M., OGIESTE, J. S., HORI, O., MOSS, R. A. & SCHMIDT, A. M. 1997. Activation of the receptor for advanced glycation end products triggers a p21(ras)-dependent mitogen-activated protein kinase pathway regulated by oxidant stress. *J Biol Chem*, 272, 17810-4.
- LANGLEY, J. & ADAMS, G. 2007. Insulin-based regimens decrease mortality rates in critically ill patients: a systematic review. *Diabetes Metab Res Rev*, 23, 184-92.
- LECLERC, E., FRITZ, G., WEIBEL, M., HEIZMANN, C. W. & GALICHET, A. 2007. S100B and S100A6 differentially modulate cell survival by interacting with distinct RAGE (receptor for advanced glycation end products) immunoglobulin domains. *J Biol Chem*, 282, 31317-31.
- LEDERER, M. O. & KLAIBER, R. G. 1999. Cross-linking of proteins by maillard processes: characterization and detection of lysine-arginine cross-links derived from glyoxal and methylglyoxal. *Bioorganic & Medicinal Chemistry*, 7, 2499-2507.
- LEE, B., PARK, J., LEE, Y., CHO, M., KIM, Y., & HENDRICKS, D. 1999. Effect of carnosine and related compounds on glucose oxidation and protein glycation in vitro. *Korean Society for Biochemistry and Molecular Biology*, 32, 370-378.
- LEE, J. H., PARVEEN, A., DO, M. H., KANG, M. C., YUMNAM, S. & KIM, S. Y. 2020. Molecular mechanisms of methylglyoxal-induced aortic endothelial dysfunction in human vascular endothelial cells. *Cell Death & Disease*, 11, 403.
- LEE, W. L. & SLUTSKY, A. S. 2010. Sepsis and endothelial permeability. *N Engl J Med*, 363, 689-91.

- LEVY, M. M., FINK, M. P., MARSHALL, J. C., ABRAHAM, E., ANGUS, D., COOK, D., COHEN, J., OPAL, S. M., VINCENT, J. L. & RAMSAY, G. 2003. 2001 SCCM/ESICM/ACCP/ATS/SIS International Sepsis Definitions Conference. *Crit Care Med*, 31, 1250-6.
- LEVY, R. J., VIJAYASARATHY, C., RAJ, N. R., AVADHANI, N. G. & DEUTSCHMAN, C. S. 2004. Competitive and noncompetitive inhibition of myocardial cytochrome C oxidase in sepsis. *Shock*, 21, 110-4.
- LI, J. H., HUANG, X. R., ZHU, H. J., OLDFIELD, M., COOPER, M., TRUONG, L. D., JOHNSON, R. J. & LAN, H. Y. 2004. Advanced glycation end products activate Smad signaling via TGF-beta-dependent and independent mechanisms: implications for diabetic renal and vascular disease. *Faseb j*, 18, 176-8.
- LI, P., ALLEN, H., BANERJEE, S., FRANKLIN, S., HERZOG, L., JOHNSTON, C., MCDOWELL, J., PASKIND, M., RODMAN, L., SALFELD, J. & ET AL. 1995. Mice deficient in IL-1 beta-converting enzyme are defective in production of mature IL-1 beta and resistant to endotoxic shock. *Cell*, 80, 401-11.
- LI, P., ALLEN, H., BANERJEE, S. & SESHADRI, T. 1997. Characterization of mice deficient in interleukin-1 beta converting enzyme. *J Cell Biochem*, 64, 27-32.
- LI, Q., ZHANG, Q., WANG, C., LIU, X., LI, N. & LI, J. 2009. Disruption of tight junctions during polymicrobial sepsis in vivo. 218, 210-221.
- LI, W., MALONEY, R. E. & AW, T. Y. 2015. High glucose, glucose fluctuation and carbonyl stress enhance brain microvascular endothelial barrier dysfunction: Implications for diabetic cerebral microvasculature. *Redox Biology*, 5, 80-90.
- LI, Y., FESSEL, G., GEORGIADIS, M. & SNEDEKER, J. G. 2013. Advanced glycation end-products diminish tendon collagen fiber sliding. *Matrix Biology*, 32, 169-177.
- LIDE, D. R. 2005. CRC Handbook of Chemistry and Physics: A Ready-Reference of Chemical and Physical Data, 85th ed Edited (National Institute of Standards and Technology). CRC Press LLC: Boca Raton, FL. 2004. 2712 pp. \$139.99. ISBN 0-8493-0485-7. *Journal of the American Chemical Society*, 127, 4542-4542.
- LIN, J., ARAS, M., KOLIBABKA, M., KERN, L., FRIEDRICHS, P., FRIEDRICHS, J., JÄRGEN, P., DIETRICH, N., FLEMING, T. & HAMMES, H.-P. 2014. Methylglyoxal administration induces inflammatory response and microglial activation in the mouse retina. *Diabetologie und Stoffwechsel*, 9.
- LO, T. W., WESTWOOD, M. E., MCLELLAN, A. C., SELWOOD, T. & THORNALLEY, P. J. 1994a. Binding and modification of proteins by methylglyoxal under physiological conditions. A kinetic and mechanistic study with N alpha-acetylarginine, N alpha-acetylcysteine, and N alpha-acetyllysine, and bovine serum albumin. *J Biol Chem*, 269, 32299-305.
- LO, T. W. C., SELWOOD, T. & THORNALLEY, P. J. 1994b. The reaction of methylglyoxal with aminoguanidine under physiological conditions and prevention of methylglyoxal binding to plasma proteins. *Biochemical Pharmacology*, 48, 1865-1870.
- LÖBNER, J., DEGEN, J. & HENLE, T. 2015. Creatine Is a Scavenger for Methylglyoxal under Physiological Conditions via Formation of N-(4-Methyl-5-oxo-1-imidazolin-2-yl)sarcosine (MG-HCr). *Journal of Agricultural and Food Chemistry*, 63, 2249-2256.
- LOHMANN, K. 1932. Beitrag zur enzymatischen Umwandlung von synthetischem Methylglyoxal in Milchsäure. *Biochemie*, 254, 332-353.
- LOPES-PIRES, M. E., FRADE-GUANAES, J. O. & QUINLAN, G. J. 2022. Clotting Dysfunction in Sepsis: A Role for ROS and Potential for Therapeutic Intervention. *Antioxidants*, 11, 88
- LORENTE, L., MARTÍN, M. M., SOLÉ-VIOLÁN, J., BLANQUER, J., LABARTA, L., DÍAZ, C., BORREGUERO-LEÓN, J. M., ORBE, J., RODRÍGUEZ, J. A., JIMÉNEZ, A. & PÁRAMO, J. A. 2014. Association of Sepsis-Related Mortality with Early Increase of TIMP-1/MMP-9 Ratio. *PLOS ONE*, 9, e94318.
- LOSSER, M. R., DAMOISEL, C. & PAYEN, D. 2010. Bench-to-bedside review: Glucose and stress conditions in the intensive care unit. *Crit Care*, 14, 231.
- LOWES, D. A., WEBSTER, N. R., MURPHY, M. P. & GALLEY, H. F. 2013. Antioxidants that protect mitochondria reduce interleukin-6 and oxidative stress, improve mitochondrial function, and reduce biochemical markers of organ dysfunction in a rat model of acute sepsis. *Br J Anaesth*, 110, 472-80.



- LU, J., RANDELL, E., HAN, Y., ADELI, K., KRAHN, J. & MENG, Q. H. 2011. Increased plasma methylglyoxal level, inflammation, and vascular endothelial dysfunction in diabetic nephropathy. *Clinical Biochemistry*, 44, 307-311.
- MACIAG, T., HOOVER, G., STEMERMAN, M. & WEINSTEIN, R. J. T. J. O. C. B. 1981. Serial propagation of human endothelial cells in vitro. 91, 420-426.
- MAESSEN, D. E. M., STEHOUWER, C. D. A. & SCHALKWIJK, C. G. 2015. The role of methylglyoxal and the glyoxalase system in diabetes and other age-related diseases. *Clinical Science*, 128, 839-861.
- MÄKINEN, V.-P., CIVELEK, M., MENG, Q., ZHANG, B., ZHU, J., LEVIAN, C., HUAN, T., SEGRÈ, A. V., GHOSH, S., VIVAR, J., NIKPAY, M., STEWART, A. F. R., NELSON, C. P., WILLENBORG, C., ERDMANN, J., BLAKENBERG, S., O'DONNELL, C. J., MÄRZ, W., LAAKSONEN, R., EPSTEIN, S. E., KATHIRESAN, S., SHAH, S. H., HAZEN, S. L., REILLY, M. P., THE CORONARY, A. D. G.-W. R., META-ANALYSIS, C., LUSIS, A. J., SAMANI, N. J., SCHUNKERT, H., QUERTERMOUS, T., MCPHERSON, R., YANG, X. & ASSIMES, T. L. 2014. Integrative Genomics Reveals Novel Molecular Pathways and Gene Networks for Coronary Artery Disease. *PLOS Genetics*, 10, e1004502.
- MAO, K., CHEN, S., CHEN, M., MA, Y., WANG, Y., HUANG, B., HE, Z., ZENG, Y., HU, Y., SUN, S., LI, J., WU, X., WANG, X., STROBER, W., CHEN, C., MENG, G. & SUN, B. 2013. Nitric oxide suppresses NLRP3 inflammasome activation and protects against LPS-induced septic shock. *Cell Res*, 23, 201-12.
- MARIK, P. E. & BELLOMO, R. 2013. Stress hyperglycemia: an essential survival response! *Crit Care*, 17, 305.
- MARIK, P. E. & RAGHAVAN, M. 2004. Stress-hyperglycemia, insulin and immunomodulation in sepsis. *Intensive Care Med*, 30, 748-56.
- MCQUAID, K. E. & KEENAN, A. K. 1997. Endothelial barrier dysfunction and oxidative stress: roles for nitric oxide? *Exp Physiol*, 82, 369-76.
- MCVICAR, C. M., WARD, M., COLHOUN, L. M., GUDURIC-FUCHS, J., BIERHAUS, A., FLEMING, T., SCHLOTTERER, A., KOLIBABKA, M., HAMMES, H.-P., CHEN, M. & STITT, A. W. 2015. Role of the receptor for advanced glycation endproducts (RAGE) in retinal vasodegenerative pathology during diabetes in mice. *Diabetologia*, 58, 1129-1137.
- MEIR, M., BURKARD, N., UNGEWIß, H., DIEFENBACHER, M., FLEMMING, S., KANNAPIN, F., GERMER, C.-T., SCHWEINLIN, M., METZGER, M., WASCHKE, J. & SCHLEGEL, N. 2019. Neurotrophic factor GDNF regulates intestinal barrier function in inflammatory bowel disease. *Journal of clinical investigation*.
- MEY, J. T. & HAUS, J. M. 2018. Dicarbonyl Stress and Glyoxalase-1 in Skeletal Muscle: Implications for Insulin Resistance and Type 2 Diabetes. 5.
- MICHALEK, R. D., GERRIETS, V. A., JACOBS, S. R., MACINTYRE, A. N., MACIVER, N. J., MASON, E. F., SULLIVAN, S. A., NICHOLS, A. G. & RATHMELL, J. C. 2011. Cutting edge: distinct glycolytic and lipid oxidative metabolic programs are essential for effector and regulatory CD4<sup>+</sup> T cell subsets. *J Immunol*, 186, 3299-303.
- MIN, J., SENUT, M. C., RAJANIKANT, K., GREENBERG, E., BANDAGI, R., ZEMKE, D., MOUSA, A., KASSAB, M., FAROOQ, M. U., GUPTA, R. & MAJID, A. 2008. Differential neuroprotective effects of carnosine, anserine, and N-acetyl carnosine against permanent focal ischemia. *J Neurosci Res*, 86, 2984-91.
- MOKHTARI, V., AFSHARIAN, P., SHAHHOSEINI, M., KALANTAR, S. M. & MOINI, A. 2017. A Review on Various Uses of N-Acetyl Cysteine. *CellJ*, 19, 11-17.
- MOON, J. S., HISATA, S., PARK, M. A., DENICOLA, G. M., RYTER, S. W., NAKAHIRA, K. & CHOI, A. M. K. 2015. mTORC1-Induced HK1-Dependent Glycolysis Regulates NLRP3 Inflammasome Activation. *Cell Rep*, 12, 102-115.
- MORARU, A., WIEDERSTEIN, J., PFAFF, D., FLEMING, T., MILLER, A. K., NAWROTH, P. & TELEMANN, A. A. 2018. Elevated Levels of the Reactive Metabolite Methylglyoxal Recapitulate Progression of Type 2 Diabetes. *Cell Metabolism*, 27, 926-934.e8.
- MORCOS, M., DU, X., PFISTERER, F., HUTTER, H., SAYED, A. A., THORNALLEY, P., AHMED, N., BAYNES, J., THORPE, S., KUKUDOV, G., SCHLOTTERER, A., BOZORGMEHR, F., EL BAKI, R. A., STERN, D., MOEHRLEN, F., IBRAHIM, Y., OIKONOMOU, D., HAMANN, A., BECKER, C., ZEIER, M.,

- SCHWENGER, V., MIFTARI, N., HUMPERT, P., HAMMES, H. P., BUECHLER, M., BIERHAUS, A., BROWNLEE, M. & NAWROTH, P. P. 2008. Glyoxalase-1 prevents mitochondrial protein modification and enhances lifespan in *Caenorhabditis elegans*. *Aging Cell*, 7, 260-9.
- MOVAT, H. Z., BURROWES, C. E., CYBULSKY, M. I. & DINARELLO, C. A. 1987. Acute inflammation and a Shwartzman-like reaction induced by interleukin-1 and tumor necrosis factor. Synergistic action of the cytokines in the induction of inflammation and microvascular injury. *Am J Pathol*, 129, 463-76.
- MURATA-KAMIYA, N. & KAMIYA, H. 2001. Methylglyoxal, an endogenous aldehyde, crosslinks DNA polymerase and the substrate DNA. *Nucleic Acids Research*, 29, 3433-3438.
- NAKAYAMA, K., NAKAYAMA, M., IWABUCHI, M., TERAWAKI, H., SATO, T., KOHNO, M. & ITO, S. 2008. Plasma  $\alpha$ -Oxoaldehyde Levels in Diabetic and Nondiabetic Chronic Kidney Disease Patients. *American Journal of Nephrology*, 28, 871-878.
- NAM, H.-K., JEONG, S.-R., PYO, M. C., HA, S.-K., NAM, M.-H. & LEE, K.-W. 2021. Methylglyoxal-Derived Advanced Glycation End Products (AGE4) Promote Cell Proliferation and Survival in Renal Cell Carcinoma Cells through the RAGE/Akt/ERK Signaling Pathways. *Biological and Pharmaceutical Bulletin*, 44, 1697-1706.
- NI, J., LIN, M., JIN, Y., LI, J., GUO, Y., ZHOU, J., HONG, G., ZHAO, G. & LU, Z. 2019. Gas6 Attenuates Sepsis-Induced Tight Junction Injury and Vascular Endothelial Hyperpermeability via the Axl/NF- $\kappa$ B Signaling Pathway. *Front Pharmacol*, 10, 662.
- NICOLAY, J. P., SCHNEIDER, J., NIEMOELLER, O. M., ARTUNC, F., PORTERO-OTIN, M., HAIK, G., JR., THORNALLEY, P. J., SCHLEICHER, E., WIEDER, T. & LANG, F. 2006. Stimulation of suicidal erythrocyte death by methylglyoxal. *Cell Physiol Biochem*, 18, 223-32.
- NIGRO, C., RACITI, G. A., LEONE, A., FLEMING, T. H., LONGO, M., PREVENZANO, I., FIORY, F., MIRRA, P., D'ESPOSITO, V., ULIANICH, L., NAWROTH, P. P., FORMISANO, P., BEGUINOT, F. & MIELE, C. 2014. Methylglyoxal impairs endothelial insulin sensitivity both in vitro and in vivo. *Diabetologia*, 57, 1485-1494.
- NIN, J. W., JORSAL, A., FERREIRA, I., SCHALKWIJK, C. G., PRINS, M. H., PARVING, H.-H., TARNOW, L., ROSSING, P. & STEHOUWER, C. D. 2011. Higher Plasma Levels of Advanced Glycation End Products Are Associated With Incident Cardiovascular Disease and All-Cause Mortality in Type 1 Diabetes: A 12-year follow-up study. *Diabetes Care*, 34, 442-447.
- O'NEILL, L. A., KISHTON, R. J. & RATHMELL, J. 2016. A guide to immunometabolism for immunologists. *Nat Rev Immunol*, 16, 553-65.
- OGAWA, S., NAKAYAMA, K., NAKAYAMA, M., MORI, T., MATSUSHIMA, M., OKAMURA, M., SENDA, M., NAKO, K., MIYATA, T. & ITO, S. 2010. Methylglyoxal is a predictor in type 2 diabetic patients of intima-media thickening and elevation of blood pressure. *Hypertension*, 56, 471-6.
- OGURA, M. & KITAMURA, M. 1998. Oxidant stress incites spreading of macrophages via extracellular signal-regulated kinases and p38 mitogen-activated protein kinase. *J Immunol*, 161, 3569-74.
- OKUSAWA, S., GELFAND, J. A., IKEJIMA, T., CONNOLLY, R. J. & DINARELLO, C. A. 1988. Interleukin 1 induces a shock-like state in rabbits. Synergism with tumor necrosis factor and the effect of cyclooxygenase inhibition. *J Clin Invest*, 81, 1162-72.
- ONAT, D., BRILLON, D., COLOMBO, P. C. & SCHMIDT, A. M. 2011. Human vascular endothelial cells: a model system for studying vascular inflammation in diabetes and atherosclerosis. *Curr Diab Rep*, 11, 193-202.
- OPAL, S. M. & VAN DER POLL, T. 2015. Endothelial barrier dysfunction in septic shock. 277, 277-293.
- OUYANG, J., ZHANG, Z.-H., ZHOU, Y.-X., NIU, W.-C., ZHOU, F., SHEN, C.-B., CHEN, R.-G. & LI, X. 2016. Up-regulation of Tight-Junction Proteins by p38 Mitogen-Activated Protein Kinase/p53 Inhibition Leads to a Reduction of Injury to the Intestinal Mucosal Barrier in Severe Acute Pancreatitis. 45, 1136-1144.
- PALSSON-MCDERMOTT, E. M. & O'NEILL, L. A. 2013. The Warburg effect then and now: from cancer to inflammatory diseases. *Bioessays*, 35, 965-73.
- PARIHAR, A., PARIHAR, M. S., MILNER, S. & BHAT, S. 2008. Oxidative stress and anti-oxidative mobilization in burn injury. *Burns*, 34, 6-17.

- PEARSON, G., ROBINSON, F., BEERS GIBSON, T., XU, B. E., KARANDIKAR, M., BERMAN, K. & COBB, M. H. 2001. Mitogen-activated protein (MAP) kinase pathways: regulation and physiological functions. *Endocr Rev*, 22, 153-83.
- PERRY, S. W., EPSTEIN, L. G. & GELBARD, H. A. 1997. In situ trypan blue staining of monolayer cell cultures for permanent fixation and mounting. *Biotechniques*, 22, 1020-1, 1024.
- PETECCHIA, L., SABATINI, F., USAI, C., CACI, E., VARELIO, L. & ROSSI, G. A. 2012. Cytokines induce tight junction disassembly in airway cells via an EGFR-dependent MAPK/ERK1/2-pathway. *Lab Invest*, 92, 1140-8.
- PETERS, V., CALABRESE, V., FORSBERG, E., VOLK, N., FLEMING, T., BAELDE, H., WEIGAND, T., THIEL, C., TROVATO, A., SCUTO, M., MODAFFERI, S. & SCHMITT, C. P. 2018. Protective Actions of Anserine Under Diabetic Conditions. *Int J Mol Sci*, 19.
- PETERS, V., JANSEN, E. E., JAKOBS, C., RIEDL, E., JANSSEN, B., YARD, B. A., WEDEL, J., HOFFMANN, G. F., ZSCHOCKE, J., GOTTHARDT, D., FISCHER, C. & KÖPPEL, H. 2011. Anserine inhibits carnosine degradation but in human serum carnosinase (CN1) is not correlated with histidine dipeptide concentration. *Clin Chim Acta*, 412, 263-7.
- PETERS, V., SCHMITT, C. P., ZSCHOCKE, J., GROSS, M. L., BRISMAR, K. & FORSBERG, E. 2012. Carnosine treatment largely prevents alterations of renal carnosine metabolism in diabetic mice. *Amino Acids*, 42, 2411-6.
- PODEROSO, J. J., CARRERAS, M. C., LISDERO, C., RIOBÓ, N., SCHÖPFER, F. & BOVERIS, A. 1996. Nitric oxide inhibits electron transfer and increases superoxide radical production in rat heart mitochondria and submitochondrial particles. *Arch Biochem Biophys*, 328, 85-92.
- POLYKRETIS, P., LUCHINAT, E., BOSCARO, F. & BANCI, L. 2020. Methylglyoxal interaction with superoxide dismutase 1. *Redox Biology*, 30, 101421.
- PRADÈRE, J.-P., HERNANDEZ, C., KOPPE, C., FRIEDMAN, R. A., LUEDDE, T. & SCHWABE, R. F. J. S. S. 2016. Negative regulation of NF- $\kappa$ B p65 activity by serine 536 phosphorylation. 9, ra85-ra85.
- PRANTNER, D., NALLAR, S., RICHARD, K., SPIEGEL, D., COLLINS, K. D. & VOGEL, S. N. 2021. Classically activated mouse macrophages produce methylglyoxal that induces a TLR4- and RAGE-independent proinflammatory response. *Journal of Leukocyte Biology*, 109, 605-619.
- PRASAD, K. & MISHRA, M. 2017. Do Advanced Glycation End Products and Its Receptor Play a Role in Pathophysiology of Hypertension? *Int J Angiol*, 26, 001-011.
- PRAUCHNER, C. A. 2017. Oxidative stress in sepsis: Pathophysiological implications justifying antioxidant co-therapy. *Burns*, 43, 471-485.
- PREISER, J. C., ICHAI, C., ORBAN, J. C. & GROENEVELD, A. B. 2014. Metabolic response to the stress of critical illness. *Br J Anaesth*, 113, 945-54.
- PUMMI, K. P., HEAPE, A. M., GRÉNMAN, R. A., PELTONEN, J. T. & PELTONEN, S. A. 2004. Tight junction proteins ZO-1, occludin, and claudins in developing and adult human perineurium. *J Histochem Cytochem*, 52, 1037-46.
- RABBANI, N., CHITTARI, M. V., BODMER, C. W., ZEHNDER, D., CERIELLO, A. & THORNALLEY, P. J. 2010. Increased Glycation and Oxidative Damage to Apolipoprotein B100 of LDL Cholesterol in Patients With Type 2 Diabetes and Effect of Metformin. *Diabetes*, 59, 1038-1045.
- RABBANI, N., GODFREY, L., XUE, M., SHAHEEN, F., GEOFFRION, M., MILNE, R. & THORNALLEY, P. J. 2011. Glycation of LDL by Methylglyoxal Increases Arterial Atherogenicity: A Possible Contributor to Increased Risk of Cardiovascular Disease in Diabetes. *Diabetes*, 60, 1973-1980.
- RABBANI, N. & THORNALLEY, P. J. 2008. Dicarbonyls linked to damage in the powerhouse: glycation of mitochondrial proteins and oxidative stress. *Biochem Soc Trans*, 36, 1045-50.
- RABBANI, N. & THORNALLEY, P. J. 2014. Measurement of methylglyoxal by stable isotopic dilution analysis LC-MS/MS with corroborative prediction in physiological samples. *Nat Protoc*, 9, 1969-79.
- RABBANI, N. & THORNALLEY, P. J. 2018. Advanced glycation end products in the pathogenesis of chronic kidney disease. *Kidney International*, 93, 803-813.
- RABBANI, N., XUE, M. & THORNALLEY, P. J. 2016. Dicarbonyls and glyoxalase in disease mechanisms and clinical therapeutics. *Glycoconj J*, 33, 513-25.

- RACHMAN, H., KIM, N., ULRICHS, T., BAUMANN, S., PRADL, L., NASSER EDDINE, A., BILD, M., ROTHER, M., KUBAN, R. J., LEE, J. S., HURWITZ, R., BRINKMANN, V., KOSMIADI, G. A. & KAUFMANN, S. H. 2006. Critical role of methylglyoxal and AGE in mycobacteria-induced macrophage apoptosis and activation. *PLoS One*, 1, e29.
- RADEVA, M. Y. & WASCHKE, J. 2018. Mind the gap: mechanisms regulating the endothelial barrier. *Acta Physiol (Oxf)*, 222.
- RADU, M. & CHERNOFF, J. 2013. An in vivo assay to test blood vessel permeability. *Journal of visualized experiments : JoVE*.
- REINHART, K., BAYER, O., BRUNKHORST, F. & MEISNER, M. 2002. Markers of endothelial damage in organ dysfunction and sepsis. *Crit Care Med*, 30, S302-12.
- RHIM, J. S., TSAI, W. P., CHEN, Z. Q., CHEN, Z., VAN WAES, C., BURGER, A. M. & LAUTENBERGER, J. A. 1998. A human vascular endothelial cell model to study angiogenesis and tumorigenesis. *Carcinogenesis*, 19, 673-81.
- RIBOULET-CHAVEY, A., PIERRON, A., DURAND, I., MURDACA, J., GIUDICELLI, J. & VAN OBBERGHEN, E. 2006. Methylglyoxal Impairs the Insulin Signaling Pathways Independently of the Formation of Intracellular Reactive Oxygen Species. *Diabetes*, 55, 1289-1299.
- RITTHALER, U., DENG, Y., ZHANG, Y., GRETEN, J., ABEL, M., SIDO, B., ALLENBERG, J., OTTO, G., ROTH, H., BIERHAUS, A. & ET AL. 1995. Expression of receptors for advanced glycation end products in peripheral occlusive vascular disease. *Am J Pathol*, 146, 688-94.
- RODNICK, K. J., HOLMAN, R. W., ROPSKI, P. S., HUANG, M. & SWISLOCKI, A. L. M. 2017. A Perspective on Reagent Diversity and Non-covalent Binding of Reactive Carbonyl Species (RCS) and Effector Reagents in Non-enzymatic Glycation (NEG): Mechanistic Considerations and Implications for Future Research. 5.
- RODRÍGUEZ-PRADOS, J. C., TRAVÉS, P. G., CUENCA, J., RICO, D., ARAGONÉS, J., MARTÍN-SANZ, P., CASCANTE, M. & BOSCA, L. 2010. Substrate fate in activated macrophages: a comparison between innate, classic, and alternative activation. *J Immunol*, 185, 605-14.
- ROHLENOVA, K., VEYS, K., MIRANDA-SANTOS, I., DE BOCK, K. & CARMELIET, P. 2018. Endothelial Cell Metabolism in Health and Disease. *Trends in Cell Biology*, 28, 224-236.
- ROM, S., HELDT, N. A., GAJGHATE, S., SELIGA, A., REICHENBACH, N. L. & PERSIDSKY, Y. 2020. Hyperglycemia and advanced glycation end products disrupt BBB and promote occludin and claudin-5 protein secretion on extracellular microvesicles. *Sci Rep*, 10, 7274.
- ROSE-JOHN, S. 2017. The Soluble Interleukin 6 Receptor: Advanced Therapeutic Options in Inflammation. *Clinical Pharmacology & Therapeutics*, 102, 591-598.
- ROUSSET, S., EMRE, Y., JOIN-LAMBERT, O., HURTAUD, C., RICQUIER, D. & CASSARD-DOULCIER, A. M. 2006. The uncoupling protein 2 modulates the cytokine balance in innate immunity. *Cytokine*, 35, 135-42.
- RUDD, K. E., JOHNSON, S. C., AGESA, K. M., SHACKELFORD, K. A., TSOI, D., KIEVLAN, D. R., COLOMBARA, D. V., IKUTA, K. S., KISSOON, N., FINFER, S., FLEISCHMANN-STRUZEK, C., MACHADO, F. R., REINHART, K. K., ROWAN, K., SEYMOUR, C. W., WATSON, R. S., WEST, T. E., MARINHO, F., HAY, S. I., LOZANO, R., LOPEZ, A. D., ANGUS, D. C., MURRAY, C. J. L. & NAGHAVI, M. 2020. Global, regional, and national sepsis incidence and mortality, 1990-2017: analysis for the Global Burden of Disease Study. *Lancet*, 395, 200-211.
- RUIZ-REMOLINA, L., OLLAURI-IBÁÑEZ, C., PÉREZ-ROQUE, L., NÚÑEZ-GÓMEZ, E., PÉREZ-BARRIOCANAL, F., LÓPEZ-NOVOA, J. M., PERICACHO, M. & RODRÍGUEZ-BARBERO, A. 2017. Circulating soluble endoglin modifies the inflammatory response in mice. *PLoS One*, 12, e0188204.
- RYLE, C. & DONAGHY, M. 1995. Non-enzymatic glycation of peripheral nerve proteins in human diabetics. *Journal of the Neurological Sciences*, 129, 62-68.
- RYTER, S. W., ALAM, J. & CHOI, A. M. 2006. Heme oxygenase-1/carbon monoxide: from basic science to therapeutic applications. *Physiol Rev*, 86, 583-650.
- SAKANO, T., EGUSA, A. S., KAWAUCHI, Y., WU, J., NISHIMURA, T., NAKAO, N., KURAMOTO, A., KAWASHIMA, T., SHIOTANI, S., OKADA, Y., SATO, K. & YANAI, N. 2022. Pharmacokinetics and

- tissue distribution of orally administrated imidazole dipeptides in carnosine synthase gene knockout mice. *Bioscience, Biotechnology, and Biochemistry*, 86, 1276-1285.
- SAKELLARIOU, S., FRAGKOU, P., LEVIDOU, G., GARGALIONIS, A. N., PIPERI, C., DALAGIORGOU, G., ADAMOPOULOS, C., SAETTA, A., AGROGIANNIS, G., THEOHARI, I., SOUGIOULTZIS, S., TSIOLI, P., KARAVOKYROS, I., TSAVARIS, N., KOSTAKIS, I. D., ZIZI-SERBETZOGLOU, A., VANDOROS, G. P., PATSOURIS, E. & KORKOLOPOULOU, P. 2016. Clinical significance of AGE-RAGE axis in colorectal cancer: associations with glyoxalase-I, adiponectin receptor expression and prognosis. *BMC Cancer*, 16, 174.
- SCHALKWIJK, C. G. 2015. Vascular AGE-ing by methylglyoxal: the past, the present and the future. *Diabetologia*, 58, 1715-1719.
- SCHALKWIJK, C. G. & MIYATA, T. 2012. Early- and advanced non-enzymatic glycation in diabetic vascular complications: the search for therapeutics. *Amino Acids*, 42, 1193-1204.
- SCHALKWIJK, CASPER G. & STEHOUWER, COEN D. A. 2005. Vascular complications in diabetes mellitus: the role of endothelial dysfunction. *Clinical Science*, 109, 143-159.
- SCHALKWIJK, C. G., STEHOUWER, C. D. A. & VAN HINSBERGH, V. W. M. 2004. Fructose-mediated non-enzymatic glycation: sweet coupling or bad modification. 20, 369-382.
- SCHALKWIJK, C. G., VAN BEZU, J., VAN DER SCHORS, R. C., UCHIDA, K., STEHOUWER, C. D. A. & VAN HINSBERGH, V. W. M. 2006. Heat-shock protein 27 is a major methylglyoxal-modified protein in endothelial cells. 580, 1565-1570.
- SCHMIDT, L. E. & DALHOFF, K. 2001. Risk factors in the development of adverse reactions to N-acetylcysteine in patients with paracetamol poisoning. *Br J Clin Pharmacol*, 51, 87-91.
- SCHÖNHERR, J. 2002. Analysis of products of animal origin in feeds by determination of carnosine and related dipeptides by high-performance liquid chromatography. *J Agric Food Chem*, 50, 1945-50.
- SCHRECK, R., RIEBER, P. & BAEUERLE, P. A. 1991. Reactive oxygen intermediates as apparently widely used messengers in the activation of the NF-kappa B transcription factor and HIV-1. *Embo j*, 10, 2247-58.
- SENA, C. M., MATAFOME, P., CRISÓSTOMO, J., RODRIGUES, L., FERNANDES, R., PEREIRA, P. & SEIÇA, R. M. 2012. Methylglyoxal promotes oxidative stress and endothelial dysfunction. *Pharmacological Research*, 65, 497-506.
- SEO, K., KI, S. H. & SHIN, S. M. 2014. Methylglyoxal induces mitochondrial dysfunction and cell death in liver. *Toxicol Res*, 30, 193-8.
- SHI, J. H. & SUN, S. C. 2018. Tumor Necrosis Factor Receptor-Associated Factor Regulation of Nuclear Factor  $\kappa$ B and Mitogen-Activated Protein Kinase Pathways. *Front Immunol*, 9, 1849.
- SHI, L. Z., WANG, R., HUANG, G., VOGEL, P., NEALE, G., GREEN, D. R. & CHI, H. 2011. HIF1 $\alpha$ -dependent glycolytic pathway orchestrates a metabolic checkpoint for the differentiation of TH17 and Treg cells. *J Exp Med*, 208, 1367-76.
- SHINOHARA, M., THORNALLEY, P. J., GIARDINO, I., BEISSWENGER, P., THORPE, S. R., ONORATO, J. & BROWNLEE, M. 1998. Overexpression of glyoxalase-I in bovine endothelial cells inhibits intracellular advanced glycation endproduct formation and prevents hyperglycemia-induced increases in macromolecular endocytosis. *The Journal of Clinical Investigation*, 101, 1142-1147.
- SINGER, M., DEUTSCHMAN, C. S., SEYMOUR, C., SHANKAR-HARI, M., ANNANE, D., BAUER, M., BELLOMO, R., BERNARD, G. R., CHICHE, J. D., COOPERSMITH, C. M., HOTCHKISS, R. S., LEVY, M. M., MARSHALL, J. C., MARTIN, G. S., OPAL, S. M., RUBENFELD, G. D., POLL, T. D., VINCENT, J. L. & ANGUS, D. C. 2016. The Third International Consensus Definitions for Sepsis and Septic Shock (Sepsis-3). *JAMA*, 315, 801-801.
- SJÖVALL, F., MOROTA, S., ASANDER FROSTNER, E., HANSSON, M. J. & ELMÉR, E. 2014. Cytokine and nitric oxide levels in patients with sepsis--temporal evolution and relation to platelet mitochondrial respiratory function. *PLoS One*, 9, e97673.

- SJÖVALL, F., MOROTA, S., HANSSON, M. J., FRIBERG, H., GNAIGER, E. & ELMÉR, E. 2010. Temporal increase of platelet mitochondrial respiration is negatively associated with clinical outcome in patients with sepsis. *Crit Care*, 14, R214.
- SMITH, P. K., KROHN, R. I., HERMANSON, G. T., MALLIA, A. K., GARTNER, F. H., PROVENZANO, M. D., FUJIMOTO, E. K., GOEKE, N. M., OLSON, B. J. & KLENK, D. C. 1985. Measurement of protein using bicinchoninic acid. *Anal Biochem*, 150, 76-85.
- SOULIS-LIPAROTA, T., COOPER, M., PAPAZOGLU, D., CLARKE, B. & JERUMS, G. 1991. Retardation by Aminoguanidine of Development of Albuminuria, Mesangial Expansion, and Tissue Fluorescence in Streptozocin-Induced Diabetic Rat. *Diabetes*, 40, 1328-1334.
- SOULIS, T., COOPER, M. E., VRANES, D., BUCALA, R. & JERUMS, G. 1996. Effects of aminoguanidine in preventing experimental diabetic nephropathy are related to the duration of treatment. *Kidney International*, 50, 627-634.
- SRINIVASAN, B., KOLLI, A. R., ESCH, M. B., ABACI, H. E., SHULER, M. L. & HICKMAN, J. J. 2015. TEER measurement techniques for in vitro barrier model systems. *J Lab Autom*, 20, 107-26.
- STEHOUWER, C. A., ZELDENRUST, G. C., DEN OTTOLANDER, G. H., HACKENG, W. H. L., DONKER, A. J. M. & NAUTA, J. J. P. 1992. Urinary albumin excretion, cardiovascular disease, and endothelial dysfunction in non-insulin-dependent diabetes mellitus. *The Lancet*, 340, 319-323.
- STERN, D., YAN, S. D., YAN, S. F. & SCHMIDT, A. M. 2002. Receptor for advanced glycation endproducts: a multiligand receptor magnifying cell stress in diverse pathologic settings. *Adv Drug Deliv Rev*, 54, 1615-25.
- STITT, A. W., CURTIS, T. M., CHEN, M., MEDINA, R. J., MCKAY, G. J., JENKINS, A., GARDINER, T. A., LYONS, T. J., HAMMES, H.-P., SIMÓ, R. & LOIS, N. 2016. The progress in understanding and treatment of diabetic retinopathy. *Progress in Retinal and Eye Research*, 51, 156-186.
- STOBER, V. P., LIM, Y. P., OPAL, S., ZHUO, L., KIMATA, K. & GARANTZIOTIS, S. 2019. Inter- $\alpha$ -inhibitor Ameliorates Endothelial Inflammation in Sepsis. *Lung*, 197, 361-369.
- STRATMANN, B., ENGELBRECHT, B., ESPELAGE, B. C., KLUSMEIER, N., TIEMANN, J., GAWLOWSKI, T., MATTERN, Y., EISENACHER, M., MEYER, H. E., RABBANI, N., THORNALLEY, P. J., TSCHOEPE, D., POSCHMANN, G. & STÜHLER, K. 2016. Glyoxalase 1-knockdown in human aortic endothelial cells – effect on the proteome and endothelial function estimates. *Scientific Reports*, 6, 37737-37737.
- STROBER, W. 2015. Trypan Blue Exclusion Test of Cell Viability. *Current protocols in immunology / edited by John E. Coligan ... [et al.]*, 111, 1-3.
- SU, Y., QADRI, S. M., CAYABYAB, F. S., WU, L. & LIU, L. 2014. Regulation of methylglyoxal-elicited leukocyte recruitment by endothelial SGK1/GSK3 signaling. *Biochim Biophys Acta*, 1843, 2481-91.
- SUGIMOTO, K., YASUJIMA, M. & YAGIHASHI, S. 2008. Role of Advanced Glycation End Products in Diabetic Neuropathy. *Current Pharmaceutical Design*, 14, 953-961.
- SZWERGOLD, B. S. 2005. Carnosine and anserine act as effective transglycating agents in decomposition of aldose-derived Schiff bases. *Biochem Biophys Res Commun*, 336, 36-41.
- TAGUCHI, A., BLOOD, D. C., DEL TORO, G., CANET, A., LEE, D. C., QU, W., TANJI, N., LU, Y., LALLA, E., FU, C., HOFMANN, M. A., KISLINGER, T., INGRAM, M., LU, A., TANAKA, H., HORI, O., OGAWA, S., STERN, D. M. & SCHMIDT, A. M. 2000. Blockade of RAGE-amphoterin signalling suppresses tumour growth and metastases. *Nature*, 405, 354-60.
- TAMAE, D., LIM, P., WUENSCHHELL, G. E. & TERMINI, J. 2011. Mutagenesis and Repair Induced by the DNA Advanced Glycation End Product N2-1-(Carboxyethyl)-2'-deoxyguanosine in Human Cells. *Biochemistry*, 50, 2321-2329.
- TEUFEL, M., SAUDEK, V., LEDIG, J. P., BERNHARDT, A., BOULARAND, S., CARREAU, A., CAIRNS, N. J., CARTER, C., COWLEY, D. J., DUVERGER, D., GANZHORN, A. J., GUENET, C., HEINTZELMANN, B., LAUCHER, V., SAUVAGE, C. & SMIRNOVA, T. 2003. Sequence identification and characterization of human carnosinase and a closely related non-specific dipeptidase. *J Biol Chem*, 278, 6521-31.

- THORNALLEY, P. J. 1988. Modification of the glyoxalase system in human red blood cells by glucose in vitro. *Biochemical Journal*, 254, 751-755.
- THORNALLEY, P. J. 1998. Glutathione-dependent detoxification of alpha-oxoaldehydes by the glyoxalase system: involvement in disease mechanisms and antiproliferative activity of glyoxalase I inhibitors. *Chem Biol Interact*, 111-112, 137-51.
- THORNALLEY, P. J. 2008. Protein and nucleotide damage by glyoxal and methylglyoxal in physiological systems--role in ageing and disease. *Drug Metabol Drug Interact*, 23, 125-50.
- THORNALLEY, P. J., BATTAH, S., AHMED, N., KARACHALIAS, N., AGALOU, S., BABAEI-JADIDI, R. & DAWNAY, A. 2003. Quantitative screening of advanced glycation endproducts in cellular and extracellular proteins by tandem mass spectrometry. *Biochemical Journal*, 375, 581-592.
- THORNALLEY, P. J., LANGBORG, A. & MINHAS, H. S. 1999. Formation of glyoxal, methylglyoxal and 3-deoxyglucosone in the glycation of proteins by glucose. *Biochem J*, 344 Pt 1, 109-16.
- TIBBLES, L. A., ING, Y. L., KIEFER, F., CHAN, J., ISCOVE, N., WOODGETT, J. R. & LASSAM, N. J. 1996. MLK-3 activates the SAPK/JNK and p38/RK pathways via SEK1 and MKK3/6. *Embo j*, 15, 7026-35.
- TIGUE, C. C., MCKOY, J. M., EVENS, A. M., TRIFILIO, S. M., TALLMAN, M. S. & BENNETT, C. L. 2007. Granulocyte-colony stimulating factor administration to healthy individuals and persons with chronic neutropenia or cancer: an overview of safety considerations from the Research on Adverse Drug Events and Reports project. *Bone Marrow Transplant*, 40, 185-92.
- TONKS, N. K. 2005. Redox redux: revisiting PTPs and the control of cell signaling. *Cell*, 121, 667-70.
- TOSCANO, M. G., GANEA, D. & GAMERO, A. M. 2011. Cecal ligation puncture procedure. *J Vis Exp*.
- TREDGET, E. E., YU, Y. M., ZHONG, S., BURINI, R., OKUSAWA, S., GELFAND, J. A., DINARELLO, C. A., YOUNG, V., BURKE, J. J. A. J. O. P.-E. & METABOLISM 1988. Role of interleukin 1 and tumor necrosis factor on energy metabolism in rabbits. 255, E760-E768.
- TURK, Z., ČAVLOVIĆ-NAGLIĆ, M. & TURK, N. 2011. Relationship of methylglyoxal-adduct biogenesis to LDL and triglyceride levels in diabetics. *Life Sciences*, 89, 485-490.
- UCHIMIDO, R., SCHMIDT, E. P. & SHAPIRO, N. I. 2019. The glycocalyx: a novel diagnostic and therapeutic target in sepsis. *Crit Care*, 23, 16.
- UHLE, F., LICHTENSTERN, C., BRENNER, T., FLEMING, T., KOCH, C., HECKER, A., HEISS, C., NAWROTH, P. P., HOFER, S., WEIGAND, M. A. & WEISMÜLLER, K. 2015. Role of the RAGE Axis during the Immune Response after Severe Trauma: A Prospective Pilot Study. *Mediators Inflamm*, 2015, 691491.
- UHLE, F., WEITERER, S., SIEGLER, B. H., BRENNER, T., LICHTENSTERN, C. & WEIGAND, M. A. 2017. Advanced glycation endproducts induce self- and cross-tolerance in monocytes. *Inflamm Res*, 66, 961-968.
- USATYUK, P. V., VEPA, S., WATKINS, T., HE, D., PARINANDI, N. L. & NATARAJAN, V. 2003. Redox regulation of reactive oxygen species-induced p38 MAP kinase activation and barrier dysfunction in lung microvascular endothelial cells. *Antioxid Redox Signal*, 5, 723-30.
- VAN EUPEN, M. G. A., SCHRAM, M. T., COLHOUN, H. M., HANSEN, N. M. J., NIESSEN, H. W. M., TARNOW, L., PARVING, H. H., ROSSING, P., STEHOUWER, C. D. A. & SCHALKWIJK, C. G. 2013. The methylglyoxal-derived AGE tetrahydropyrimidine is increased in plasma of individuals with type 1 diabetes mellitus and in atherosclerotic lesions and is associated with sVCAM-1. *Diabetologia*, 56, 1845-1855.
- VANASCO, V., SAEZ, T., MAGNANI, N. D., PEREYRA, L., MARCHINI, T., CORACH, A., VACCARO, M. I., CORACH, D., EVELSON, P. & ALVAREZ, S. 2014. Cardiac mitochondrial biogenesis in endotoxemia is not accompanied by mitochondrial function recovery. *Free Radic Biol Med*, 77, 1-9.
- VANDERJAGT, D. L. 2008. Methylglyoxal, diabetes mellitus and diabetic complications. *Drug Metabol Drug Interact*, 23, 93-124.
- VANDOOREN, J., GEURTS, N., MARTENS, E., VAN DEN STEEN, P. E. & OPDENAKKER, G. 2013. Zymography methods for visualizing hydrolytic enzymes. *Nat Methods*, 10, 211-20.
- VANHOUTTE, P. M. 1998. Endothelial dysfunction and vascular disease. *Verh K Acad Geneesk Belg*, 60, 251-66.

- VEECH, R. L., RAIJMAN, L., DALZIEL, K. & KREBS, H. A. 1969. Disequilibrium in the triose phosphate isomerase system in rat liver. *Biochem J*, 115, 837-42.
- VIGNERON, C., PY, B. F., MONNERET, G. & VENET, F. 2023. The double sides of NLRP3 inflammasome activation in sepsis. *Clin Sci (Lond)*, 137, 333-351.
- VINCE, J. E. & SILKE, J. 2016. The intersection of cell death and inflammasome activation. *Cell Mol Life Sci*, 73, 2349-67.
- VISTOLI, G., COLZANI, M., MAZZOLARI, A., GILARDONI, E., RIVALETTO, C., CARINI, M. & ALDINI, G. 2017. Quenching activity of carnosine derivatives towards reactive carbonyl species: Focus on  $\alpha$ -(methylglyoxal) and  $\beta$ -(malondialdehyde) dicarbonyls. *Biochemical and Biophysical Research Communications*, 492, 487-492.
- VISTOLI, G., COLZANI, M., MAZZOLARI, A., MADDIS, D. D., GRAZIOSO, G., PEDRETTI, A., CARINI, M. & ALDINI, G. 2016. Computational approaches in the rational design of improved carbonyl quenchers: focus on histidine containing dipeptides. *Future Med Chem*, 8, 1721-37.
- VLAHOPOULOS, S. & ZOUMPOURLIS, V. C. 2004. JNK: a key modulator of intracellular signaling. *Biochemistry (Mosc)*, 69, 844-54.
- VLISSARA, H., BROWNLEE, M. & CERAMI, A. 1983. Excessive Nonenzymatic Glycosylation of Peripheral and Central Nervous System Myelin Components in Diabetic Rats. *Diabetes*, 32, 670-674.
- WANG, H., MENG, Q. H., GORDON, J. R., KHANDWALA, H. & WU, L. 2007. Proinflammatory and proapoptotic effects of methylglyoxal on neutrophils from patients with type 2 diabetes mellitus. *Clinical Biochemistry*, 40, 1232-1239.
- WANG, J. & LENARDO, M. J. 2000. Roles of caspases in apoptosis, development, and cytokine maturation revealed by homozygous gene deficiencies. *J Cell Sci*, 113 ( Pt 5), 753-7.
- WANG, X., WANG, Y.-S., ZENG, Q.-L., QIU, C.-Y., HE, Y.-Y., WU, Z.-H., HE, Y.-J., SHANG, T., ZHANG, H.-K., ZHU, Q.-Q. & LI, D.-L. 2022. The role of RAGE, MAPK and NF- $\kappa$ B pathway in the advanced glycation end-products induced HUVECs dysfunction. *Vascular Investigation and Therapy*, 5, 80-87.
- WANG, Y., HALL, L., KUJAWA, M., LI, H., ZHANG, X., O'MEARA, M., ICHINOSE, T. & WANG, J. 2019. Methylglyoxal Triggers Human Aortic Endothelial Cell Dysfunction via Modulating K ATP /MAPK pathway. *American Journal of Physiology-Cell Physiology*, 317.
- WAQAS, K., CHEN, J., RIVADENEIRA, F., UITTERLINDEN, A. G., VOORTMAN, T. & ZILLIKENS, M. C. 2022. Skin Autofluorescence, a Noninvasive Biomarker of Advanced Glycation End-products, Is Associated With Frailty: The Rotterdam Study. *J Gerontol A Biol Sci Med Sci*, 77, 2032-2039.
- WARBURG, O., POSENER, K., NEGELEIN, E. 1924. Über den Stoffwechsel der Carcinomzelle. *Biochemische Zeitschrift*, 152, 309-344.
- WARD, R. A. & MCLEISH, K. R. 2004. Methylglyoxal: a stimulus to neutrophil oxygen radical production in chronic renal failure? *Nephrology Dialysis Transplantation*, 19, 1702-1707.
- WATSON, P. M., PATERSON, J. C., THOM, G., GINMAN, U., LUNDQUIST, S. & WEBSTER, C. I. 2013. Modelling the endothelial blood-CNS barriers: a method for the production of robust in vitro models of the rat blood-brain barrier and blood-spinal cord barrier. *BMC Neurosci*, 14, 59.
- WEIGAND, M. A., HÖRNER, C., BARDENHEUER, H. J. & BOUCHON, A. 2004. The systemic inflammatory response syndrome. *Best Pract Res Clin Anaesthesiol*, 18, 455-75.
- WEINBAUM, S., TARBELL, J. M. & DAMIANO, E. R. 2007. The structure and function of the endothelial glycocalyx layer. *Annu Rev Biomed Eng*, 9, 121-67.
- WELTEN, A. G., SCHALKWIJK, C. G., TER WEE, P. M., MEIJER, S., VAN DEN BORN, J. & BEELEN, R. J. J. P. D. I. 2003. Single exposure of mesothelial cells to glucose degradation products (GDPs) yields early advanced glycation end-products (AGEs) and a proinflammatory response. 23, 213-221.
- WEST, A. P., BRODSKY, I. E., RAHNER, C., WOO, D. K., ERDJUMENT-BROMAGE, H., TEMPST, P., WALSH, M. C., CHOI, Y., SHADEL, G. S. & GHOSH, S. 2011a. TLR signalling augments macrophage bactericidal activity through mitochondrial ROS. *Nature*, 472, 476-80.
- WEST, A. P., SHADEL, G. S. & GHOSH, S. 2011b. Mitochondria in innate immune responses. *Nat Rev Immunol*, 11, 389-402.



- WESTWOOD, M. E., ARGIROV, O. K., ABORDO, E. A. & THORNALLEY, P. J. 1997. Methylglyoxal-modified arginine residues--a signal for receptor-mediated endocytosis and degradation of proteins by monocytic THP-1 cells. *Biochim Biophys Acta*, 1356, 84-94.
- WESTWOOD, M. E. & THORNALLEY, P. J. 1996. Induction of synthesis and secretion of interleukin 1 beta in the human monocytic THP-1 cells by human serum albumins modified with methylglyoxal and advanced glycation endproducts. *Immunol Lett*, 50, 17-21.
- WIECHELMAN, K. J., BRAUN, R. D. & FITZPATRICK, J. D. 1988. Investigation of the bicinchoninic acid protein assay: identification of the groups responsible for color formation. *Anal Biochem*, 175, 231-7.
- WIENER, R. S., WIENER, D. C. & LARSON, R. J. 2008. Benefits and risks of tight glucose control in critically ill adults: a meta-analysis. *Jama*, 300, 933-44.
- WU, G. 2020. Important roles of dietary taurine, creatine, carnosine, anserine and 4-hydroxyproline in human nutrition and health. *Amino Acids*, 52, 329-360.
- WU, H., LIU, J., LI, W., LIU, G. & LI, Z. 2016. LncRNA-HOTAIR promotes TNF- $\alpha$  production in cardiomyocytes of LPS-induced sepsis mice by activating NF- $\kappa$ B pathway. *Biochem Biophys Res Commun*, 471, 240-6.
- WU, L. 2005. The pro-oxidant role of methylglyoxal in mesenteric artery smooth muscle cells. *Can J Physiol Pharmacol*, 83, 63-8.
- WU, L. & JUURLINK, B. H. 2002. Increased methylglyoxal and oxidative stress in hypertensive rat vascular smooth muscle cells. *Hypertension*, 39, 809-14.
- WUENSCHHELL, G. E., TAMAE, D., CERCILLIUX, A., YAMANAKA, R., YU, C. & TERMINI, J. 2010. Mutagenic Potential of DNA Glycation: Miscoding by (R)- and (S)-N2-(1-Carboxyethyl)-2'-deoxyguanosine. *Biochemistry*, 49, 1814-1821.
- XIONG, Z., DING, J., ZHOU, J., YAO, S., ZHENG, J. & GUO, X. 2020. Correlation between the HIF-1 $\alpha$ /Notch signaling pathway and Modic changes in nucleus pulposus cells isolated from patients with low back pain. *BMC musculoskeletal disorders*, 21.
- XU, D. & KYRIAKIS, J. M. 2003. Phosphatidylinositol 3'-Kinase-dependent Activation of Renal Mesangial Cell Ki-Ras and ERK by Advanced Glycation End Products\*. *Journal of Biological Chemistry*, 278, 39349-39355.
- YAMAWAKI, H., SAITO, K., OKADA, M. & HARA, Y. 2008. Methylglyoxal mediates vascular inflammation via JNK and p38 in human endothelial cells. *American Journal of Physiology-Cell Physiology*, 295, C1510-C1517.
- YANG, C. T., MENG, F. H., CHEN, L., LI, X., CEN, L. J., WEN, Y. H., LI, C. C. & ZHANG, H. 2017. Inhibition of Methylglyoxal-Induced AGEs/RAGE Expression Contributes to Dermal Protection by N-Acetyl-L-Cysteine. *Cell Physiol Biochem*, 41, 742-754.
- YANG, H., ZHOU, W., MA, S. & MA, X. 2020. [Effect of dexmedetomidine on expression of tight junction protein ZO-1 in kidney tissue of rats with acute kidney injury induced by sepsis]. *Zhonghua Wei Zhong Bing Ji Jiu Yi Xue*, 32, 1467-1471.
- YAO, D. & BROWNLEE, M. 2010. Hyperglycemia-induced reactive oxygen species increase expression of the receptor for advanced glycation end products (RAGE) and RAGE ligands. *Diabetes*, 59, 249-55.
- YAU, J. W. Y., ROGERS, S. L., KAWASAKI, R., LAMOUREUX, E. L., KOWALSKI, J. W., BEK, T., CHEN, S.-J., DEKKER, J. M., FLETCHER, A., GRAUSLUND, J., HAFFNER, S., HAMMAN, R. F., IKRAM, M. K., KAYAMA, T., KLEIN, B. E. K., KLEIN, R., KRISHNAIAH, S., MAYURASAKORN, K., O'HARE, J. P., ORCHARD, T. J., PORTA, M., REMA, M., ROY, M. S., SHARMA, T., SHAW, J., TAYLOR, H., TIELSCH, J. M., VARMA, R., WANG, J. J., WANG, N., WEST, S., XU, L., YASUDA, M., ZHANG, X., MITCHELL, P., WONG, T. Y. & GROUP, F. T. M.-A. F. E. D. S. 2012. Global Prevalence and Major Risk Factors of Diabetic Retinopathy. *Diabetes Care*, 35, 556-564.
- YEH, C.-H., STURGIS, L., HAIDACHER, J., ZHANG, X.-N., SHERWOOD, S. J., BJERCKE, R. J., JUHASZ, O., CROW, M. T., TILTON, R. G. & DENNER, L. 2001. Requirement for p38 and p44/p42 Mitogen-Activated Protein Kinases in RAGE-Mediated Nuclear Factor- $\kappa$ B Transcriptional Activation and Cytokine Secretion. *Diabetes*, 50, 1495-1504.

- YOSEPH, B. P., KLINGENSMITH, N. J., LIANG, Z., BREED, E. R., BURD, E. M., MITTAL, R., DOMINGUEZ, J. A., PETRIE, B., FORD, M. L. & COOPERSMITH, C. M. 2016. Mechanisms of Intestinal Barrier Dysfunction in Sepsis. *Shock*, 46, 52-9.
- YOUNG, D. A., LOWE, L. D. & CLARK, S. C. 1990. Comparison of the effects of IL-3, granulocyte-macrophage colony-stimulating factor, and macrophage colony-stimulating factor in supporting monocyte differentiation in culture. Analysis of macrophage antibody-dependent cellular cytotoxicity. *J Immunol*, 145, 607-15.
- YU, J., SUN, X., GOIE, J. Y. G. & ZHANG, Y. 2020. Regulation of Host Immune Responses against Influenza A Virus Infection by Mitogen-Activated Protein Kinases (MAPKs). *Microorganisms*, 8.
- ZENG, G., CHEN, D., ZHOU, R., ZHAO, X., YE, C., TAO, H., SHENG, W. & WU, Y. 2022. Combination of C-reactive protein, procalcitonin, IL-6, IL-8, and IL-10 for early diagnosis of hyperinflammatory state and organ dysfunction in pediatric sepsis. 36, e24505.
- ZHANG, M. M., ONG, C. L., WALKER, M. J. & MCEWAN, A. G. 2016. Defence against methylglyoxal in Group A Streptococcus: a role for Glyoxylase I in bacterial virulence and survival in neutrophils? *Pathog Dis*, 74.
- ZHANG, S., ZHENG, S., WANG, X., SHI, Q., WANG, X., YUAN, S. & WANG, G. 2015. Carbon Monoxide-Releasing Molecule-2 Reduces Intestinal Epithelial Tight-Junction Damage and Mortality in Septic Rats. *PLoS one*, 10, e0145988.
- ZHONG, H., VOLL, R. E. & GHOSH, S. 1998. Phosphorylation of NF- $\kappa$ B p65 by PKA Stimulates Transcriptional Activity by Promoting a Novel Bivalent Interaction with the Coactivator CBP/p300. *Molecular Cell*, 1, 661-671.
- ZHOU, H., ZHENG, X. Q., ZHANG, Z. J. & TENG, G. J. 2009. [Effects of N-acetylcysteine upon methylglyoxal-induced damage in hippocampal neuronal cells]. *Zhonghua Yi Xue Za Zhi*, 89, 2789-92.
- ZHOU, Q., CHENG, K.-W., GONG, J., LI, E. T. S. & WANG, M. 2019. Apigenin and its methylglyoxal-adduct inhibit advanced glycation end products-induced oxidative stress and inflammation in endothelial cells. *Biochemical Pharmacology*, 166, 231-241.
- ZHOU, R., YAZDI, A. S., MENU, P. & TSCHOPP, J. 2011. A role for mitochondria in NLRP3 inflammasome activation. *Nature*, 469, 221-5.

## 8. Personal contribution to data collection

The present work was partly associated to the SFB project 1118 (Reactive metabolites as a cause of diabetic consequential damage) with the support of the sub-project C05 *The importance of carnosine metabolism in protection against diabetic late damage by reactive metabolites*, sub-project leader Prof. (apl.) Dr. rer. nat. Verena Peters and Mr. Apl. Prof. Dr. med. Claus Peter Schmitt. All animal experiments were carried out together with Ute Krauser. The i.v. injection of Evans Blue was performed by Dr. rer. nat. Laura Kummer. The IF and IHC stains as well as the zymography were previously established by Dr. sc. hum. Maria Bartosova. The HPLC for the Ans concentrations were carried out by Kristina Klingbeil in the laboratory of I - General Pediatrics, Neuropediatrics, Metabolism, Gastroenterology, Nephrology, part of the Center for Pediatric and Adolescent Medicine, the evaluation was carried out by Prof. (apl.) Dr. rer. nat. Verena Peters.

# Curriculum Vitae

## PERSONAL INFORMATION

Name: Nadia Gallenstein  
Date of Birth: 06.10.1991  
Place of Birth: Mannheim  
Nationality: German  
Marital Status: single

## PRIMARY AND SECONDARY SCHOOLS

1997-2001 Vogelstang Primary school  
2001-2010 Geschwister-Scholl-Gymnasium (High school)  
24.06.2010 High school graduation (German Abitur)

## UNIVERSITY

2011-2014 Studies of Ecotrophology  
22.10. 2014 Bachelor of Science Ecotrophology (overall grade: 2.8)  
2014-2016 Studies of cell biology and physiology  
06.10.2016 Master of Science Cell biology and physiology (overall grade: 1.9)

## PROFESSIONAL CAREER/EXPERIENCE

01.10.2016- 31.12.2016 Research assistant at Paul-Ehrlich-Institute  
Division of Immunology, Unit 3/0  
01.02.2018- to date Scientific employee at the University Hospital Heidelberg with  
doctorate  
26.02.2018-02.03.2018 Course on Laboratory Animals Function A and D

Heidelberg, 25.05.2023

## Acknowledgements

First, I would like to thank Prof. Dr. med. Markus A. Weigand, who gave me the opportunity to do my doctoral thesis in the Clinic for Anesthesiology, but above all for taking on the role of doctoral supervisor after the structural change at the clinic without hesitation. As a supervisor, you always had a positive word for me and always supported my new ideas. Special thanks go to Prof. Dr. med. Thorsten Brenner and Dr. med. Thomas Schmoch, who brought my project to life in the first place, making my thesis possible and who accompanied me to the end despite the distance. Prof. Dr. med. Claus Peter Schmitt and Prof. Dr. rer. nat. Verena Peters I would like to thank for the close cooperation and support. Your expertise from different perspectives has repeatedly led to new approaches and without you this project would not have been possible. Extraordinary thanks go to Ute Krauser (Üt) for any support with my experiments, especially the many hours in the animal stable, but also, above all, for your mental and personal support. I don't know what I would have done without you, our connection is unique and priceless. Prof. Dr. sc. hum. Konstanze Plaschke I would like to thank for any support regarding the animal applications and for taking over my animal experiment management without hesitation, even though we hardly knew each other. You have always offered your support and without you this project would not have been possible. I would like to thank Judith Schenz for the opportunity to carry out my experiments in the central research laboratory of the Clinic for Anesthesiology and for having me involved in her working group on immune metabolism and epigenetics in (systemic) immune reactions. I would like to thank Dr. rer. nat. Laura Kummer for her experimental support, all advice and scientific as well as personal discussions. You made the time in the laboratory a really great time and a multi-faceted friendship was formed here, too, which continues to exist. Dr. sc. hum. Maria Bartosova I would like to thank for the introduction to working with endothelial cells, all the advice and her positive attitude. I am very happy that work colleagues have become friends. I would like to thank Dr. sc. hum. Tilman Pfeffer for the cross-departmental coherency and for your diverse scientific and mental support, which has continued to this day. I would like to thank the members of the AG Schenz and the general laboratory (Jessica Löffler, Sabine Stegmaier, Jan Pfister, Lucas Tichy) as well as the members of the pediatric nephrology laboratory (Jana Heigwer, Iva Marinovic, Eszter Levai) and the metabolism laboratory for the pleasant working atmosphere and so many fun hours in the lab. I would like to thank the IBF employees of the KEB (especially Ilona Krämer and Silvio Krasemann) for all the support with my animal experiment and for many a funny chat. I would like to thank Sarah Zimmer and Annabelle Schmitt from the laboratory for general, visceral and transplant surgery for our kitchen meetings, which were very enriching both scientifically and on a friendly level. Finally, great thanks go to my friends and family. You covered all the highs and lows of this doctoral thesis, and I would never have made it without you.

THANK YOU VERY MUCH!

## Eidesstattliche Versicherung (Affidavit)

1. Bei der eingereichten Dissertation zu dem Thema "Pathophysiology of methylglyoxal (MG)-associated endothelial cell damage in experimental sepsis" handelt es sich um meine eigenständig erbrachte Leistung.
2. Ich habe nur die angegebenen Quellen und Hilfsmittel benutzt und mich keiner unzulässigen Hilfe Dritter bedient. Insbesondere habe ich wörtlich oder sinngemäß aus anderen Werken übernommene Inhalte als solche kenntlich gemacht.
3. Die Arbeit oder Teile davon habe ich bislang nicht an einer Hochschule des In- oder Auslands als Bestandteil einer Prüfungs- oder Qualifikationsleistung vorgelegt.
4. Die Richtigkeit der vorstehenden Erklärungen bestätige ich.
5. Die Bedeutung der eidesstattlichen Versicherung und die strafrechtlichen Folgen einer unrichtigen oder unvollständigen eidesstattlichen Versicherung sind mir bekannt. Ich versichere an Eides statt, dass ich nach bestem Wissen die reine Wahrheit erkläre und nichts verschwiegen habe.

Ort und Datum Unterschrift